Testing the Origins of the Blue Ridge Escarpment

Gregory C. Bank
Master's Thesis - Defended July 27, 2001
Dept. of Geological Sciences, Virginia Tech
advisor: Dr. James Spotila
Committee members: Dr. David Harbor, Bill Henika, Dr. W. Lee Daniels

TESTING THE ORIGINS OF THE BLUE RIDGE ESCARPMENT

Gregory C. Bank

Abstract

Long, linear, high-relief escarpments mark many of the world's passive margins. These Great Escarpments have been interpreted to be the result of isostatic flexure, parallel slope retreat, and divide migration which accompanies rifting. It is unclear whether all these escarpments share this origin. Also uncertain is whether these features are formed via stable, steady-state processes or by climatic shifts or tectonic rejuvenation. The Blue Ridge Escarpment, eastern North America's great escarpment, is no different. A number of hypotheses attempt to explain the Blue Ridge Escarpment. These include lithologic variation between Blue Ridge and Piedmont rocks, the distance to ultimate base level, as well as, escarpment retreat resulting from post/syn-rift warping or faulting. We approach this problem from two directions. The first involves topographic comparisons and geologic observations to recognize and track divide migration. The second approach uses U-Th/He thermochronometry along two scarp-normal transects.

Topographic analysis used data extracted from DEMs to compare three zones – the Upland, the Piedmont and the scarp zone itself. Parameters such as relief, drainage density, hypsometry, and slope are often used as proxies for relative erosion rates and the degree of maturity of a landscape. Results from these analyses indicate that the Upland and Piedmont zones are distinct landscapes, sharing very few topographic similarities, yet neither appears significantly more erodible than the other. Examination of parameters in the proximity of the escarpment point toward more rapid erosion here. Field evidence of this rapid scarp erosion (and thus divide migration) lies in the presence of beheaded stream channels, cobble roundness, and clast provenance.

U-Th/He thermochronometry is a low temperature technique that allows us to calculate when rock cooled below 60-70C. Temperature is used as a proxy for depth, from which we can extract an exhumation rate. This method allows us to further test scarp genesis hypotheses. Preliminary results show older ages (~160) from the Upland

surface than on the Piedmont lowland (~100 Ma). This confirms that the Piedmont surface is distinct from the Upland and demonstrates that it has experienced greater erosion. There is also some indication that ages “jump” across the Bowens Creek/Brevard fault system. Lastly, the ages appear to become younger approaching the escarpment which is indicative of scarp migration. As these results are preliminary, more data is required to prove or disprove these conclusions.

Acknowledgements

I wish to thank Dr. James Spotila for advising me through this project. I wish to thank Bill Henika of the Virginia Division of Mineral Resources and Virginia Tech for his vast and invaluable knowledge of the study region and for his willingness to help with sampling field trips. In addition, I would like to express my appreciation to Dr. Peter Reiners for dating many of my samples. Thanks also go to Dr. David Harbor of Washington & Lee University and to Dr. W. Lee Daniels of Virginia Tech.

Funding

This project was funded by a Byron Cooper Geoscience Endowed Fellowship Grant and by a Geological Society of America Student Research Grant.

Table of Contents

Chapter 1: Introduction

1.1 Background

The Blue Ridge Escarpment is a striking land feature in the southern Appalachian Mountains of Virginia and North Carolina. For over 450 km, this escarpment separates the Piedmont and Blue Ridge physiographic provinces, reaches a height of over 550 m, and forms the drainage divide between the Gulf of Mexico and Atlantic Ocean. This landform is atypical of the subdued topography found throughout most of the Appalachians, in that it consists of very rugged, steep slopes (Figure 1). It also lies in a mountain belt in which orogenesis ceased over 270 Myr ago. The occurrence of two low-relief surfaces on either side of the escarpment further illustrates this landform's uniqueness in the region. As an anomalous feature, the Blue Ridge Escarpment has not escaped scrutiny and has been studied for well over a century (e.g., Hayes and Campbell, 1894; Davis, 1903; Hack, 1982). Despite a wide variety of hypotheses that attempt to explain its origin, however, none have become dominant and the escarpment's development is still poorly understood.

1.2 Previous Studies

Early studies produced anecdotal explanations for the Blue Ridge Escarpment, which laid the foundation for more recent investigations. Based on the reconstruction of presumed Tertiary and Cretaceous peneplains, Hayes and Campbell (1894) suggested that monoclinal flexure was responsible for scarp genesis. Davis (1903) introduced the idea that the escarpment developed *into*, rather than originated as, the sharp boundary and divide it presently represents. He proposed that distance to ultimate base-level caused the escarpment, citing that the Gulf of Mexico drainages are >5 times longer than Atlantic streams. This is consistent with the observation that westward-flowing streams are at grade (Wright, 1927). It is problematic, however, that higher Tertiary sea levels (e.g., the Mississippi Embayment) would have made the distance to base-level of both watersheds nearly equal (White, 1950). Hack (1982) also noted that streams draining the Blue Ridge leave the province at similar elevations (e.g., The Atlantic-draining Catawba River enters the Piedmont at an elevation of ~500 m, whereas the Gulf-draining French Broad River enters the Valley and Ridge province at ~400 m). As an alternative, Hack (1982)

suggested the highlands west of the escarpment are held up by resistant units of sandstone and quartzite, forming a high base level for the entire basin. In addition, Hack argued that the steep headwater reaches of the Atlantic drainages are eroding into the Blue Ridge plateau, which retreats steadily and maintains a steady-state topographic form. Johnson (1933) similarly proposed the escarpment was caused by the erosion of a pre-Triassic upwarping of Blue Ridge basement rock, which formed a resistant barrier to headward erosion by Atlantic drainages.

Because the escarpment is so sharp, faulting has also been considered as a possible cause. White (1950) proposed that a southeast-dipping normal fault occurs at the base of the escarpment, based on lineations and slickensided surfaces in weathered bedrock, which could have built the rugged landform.

Wright (1927) believed that several pieces of evidence ought to exist if the Blue Ridge Escarpment is to be explained by faulting. His criteria included the presence of a straight, sharp slope break at the base of the escarpment that is independent of rock structure, unequal slopes on either side of the proposed fault zone, the presence of short parallel streams draining the upthrown block, and the existence of bedrock displacement. Wright found that the trace of the base of the escarpment is much more irregular than previously thought and is parallel to sub-parallel to rock structure. He also found that the short transverse stream draining the escarpment are much more irregular than those draining block-fault mountains in the Basin and Range and thus argued against a block-faulting origin for the Blue Ridge Escarpment. The northern section of the escarpment possesses two very different slopes but further south this difference is less distinct. Lastly, Wright found no evidence for displacement along the proposed fault zone. Wright concluded that most of the field evidence did not support a fault origin for the Blue Ridge Escarpment and that some signs argued against it. Dietrich (1957) could not rule out faulting but proposed that the escarpment had retreated a considerable distance, thereby making it very unlikely to have formed as a result of isolated fault displacement. Hack (1982) also disagreed with the border fault hypothesis, citing the lack of evidence. Faults, however, are abundant in the vicinity of the scarp. The southeast-dipping Brevard Fault zone lies within 10 km of the base of the escarpment and extensional motion has been suggested (e.g., White, 1950; Roper and Justus, 1973) (Figure 2). This fault cuts

across the escarpment in northwestern Georgia, however, limiting its value as an explanation.

More recently, flexural isostasy has emerged as a popular hypothesis for the escarpment's origin (e.g. Pazzaglia and Gardner, 1994). According to this idea, large amounts of sediment were carried to the coast as the Appalachian Mountains were eroded. Deposition of this sediment caused local subsidence of the middle Atlantic margin and flexural rebound inland of the area of subsidence. Isostatic compensation due to the denudation of the mountains added to the flexural uplift. As this continues, the axis of uplift develops into a divide between eastward- and westward-draining streams. This divide is asymmetric because of its proximity to the eastern margin of North America and the resulting characteristic shape. A positive feedback loop is created, in which erosion drives isostatic uplift which in turn causes more erosion. The escarpment thus begins at the axis of flexural bulge and steadily migrates westward (Pazzaglia and Gardner, 1994).

Rift-flank uplift and subsequent erosion is an idea applied to many great escarpments. Essentially, uplift adjacent to a rift axis creates an asymmetric divide and an escarpment. The divide migrates into the newly created plateau via headward erosion. If parallel retreat occurs, the escarpment is maintained. Although briefly mentioned in review literature (Ollier, 1985), this hypothesis has not been explored in depth for eastern North America.

1.3 Other Great Escarpments worldwide

Although the Blue Ridge Escarpment has not been satisfactorily explained, it is not the only feature of its kind in the world. Great escarpments occur along many other continental margins. For example, well-studied escarpments occur in western South Africa and in southeastern Australia. South Africa's great escarpment is ~2500 km long and runs parallel to the coast, usually ~100 km or more inland. Most of the escarpment coincides with the regional asymmetric divide, which is broken only occasionally by rivers draining a 1200-m-high interior plateau (Ollier, 1985). The idea that the origin of this escarpment has been driven by erosional processes, rather than tectonic processes, emerged in the early 20th Century (Seuss, 1904). This escarpment's "step-like" pattern in

profile is attributed by King (1953, 1955) to multiple episodes of erosional rejuvenation due to base-level lowering dating from the breakup of Gondwana. More recently, Ollier (1985) proposed rift-flank uplift and widespread denudation associated with base-level lowering to explain the escarpment. Brown et al. (1990) and Gilchrist et al. (1994) present thermochronometric and offshore stratigraphic data that supports this assessment. Since rifting in the mid-Cretaceous, 0.5 – 3.5 km of denudation has occurred along southwestern Africa. Denudation has been greater along the exterior side of the escarpment, as well as greater in the Late Cretaceous than subsequently during the Cenozoic. This great escarpment therefore appears to have formed by erosional retreat of an asymmetric divide following Mesozoic rifting.

The great escarpment along southeastern Australia is much more irregular than its South African counterpart. The regional drainage divide lies inland of the escarpment. This results in an escarpment that is defined by separating the incised portions of the plateau from the unincised areas, resulting in an escarpment that follows the walls of canyons and gorges. Seidl et al. (1996) named this a "gorge-type" escarpment. The timing and mechanism driving the uplift of eastern Australian margin are also problematic. Wellman (1980) proposed that initiation of this uplift may have been linked with magmatism in the mid-Cretaceous and has been gradual but continuous ever since. The regional sedimentation record suggests cycles of erosion linked with magmatism and intervening periods of minimal denudation (Jones and Veevers, 1982). Based on these associations, Ollier (1982) proposed the escarpment was produced by rift-flank uplift and subsequent erosional retreat. This proposal was adopted by subsequent studies. Seidl et al. (1996) projected the present-day surface of the plateau to the coast to estimate the volume of material removed since rifting initiated and compared this to offshore sediment records. This mass balance approach showed that the volume eroded in their model of escarpment genesis could easily fit within the more voluminous offshore sediments. Given the possibility that the escarpment has been retreating since rifting and assuming rift-flank uplift at ~80 Myr ago, the escarpment retreat rate to its present location as defined by knickpoints is ~2 km/Myr (Weissel and Seidl, 1998). Southeast Australia thus provides an example of an escarpment that may have formed from prolonged erosion and parallel retreat following rifting. Although rift-flank uplift is currently the most popular

model for southeastern Australia's escarpment, its uniqueness as a gorge-type escarpment complicates the rift-flank model used to explain it.

1.4 Landscape Models

Landscape evolution modeling is an alternative method of exploring the genesis and behavior of great escarpments. For example, Tucker and Slingerland (1994) create a surface process model that predicts the minimum number of erosional processes required to develop an escarpment. Their model identifies four conditions requisite for long-term escarpment retreat. The first condition is the presence of bedrock channels that become more efficient with greater drainage area. The channels steepen and propagate headwardly, thus maintaining a sharp scarp. Another condition is a low rate of sediment production versus transport efficiency (i.e., transport limited). The third condition is the presence of any process that maintains a drainage divide near the escarpment crest. Lastly, and perhaps most importantly, an interior plateau with high elevation must be initially present. The higher the elevation of this surface, the more freedom streams have to dissect, thereby increasing the influence of the first three conditions. Kooi and Beaumont (1994) used a surface process model to apply different erosion variables to antecedent topography and found that conditions causing escarpment retreat without a coincident divide are rare and difficult to maintain. An escarpment is maintained through the balance of diffusive slope decline and fluvial slope steepening. If the former dominates, the escarpment will simply "melt" into the landscape. If fluvial steepening takes over, the escarpment crest will quickly retreat until it coincides with the drainage divide (Kooi and Beaumont, 1994). In a modeling study of the southeast Australia escarpment, van der Beek and Braun (1999) use a numerical surface process model, an updated version of Braun and Sambridge's (1997) CASCADE code, to examine scarp processes. The model predicts the existence of certain conditions, such as a fixed drainage divide since the opening of the Tasman Sea, that helped form the escarpment. The model also shows the importance of lithologic control on drainage morphology in southeastern Australia.

Landscape models can thus offer theoretical clues to how escarpments may develop, many of which agree that drainage divide location are vital to great escarpment

formation. However, because they cannot pin down the actual antecedent topography or climatic changes, they cannot by themselves demonstrate the evolution of a great escarpment.

1.5 Testing Hypotheses for the Origins of the Blue Ridge Escarpment

Although rift-flank uplift and erosional retreat may account for many of the world's great escarpments and seems like a reasonable theoretical explanation for escarpments in general, it is not clear whether this mechanism can be resolved with existing data for the Blue Ridge Escarpment. To investigate the long term development of great escarpments and to address the erosional history of the Appalachian Mountains, I have conducted a topographic and thermochronometric study of the Blue Ridge Escarpment. Because available techniques may only loosely constrain its topographic history, I have focused on testing specific straw-man hypotheses for its origin. The hope is that some of these hypotheses will make predictions for the erosional history of the escarpment or adjacent domains that are not supported by data and therefore permit the hypotheses to be eliminated. Of prime importance is that each hypothesis makes specific predictions about the relative degree of total exhumation experienced by different portions of the study region, about the "landscape age" of the upper and lower low-relief domains that are separated by the escarpment, and the degree of escarpment retreat. Landscape age is here considered to be the relative duration of conditions of slow erosion, which can generally be considered the background in the Appalachians. This duration can only be short (i.e. a young landscape age) if a pulse of more rapid denudation and topographic change has recently occurred. Implicit in these considerations is that modern erosional intensity is greatest along the present-day escarpment itself.

Below are described six hypotheses that summarize plausible scenarios most likely responsible for large-scale escarpment genesis. Each has been considered in one form or another by a previous researcher. Each also makes predictions that may be testable using topographic analysis or thermochronometry. These ideas are represented schematically in Figures 3-8 and summarized in Table 1. For each hypothesis, the

predicted relative exhumation, relative landscape age, and degree of escarpment migration are represented.

The first general hypothesis explains the Blue Ridge Escarpment as the product of differential erodibility between the Blue Ridge and inner Piedmont (Figure 3). Essentially, the escarpment is formed because the Piedmont is more easily eroded. This idea is not suggested by mapped bedrock variations in the region, as the escarpment is not associated with a major lithologic contact. In fact, Hack (1982) noted that the Blue Ridge Escarpment is probably the only landform in the Appalachians not attributable to lithologic control. However, subtle contrasts in foliation, metamorphic grade, chemical composition, or degree of jointing and fracturing could exist at the escarpment, which may not be mapable. In this case, differential erodibility could remain a viable hypothesis for escarpment origin. In addition, mapped lithologic contrast across the Brevard fault zone (Reed et al., 1970) could have played a role in escarpment development (Figure 2). This could lead to an association of the escarpment with the fault zone, which is discussed below. If bedrock erodibility is responsible for the escarpment, there are several predictions for the kinematics of erosion (Figure 3). First, it implies that the Piedmont has experienced more denudation than the Blue Ridge upland and thus has a younger landscape age. Second, it predicts that the escarpment should have been relatively fixed at the lithologic contact.

Another hypothesis that argues for minimal escarpment migration involves localized geodynamic uplift associated with deep crustal processes (Figure 4). The escarpment is spatially associated with a gravity anomaly low (Hack, 1982), which may correspond to a deepening of the Moho and thickening of the Grenville basement under the Blue Ridge (Pratt et al., 1988; Hubbard et al., 1991). Northeast of the Blue Ridge escarpment, both the anomaly and the Appalachian drainage divide step northwest into the Valley and Ridge province. A possible link between these is local surface uplift and exhumation associated with a geodynamic mechanism represented by the anomaly. For example, regional compressive stress may cause flow in the lower crust that abuts the thick Grenville slab to the west thus causing uplift (Battiau-Queney, 1989). The predictions of this hypothesis are a minimum amount of escarpment migration and a

localized area of major denudation and young landscape age centered at the escarpment (including both sides of the divide).

Another hypothesis predicts headward migration of the escarpment due to erosional retreat of an asymmetric divide (Figure 5). In this model, postulated by Hack (1973), Gulf of Mexico drainages are at grade, even though they are much higher than adjacent Atlantic drainages. Resistant units in the Appalachian Plateau, downstream of the Blue Ridge highlands, act as local base level for Gulf drainages, thereby preventing headward erosion. This is supported by the higher stream-length gradient indices found along the New River in the Appalachian Plateau (Hack, 1973). In contrast, the Atlantic streams are not at grade where they encounter the edge of the Blue Ridge highlands. These highlands are thus "held up" on the west by resistant bedrock, whereas the greater erosive power of the Atlantic streams maintains a retreating asymmetric divide. Adding to this may be a higher frequency of catastrophic climatic events along the eastern seaboard, which could provide Atlantic streams more erosive power (e.g., Jacobson et al., 1991). This hypothesis predicts that exhumation magnitude should be greatest to the east of the present-day escarpment, landscape age should be youngest at the escarpment and gradually increase eastward, and a moderate to significant amount of escarpment migration should have occurred (Figure 5).

The fourth hypothesis uses Cenozoic faulting and short-term migration to account for the escarpment's development (Figure 6). In this hypothesis, normal motion along a Piedmont fault occurred in recent geologic time, creating an asymmetric divide. Headward migration into this divide has moved the escarpment and divide a slight distance westward. Such a fault could be White's (1950) proposed southeast-dipping "Blue Ridge border fault" near the base of the escarpment, although the evidence for this fault is in doubt (Hack, 1982; Dietrich, 1959; Espenshade et al., 1975). Reactivation of the nearby Brevard Fault zone in a normal-motion sense has also been proposed, although it is usually associated with thrust and/or dextral motion (Roper and Justus, 1973). In either case, the fault must be located near the base of the escarpment and only a minimum amount of migration should have occurred. Total denudation and landscape age across the surfaces east of the fault and west of the escarpment would be comparable with one

another, while exhumation would be greater and landscape age younger between the fault and the escarpment (Figure 6).

The fifth hypothesis concerns rift-flank uplift followed by long-term escarpment migration (Figure 7). The Blue Ridge Escarpment is roughly parallel to a series of Late Triassic-Early Jurassic-age rift basins (Figure 2). The Dan River basin in Virginia is ~60 km from the escarpment and consists of southeast-dipping border faults with ~4 km of throw, forming an asymmetric graben with southwest-tilted strata (Costain and Coruh, 1989). Following displacement and isostatic footwall uplift in the Mesozoic, the escarpment may have begun its erosional retreat. This would be somewhat different than the traditional view of great escarpment formation by rift-flank uplift, however, given that the Newark-age grabens were not full-fledged rifts and were not continuous. In addition, the age of rifting in eastern North America is much older than in other great escarpments, requiring a much longer period of retreat and survival. The main predictions of this hypothesis are major migration (>50 km, in some places), westward-younging landscape ages from the rift basins to the escarpment, and abrupt increase in age on the upland (Figure 7).

The last hypothesis consists of escarpment formation due to flexural isostasy (Figure 8). In this model, offshore sediment loading causes subsidence of the coastal margin and flexural uplift further inland. Isostatic compensation of eroded material leads to greater uplift, while uplift leads to yet more erosion and isostatic rebound. The result is an asymmetric drainage divide which continually retreats due to a positive feedback loop (Pazzaglia and Gardner, 1994). The predictions are for major escarpment retreat, greatest exhumation magnitude, and decreasing landscape age toward the escarpment (Figure 8).

A number of these hypotheses make predictions that are very similar to one another, limiting the chances of ruling out any specific hypothesis. The origin of the Blue Ridge Escarpment may also be a combination of mechanisms. Despite these caveats, I believe these predictions can be tested and at least some of the hypotheses ruled out. To address this, I first use various topographic analyses as a proxy for relative erosion rate and landscape age of the regions adjacent to the escarpment, as well as to test whether significant escarpment migration has occurred. In Chapter 3, I use field

evidence and stream characteristics to explore the likelihood the divide migration has occurred. In Chapter 4, I constrain exhumation patterns in the region using a new technique. (U-Th)/He is a low temperature thermochronometer that is sensitive to 40º-90° C (closure temperature = T_c= ~70° C for a 10° C/Myr cooling rate) (Wolf et al., 1996). By using temperature as a proxy for depth, the spatial variation in recent exhumation can be determined and compared with the predictions of the hypotheses. With these three approaches, I aim to better constrain the origin of the Blue Ridge Escarpment.

Chapter 1 - Figure and Table Captions

Figure Captions

Figure 1 – Location map and three-dimensional perspective view of the Blue Ridge Escarpment and adjacent areas, generated from 90-m DEMs using Microdem. North is to the right on the perspective view. Note how the high-relief escarpment separates the more gentle Piedmont (bottom) and Blue Ridge upland.

Figure 2 – Line drawing of the Blue Ridge Escarpment and surrounding physiographic provinces. The escarpment is in gray while X's mark major topographic highs within the study region. Dan River Basin…

Figure 3 – Escarpment genesis by lithologic control. The three panels conceptually represent successive snap shots through time. Dashed line represent amounts of rock removed by erosion. The less resistant Piedmont is eroded more quickly than the upland, creating a high-relief transition between the provinces. At bottom, the resulting exhumation magnitude, landscape age, and escarpment migration are shown schematically.

Figure 4 - Conceptual diagram of escarpment genesis by geodynamic uplift and erosion, similar to Figure 3. Here, localized forces create an axis of swifter uplift (and thus greater exhumation magnitude). Because the new divide is nearly symmetrical, little migration is expected.

Figure 5 - Escarpment genesis by headward migration of an asymmetric divide. Streams on upland are at grade because they run into resistant units in the Valley & Ridge and Appalachian Plateau. The more vigorous Atlantic streams erode headwardly into the escarpment causing divide migration into the upland.

Figure 6 - Escarpment genesis by Cenozoic faulting and short-term migration. Normal-sense motion along a border fault in the Piedmont creates an asymmetric divide which is eroded headwardly by Atlantic streams. Degree of migration is minimal since faulting is recent.

Figure 7 - Escarpment genesis by rift-flank uplift and subsequent erosional retreat. Fault-block uplift along early Mesozoic rift axis creates an asymmetric divide which is eroded headwardly by Atlantic streams. Degree of migration can be significant due to the great length of time since rifting.

Figure 8 - Escarpment genesis by flexural loading and isostasy. Sediments eroded from Appalachian Mountains are deposited along Atlantic margin. Loading causes crustal subsidence at the margin and uplift in the interior. This uplift may have created an asymmetric bulge which is then eroded, helping to create a positive-feedback. The degree of migration may be significant depending on the timing of flexural uplift.

Table Caption

Table 1 – Summary of escarpment origin hypotheses with individual predictions

Figure 1

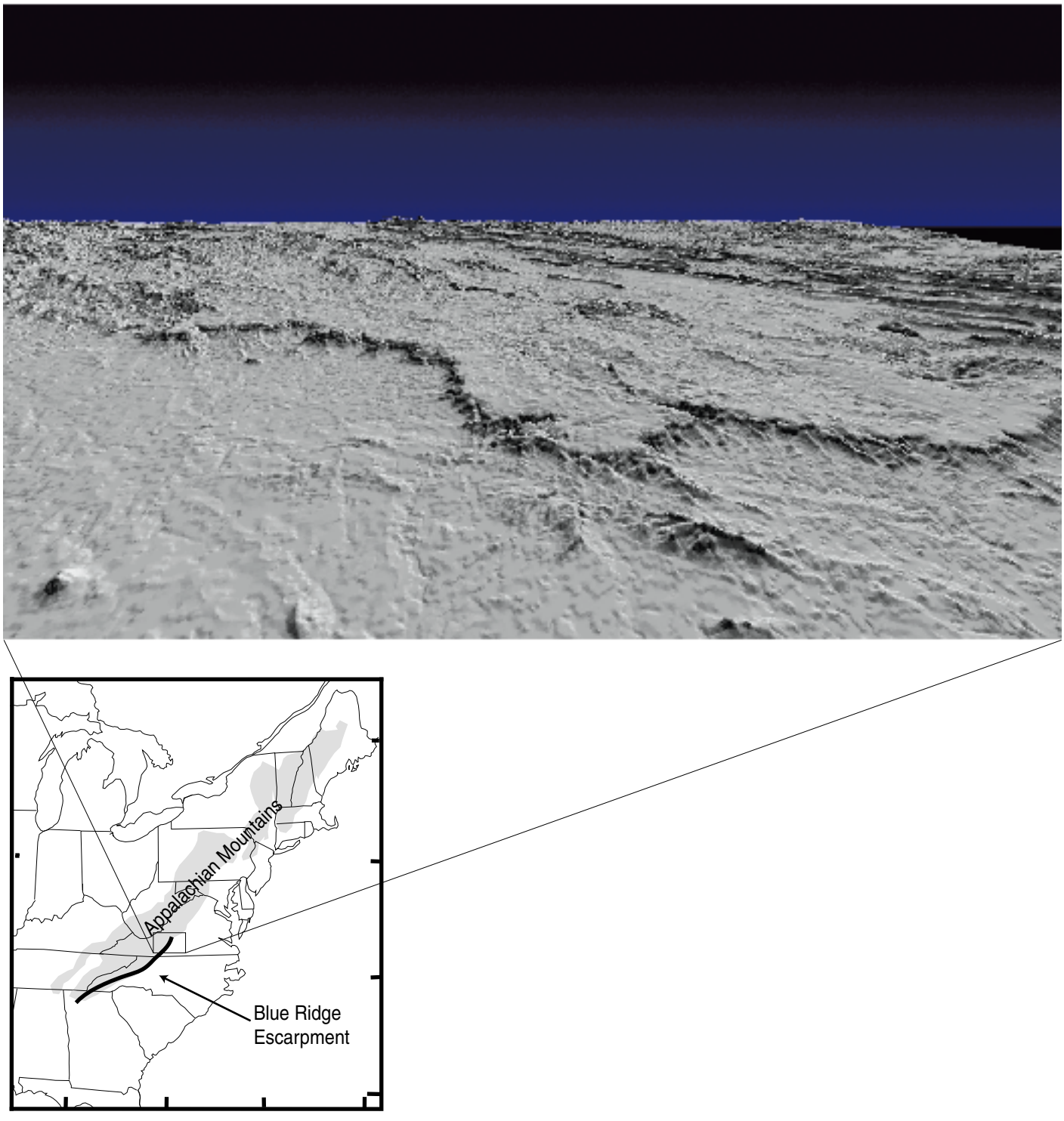

Figure 2

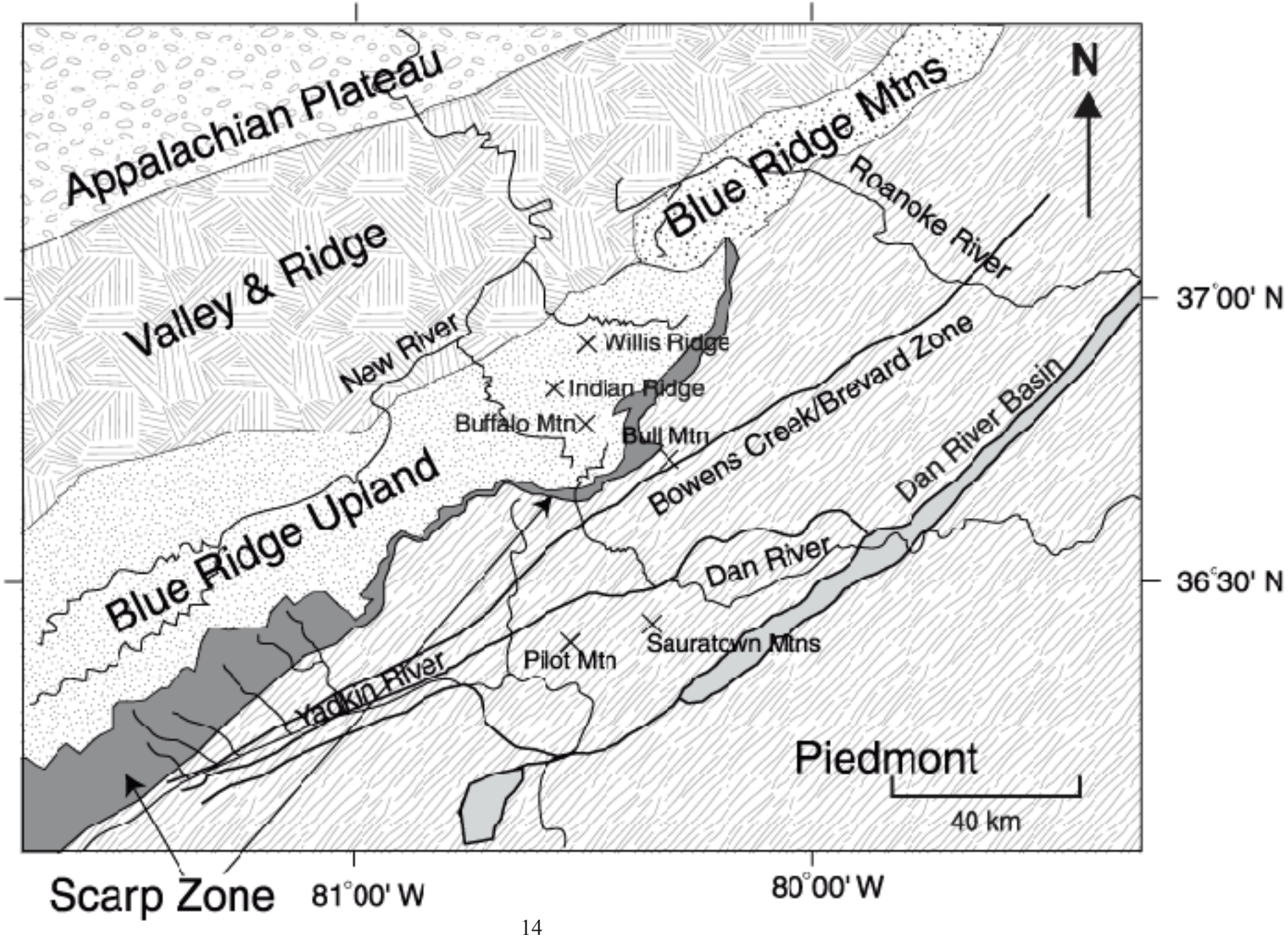
Appalachian Plateau
Valley & Ridge
Blue Ridge Mtns
Roanoke River
N
New River
Willis Ridge
Indian Ridge
Buffalo Mtn
Bull Mtn
Bowens Creek/Brevard Zone
Dan River Basin
Blue Ridge Upland
Dan River
Pilot Mtn
Sauratown Mtns
Yadkin River
Piedmont
40 km
Scarp Zone
81°00' W
80°00' W
37°00' N
36°30' N

Figure 3

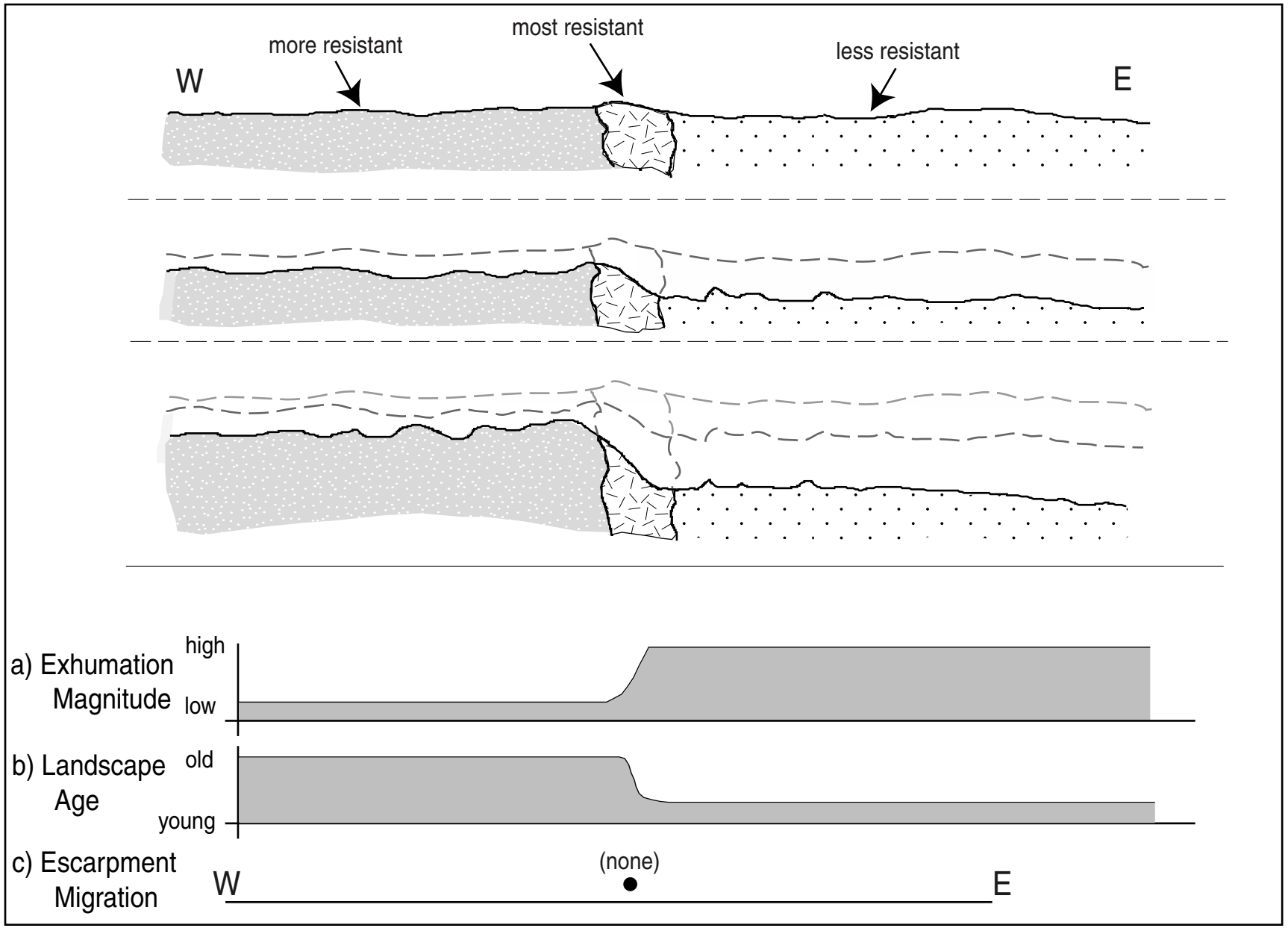
more resistant
most resistant
less resistant
W
E
a) Exhumation Magnitude
high
low
b) Landscape Age
old
young
c) Escarpment Migration
(none)
W
E

Figure 4

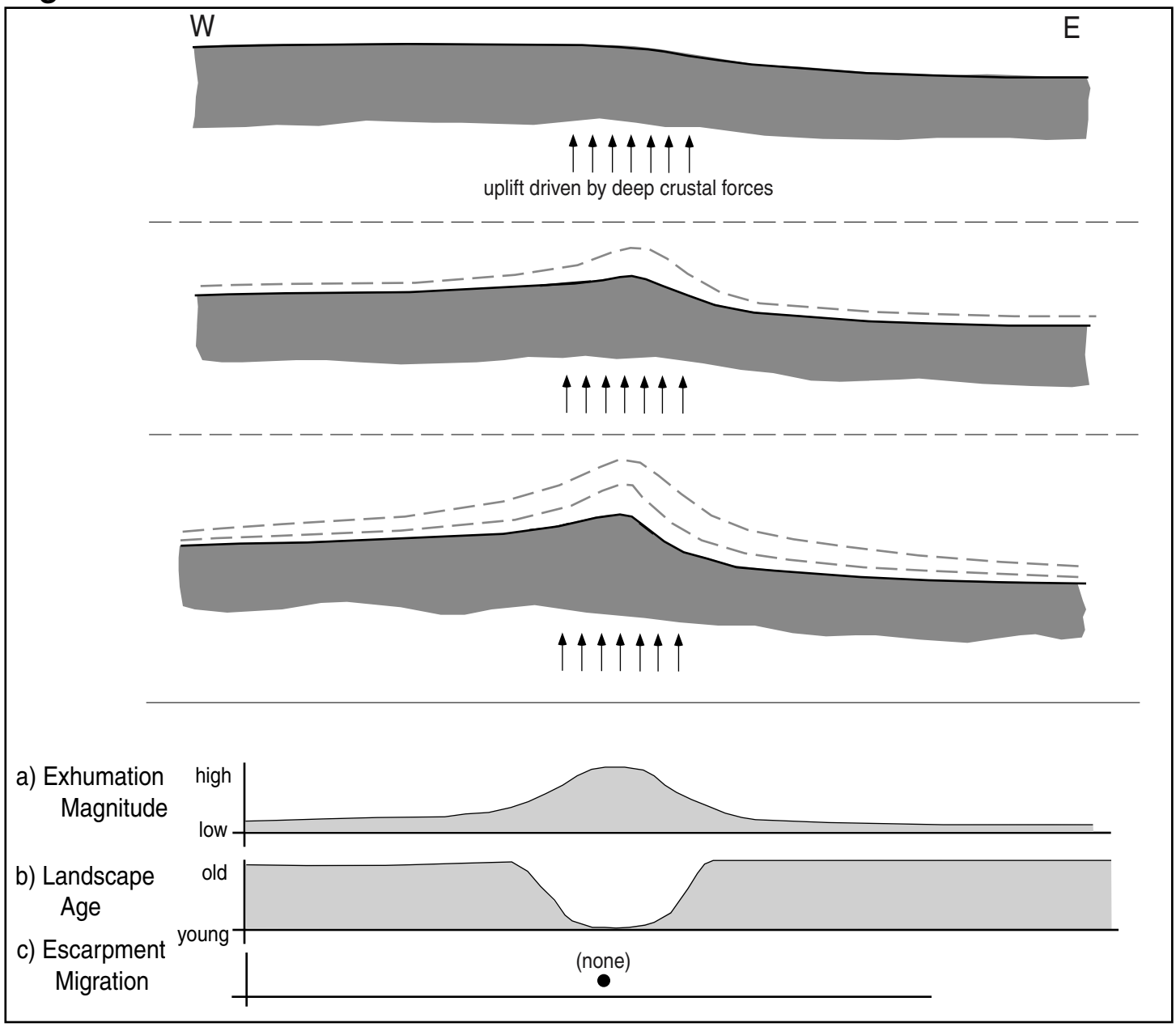
W
E
uplift driven by deep crustal forces
a) Exhumation Magnitude
high
low
b) Landscape Age
old
young
c) Escarpment Migration
(none)

Figure 5

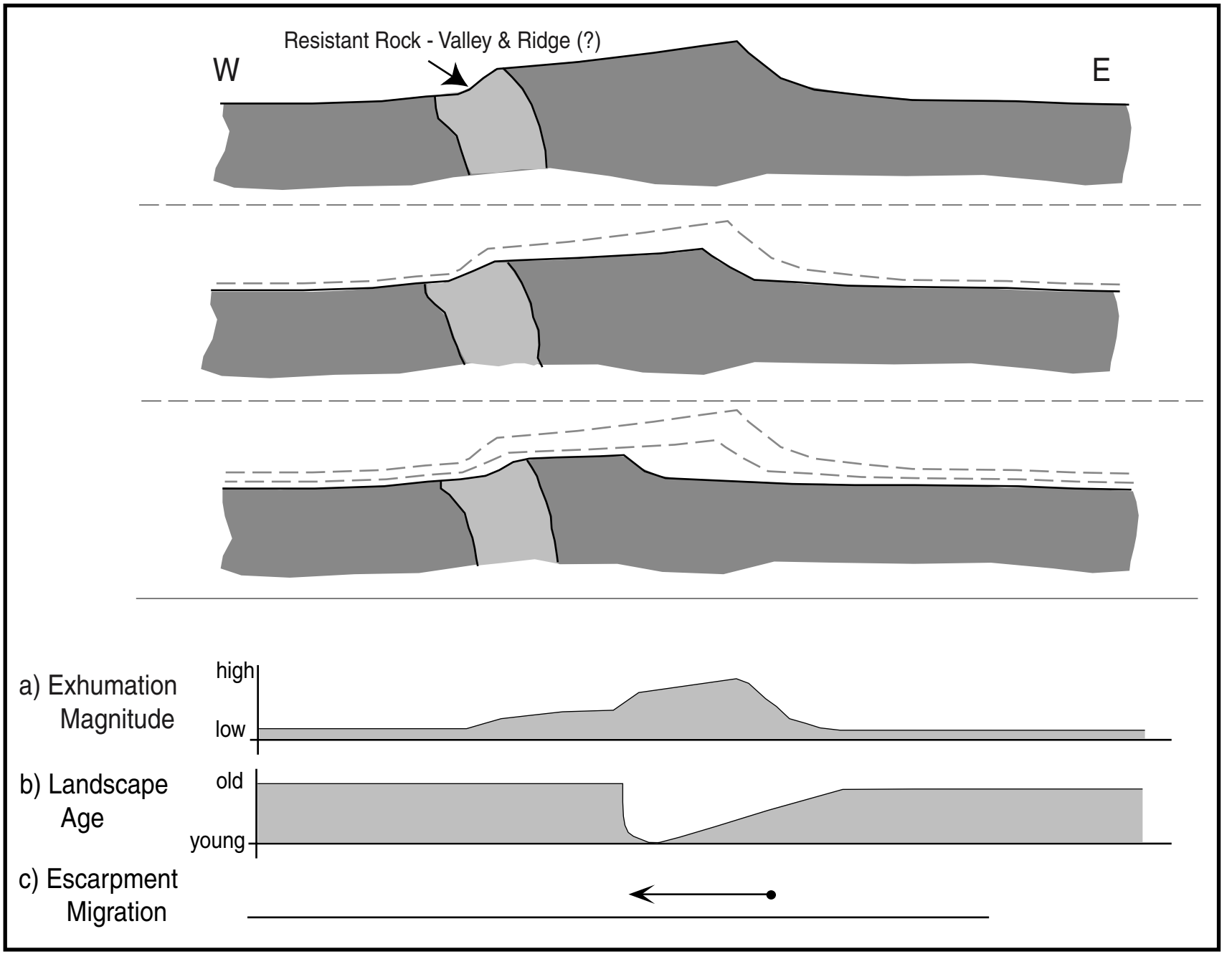
Resistant Rock - Valley & Ridge (?)
W
E
a) Exhumation Magnitude
high
low
b) Landscape Age
old
young
c) Escarpment Migration

Figure 6

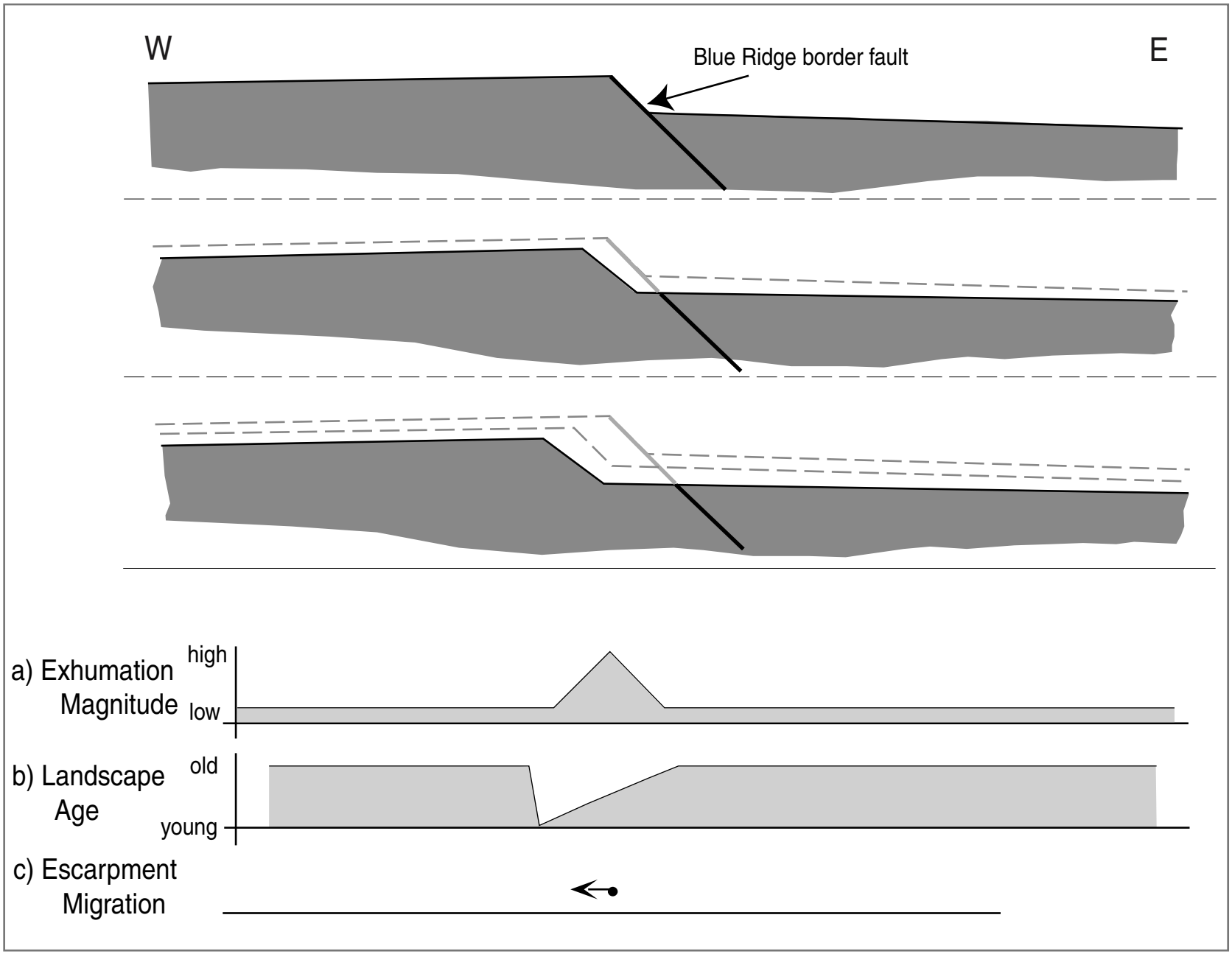
W
Blue Ridge border fault
E
a) Exhumation Magnitude
high
low
b) Landscape Age
old
young
c) Escarpment Migration

Figure 7

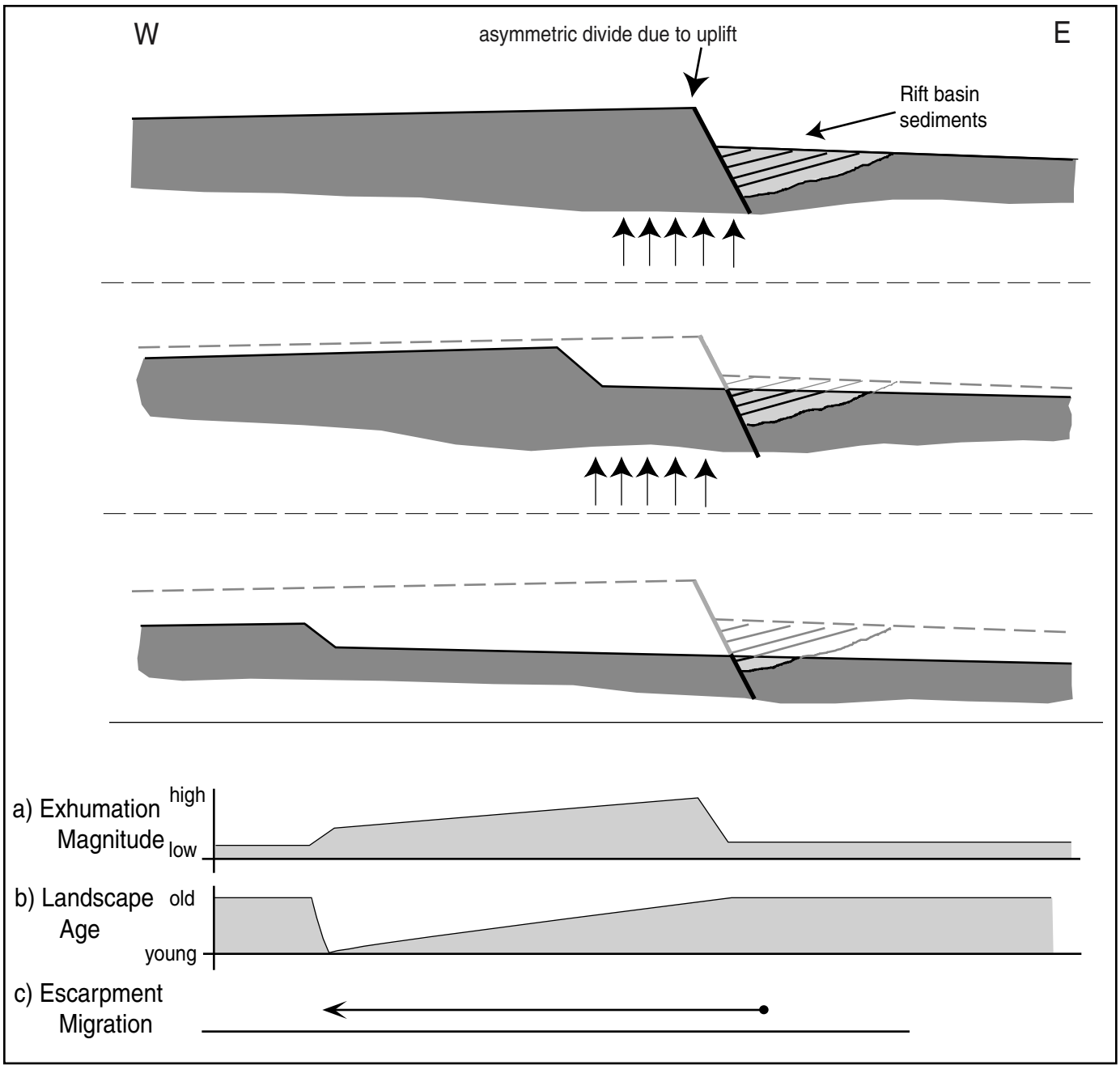
W
asymmetric divide due to uplift
E
Rift basin
sediments
a) Exhumation
Magnitude
high
low
b) Landscape
Age
old
young
c) Escarpment
Migration

Figure 8

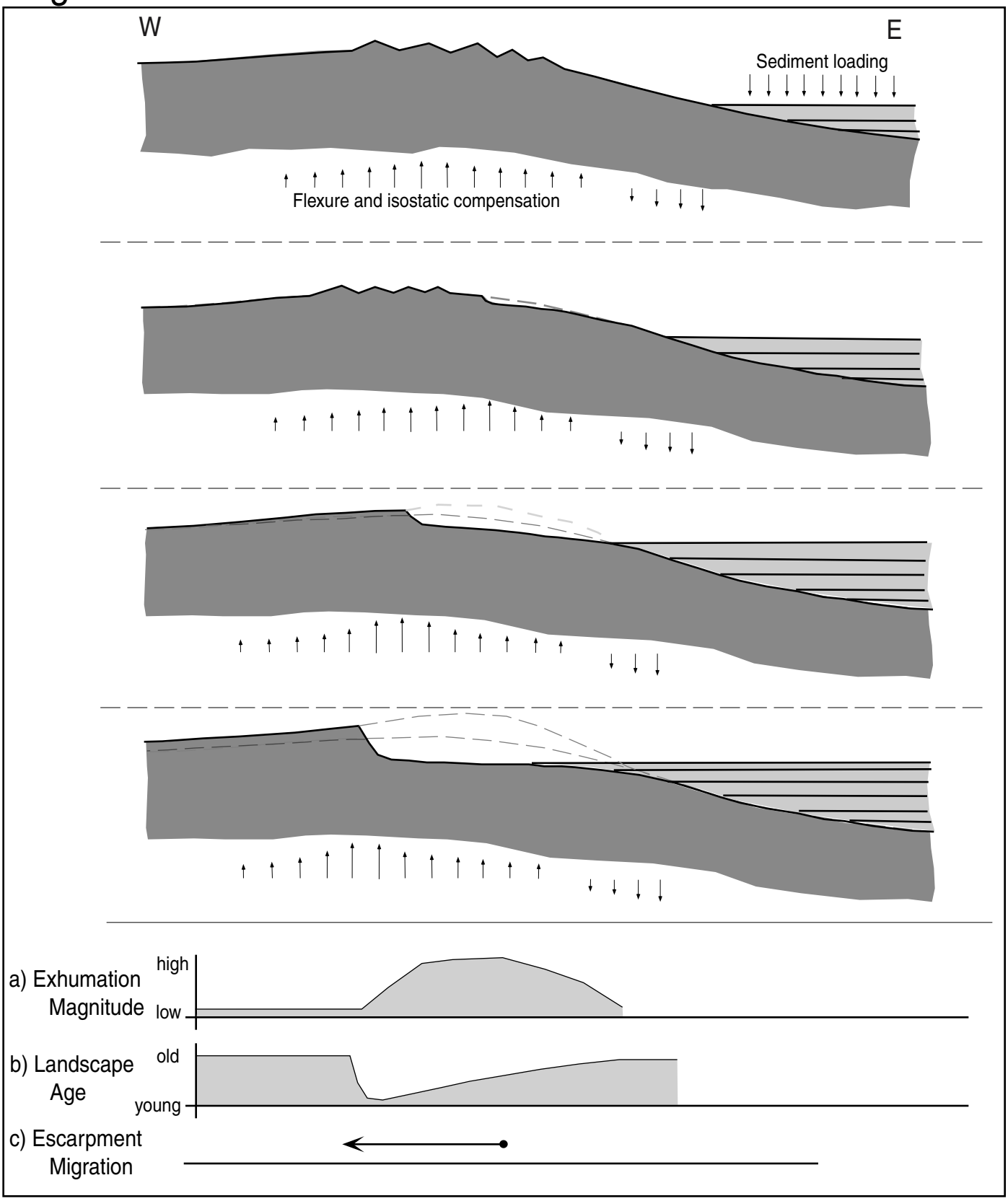
W
E
Sediment loading
Flexure and isostatic compensation
a) Exhumation Magnitude
high
low
b) Landscape Age
old
young
c) Escarpment Migration

Table 1

Hypothesis	Required Boundary conditions	Exhumation Pattern	Landscape age of surfaces	Escarpment Migration
Lithologic control	not present	~500 m more on Piedmont side	much older on upland	very little to none
Local uplift associated w/ geodynamic mechanism	not clear – there is a deep anomaly of unknown origin (Battiau-Queney, 1989)	large exhumation near Blue Ridge Escarpment (BRE) on both sides of the divide	very young at BRE, older away from it	none
Headward migration of an asymmetric divide	present – distance to base level (e.g., Davis, 1903)	nearly uniform, slightly higher in the vicinity of the escarpment	younging from Piedmont to BRE; very old on upland	moderate
Cenozoic faulting w/ short-term migration	uncertain – ambiguous border fault (White, 1950); or Brevard f.z. (Roper and Justice, 1973)	increasing exhumation from Piedmont to BRE	younging from Piedmont to BRE; very old on upland	minor
Long-term, post-rift migration	present - Dan River basin -presumed 4 km of throw/uplift	increasing exhumation from Piedmont to BRE	younging from Piedmont to BRE; very old on upland	major
Flexural isostasy	present – offshore sedimentary sequence (e.g. Pazzaglia and Gardner, 1994)	increasing exhumation from Piedmont to BRE	younging from Piedmont to BRE; very old on upland	major to moderate

Chapter 2: Topographic Analysis

2.1 Introduction

Topography is an expression of processes at work on a landscape. In many regions, topography contains clues to the processes that have shaped a landscape and how these have varied temporally and spatially (e.g., Willemin and Knuepfer, 1994; Densmore and Hovius, 2000; Snyder et al., 2000; Meigs and Sauber, 2000). Examination of topographic character is thus useful in interpreting and understanding landscape evolution.

Topographic characterization can help constrain the evolution of the Blue Ridge Escarpment in several ways. For example, denudation rate generally correlates with relief and hillslope angle in a given region (Ahnert, 1970; Whipple and Tucker, 1999). Spatial patterns of relief and slope may thus be a proxy for relative erosion rates in the study area. Other topographic indices are considered proxies for relative landscape maturity. For example, basin hypsometry has been used to differentiate basins at grade from those in disequilibrium (Strahler, 1952). Each of the hypothetical models for the origin of the Blue Ridge Escarpment requires boundary conditions for landscape development and predicts relative erosion rates for different positions in the study region (Figures 3-8). Examining topography thus allows us to compare the actual landscape to predictions of topographic history and erosional kinematics made by each hypothesis.

The initial goal of this methodology was to use topography reveal information about the evolution of the Piedmont, the Blue Ridge upland, and the Blue Ridge Escarpment domains. After analyzing the various data, I realize that, although topography often contains clues concerning landscape development, at this scale most strongly a function of process.

2.2 Methods

To extract useful inferences from topography of the Blue Ridge Escarpment region, we must first gain a general understanding of regional topographic character. The topography must then be subjected to rigorous comparisons designed to represent erosional intensity and landscape age. A basic characterization of the landscape involves the quantification of drainage patterns, hillslope angles, relief and average elevation

distribution. I first explore the variation of these parameters in the region to define and contrast geomorphic domains. This is followed by a more detailed comparison between low-relief domains above and below the escarpment as well as a detailed characterization of the escarpment topography itself. These comparisons may indicate whether the low-relief surfaces share relative landscape age or are distinct in erosional history. They may also provide hints as to whether escarpment and divide migration has occurred.

Topographic analyses were made using digital topography of the region. Digital Elevation Models (DEMs) were downloaded from the United States Geological Survey website (www.usgs.gov). Basic characterizations were made using 1-degree (latitude-longitude) DEMs with a spatial resolution of 90 meters. Detailed comparisons were made using 7.5-minute DEMs (i.e. equal to published 1:24,000 quadrangle maps) with 30-m spatial resolution. Topographic parameters were calculated using RiverTools 2.0 (distributed by *Research Systems Inc*.) and Microdem (DEM manipulation program written by Dr. Peter Guth, U.S. Naval Academy). RiverTools extracts drainage networks from the DEMs and calculates drainage basin statistics. Microdem is used to calculate slope ("hybrid (steepest + 8) algorithm"; Guth, 1995) and relief at specified wavelengths.

2.3 Initial Characterization

The escarpment separates the Blue Ridge and Piedmont physiographic provinces of the southern Appalachians (Figure 2). The study area is thus segregated into three geomorphic regions or domains (including the escarpment itself), whose individual evolution may be betrayed by unique topographic character.

The Blue Ridge province in western Virginia and northern North Carolina consists of a 30- to 40-km wide upland, characterized by gently rolling hills (~70 m relief) that are broken by isolated northeast-trending ridges (~250-300 m relief). These prominent ridges, which include Buffalo Mountain, Willis Ridge, and Indian Ridge, are thought to exist due to resistant bedrock (Dietrich, 1959) (Figure 2). The “ruggedness” (steeper with greater relief) of the upland, although much gentler than the escarpment itself, can be attributed to these resistant ridges as well as fluvial incision. Most of the upland streams flow to the New River, which drains the northwest side of the asymmetric divide (Dietrich, 1957). Upland drainage basins are characterized by dendritic flow

patterns, with noticeable control exerted by geologic structure. Control is demonstrated by confined meandering within lineaments. The Little River, trunk stream of northern portion of the upland, contains several entrenched meanders in its lower reaches. Big Reed Island Creek, which drains the area around Buffalo Mountain, shows similar character. A small number of upland basins actually flow down the escarpment to the southeast (e.g. the Dan River), such that locally the regional drainage divide is a short distance inland of the escarpment. The southeast-draining Dan River is similar in appearance to other upland streams while in its headwaters in the Meadows of Dan, but has incised a 400-m deep gorge where it flows across the escarpment. It has been suggested that the gentle Dan River headwaters have been captured from the Big Reed Island Creek basin (Dietrich, 1959; Hack, 1982).

The ~70 km-wide inner Piedmont lies southeast of the escarpment and also exhibits a low-relief character. It contains subdued, rolling hills, but lacks streams with entrenched reaches typical of the Blue Ridge upland. The Piedmont has no major resistant ridges, but is broken by isolated monadnocks. These knob-like forms, such as Pilot Mountain, the Sauratown Mountains, Fork Mountain, Turkeycock Mountain, and Smith Mountain, generally rise to 650-750 m in elevation, creating a maximum local relief of ~400 m (Dietrich, 1959) (Figure 2). The majority of the Piedmont in the study area falls within two major basins draining to the Atlantic. The Dan River flows from atop the upland down the escarpment toward the southeast before turning northeast near Danville, Virginia. To the south, the Yadkin River flows northeast, parallel to the escarpment. It makes a broad turn to the south near Winston-Salem, North Carolina. Drainage patterns within these basins are dendritic, although many of trunk streams follow paths determined by structure. For example, the upper Yadkin River follows the Yadkin Valley lineament (Reed and Bryant, 1964). These streams are also less sinuous than their upland counterparts.

The majority of the upland is underlain by metamorphic Blue Ridge rocks. The Alligator Back Formation (banded quartzo-feldspathic gneiss with abundant micaceous layers) overlies the Ashe Formation (thinly-layered sulfidic biotite-muscovite gneiss interlayered with mica schist and minor amphibolite). These units also comprise the bedrock just southwest of the escarpment. The upland is bounded on the northwest by

the Cambrian clastic stratigraphy of the Valley and Ridge metamorphosed to greenschist facies, including the Chilhowie Group (Espenshade et al., 1975). The bedrock of the inner Piedmont is similar to the Blue Ridge. Crystalline bedrock of the province consists of the Smith River Allochthon (banded biotite-plagioclase-quartz gneiss, biotite-quartz schist, and granite), the Sauratown Mountains Window (biotite gneiss and quartzite), and the Charlotte Belt (fine-grained biotite-quartz-feldspar gneiss, quartz-muscovite schist, and fine-grained laminated amphibolite). Northeast-trending structures break this bedrock into distinct lithotectonic packages. The Bowens Creek/Brevard Fault System is among the most well known (Figure 2). It is worth noting that the juxtaposition of the Piedmont and Blue Ridge lithologies along the Brevard Fault Zone may have an important relationship to escarpment origin. Another system that could be related to the escarpment is the normal faulting that bounds the inner Piedmont on the east and makes the western limit of a Triassic-Jurassic sediment-filled rift valley (the Danville Basin) (Espenshade et al., 1975).

The 90-m DEMs illustrate the distinctiveness of the escarpment's ruggedness with respect to the adjacent, more gentle domains. The escarpment is clearly defined by steep slopes between the upland and Piedmont (Figure 9). These slopes are associated with an elevation drop of 400-500 m over a distance of ~2.5-3 km. Although average slope in the broad domain from just above the escarpment to the furthest limit of its spur ridges is only ~13° (Table 2), hillslopes are locally much steeper. Based on shorter wavelength, 30-m resolution DEMs, the average slopes along the narrow (~500 m-wide), upper portion of the escarpment are typically closer to ~24°. This is nearly as steep as slopes found in actively uplifting mountain ranges (e.g. Burbank et al., 1996; Blythe et al., 2000; Ahnert, 1970). It is clear the escarpment domain is a sharp boundary between two regions of much gentler topography. This is illustrated by the elevation distribution of each domain (Figure 10). The narrow elevation distribution of the upland and Piedmont indicates their low relief, in contrast to the broad range of elevation found on the steep escarpment.

The 90-m DEMs also quantify the topographic differences between the upland and Piedmont domains. Although the surfaces appear similar (Figure 2), the average upland slope is ~ 6° greater than the Piedmont (Table 2). Relief on the upland is also

four times greater than on the Piedmont. These differences in relief and slope, also evident on the slope map of the region (Figure 9), suggest the two sides of the asymmetric divide may have experienced different erosional processes or histories.

This basic topographic characterization is useful in defining the main geomorphic domains that comprise the region. Two similar, gently-rolling surfaces are separated by a much more rugged escarpment that rivals the topographic character of active mountain belts. Viewed in more detail, however, the two low-relief surfaces also differ in their topographic character. A more rigorous analysis is required to explore what these differences may mean in terms of geomorphic evolution.

2.4 Detailed Analyses

2.4.1 Topographic comparison of Upland and Piedmont surfaces

Broad scale examinations show similarity between the upland and Piedmont surfaces, although differences in ruggedness are apparent. These differences may reflect fundamental differences in the erosional history of each domain. Examining the topography and drainage basins of the two domains in more detail will allow a more thorough comparison and may illustrate differences in their landscape age or erosional intensity.

I examined the topography of these domains in two ways. First, I compare “pristine” subsets of the upland and Piedmont surfaces to test how similar they are and explore if they have experienced similar erosional histories. These subsets typically consist of interfluves along basin divides and are regarded as "pristine" because they lack incised valleys or monadnocks. These regions are the last to experience dissection and can be considered the most mature in a landscape; any differences between them may be the result of different erosional histories. For example, in one hypothesis for the origin of the Blue Ridge Escarpment, these upper and lower surfaces are the same “peneplain” but have been separated by recent faulting (Figure 5). Detailed subset analysis will help test the predictions of this hypothesis. The second approach focuses on individual drainage

basins. Drainage basins are a fundamental geomorphic unit (Leopold et al., 1964; Strahler, 1952). They alter the landscape in response to evolving boundary conditions and therefore are the key to understanding erosional processes. Because basins are the most basic unit in the landscape, the comparisons between them are valid and can provide clues to differences in erosional character and history.

These approaches require more detailed topographic data. The smaller area covered by the subsets permit the use of higher resolution (30 m) DEMs. These comparisons also require more sophisticated topographic parameterization. I employ a number of topographic statistics beyond relief and slope to gain a more detailed perspective of differences in the landscape.

2.4.1a Topographic subset comparison

To focus on topographic subsets, I selected square subsets from USGS 30-m DEMs. Five patches from the upland and six from the Piedmont were chosen which represent unincised, low-relief areas (Figure 11). In each 25 km^2 area, I calculated elevation, slope, and wavelength-dependent relief (at wavelengths of 5 km, 0.5 km, and 0.1 km). Elevation profiles across the subsets help to further characterize the topography represented by these parameters. Hypsometric elevation curves and the hypsometric integral were also calculated for each subset. The hypsometric integral is calculated as the area under the hypsometric curve (Strahler, 1952) and is approximated by the equation (Pike & Wilson, 1971):

$$HI = \frac{\text{(mean elevation. – minimum elevation)}}{\text{(maximum elevation – minimum elevation)}}$$

These parameters express the relative ruggedness of the subset domains.

The results show that the upland subsets are consistently more rugged (Figure 12). Upland relief is nearly double that of the Piedmont on all wavelengths. Average slope on the upland subsets (11.5°) is also greater than average slope in the Piedmont (9.2°). This difference in slope is consistent with the difference in short (0.1 km) wavelength relief. For example, over 0.1 km, a uniformly sloping surface of 9.2° yields a relief of ~16 m, whereas a slope of 11.5° over the same distance yields ~20 m. These are about the same

as the average short wavelength relief in the subsets (Figure 12). At longer wavelengths, the difference in relief is greater than that predicted by the difference in slope between the upland and Piedmont, indicating that the upland has both a more rugged topographic grain (i.e. hillslope roughness) as well as a broader ridge and valley structure. Elevation profiles across these subsets illustrate this as well (Figure 13). Profiles across the Piedmont interfluves show major high-frequency but minimal low-frequency elevation variation. In contrast, the upland is more irregular at long wavelengths and has a higher amplitude (i.e. relief) short-wavelength variations that translate to higher local slopes.

The hypsometric curves show similar variation between upland and lowland subsets. Upland hypsometric curves are generally lower than Piedmont curves (Figure 14). The upland curves represent a low-relief landscape with monadnocks; the few high peaks increase the entire elevation range of the selected region (Strahler, 1952). The Piedmont curves represent a similar, low-relief landscape and are similarly shaped, yet they are higher (i.e. higher average HI; Figure 12) because the total elevation range in the subsets is less. This may also represent the lack of large monadnocks or other positive relief forms on the Piedmont. The anomalously high curve for Box 9 of the upland is due to a single, relatively deep valley that breaks the otherwise low-relief surface. The opposite relationship is true for Box 1 of the Piedmont. This subset occurs along the Dan River near Danville, Virginia and lies mostly with the river's floodplain (Figure 11). Most of this subset occurs at relatively low elevation and only the edge overlaps a region of relatively high elevation, so that the curve is shifted upwards because the elevation range is expanded. Except for these outliers from each topographic domain, the hypsometric curves cluster into two groups, indicating the subsets within each domain are self-similar.

The topographic comparison of subsets reveal differences between the Piedmont and upland domains. The implications of these differences are discussed later in conjunction with other topographic analyses.

2.4.1b Drainage Basin Comparisons

To compare individual basins, I selected three drainage basins on the upland and three on the Piedmont. These basins range in area from >900 km^2 to <200 km^2 (Figure

11). None of the Piedmont basins rise at the Blue Ridge Escarpment, thus avoiding the effects of this more rugged domain. Drainage networks were extracted from 30-m DEMs and are shown in Figure 15a and Figure 15b. For each basin, I calculated hypsometry as well as several network parameters, including drainage density, magnitude density, and sinuosity. These parameters are defined in Table 3. Each should represent to some extent the degree of drainage network development and provide clues to the erosional intensity of each basin.

Basin area-altitude plots and associated hypsometric integrals cover a wide range of values. Average hypsometric integral for the upland basins is higher (Figure 16). However, individual basin values from the Piedmont overlap those of the upland, making it difficult to discern a consistent difference between upland and Piedmont basin hypsometry.

Results show consistent differences in drainage networks between the Piedmont and the upland. Piedmont basins possess a greater drainage density and magnitude density than upland basins despite having lower relief (Figure 17). The greater magnitude density of Piedmont basins represents a higher number of 1^{st} order streams per area and may be a function of the Piedmont's higher drainage density. This is because 1^{st} order streams comprise the majority of drainage networks and drain the greatest fraction of a basin's area, and therefore have the largest influence on these parameters. To test whether the Piedmont basins contain a higher concentration of 1^{st} order streams (relative to higher order streams) than the upland, I also calculated length ratio and stream number ratio (Figure 17, Table 3). The average Piedmont values are only slightly different than for the upland and there is considerable overlap between individual basins. The Piedmont therefore does not contain an unusual concentration of 1^{st} order streams, while its higher number of 1^{st} order streams is a function of its higher drainage density.

Bifurcation ratios are another statistical representation of basin integration (Table 3) and are slightly higher for Piedmont basins (Figure 17). The ratios were carried out to 5^{th} order streams so that different size basins could be compared. A high bifurcation ratio indicates that a basin contains a higher proportion of streams that do not unite to produce higher order channels. This could indicate a more complex network along the Piedmont, but the considerable difference and overlap among all basins makes this a weak

conclusion. The sinuosity Piedmont streams is also distinct. Although sinuosity is basically identical among the upland and Piedmont streams lower than 4th order, upland basins are significantly more sinuous at higher orders (Figure 18). Two Piedmont basins actually experience a decrease in sinuosity at the highest order, although this may be related to structural control (Figure 11, 18). These differences may have important implications for inferred landscape age, as discussed below.

2.4.2 Topographic characterization of the escarpment zone

One of the critical predictions of each hypothesis for the origin of the Blue Ridge Escarpment is the occurrence of large or small amounts of migration of the escarpment through time (Figures 3-8). To test whether the topography of the escarpment domain is consistent with long-term migration, I examined how topographic parameters change with position along the inner Piedmont going away from the escarpment.

The first approach was to examine variations in ruggedness along transects normal to the escarpment. Two profiles were pieced together from 14 overlapping, 5 km x 5 km, 30-m DEM subsets (for location, Figure 11; for method, Figure 19). For each box, the total relief, average slope and hypsometric integral were calculated and plotted with respect to distance from the escarpment (Figure 20). Second, drainage density and magnitude density were calculated along the longest channel in drainage basins with headwaters at the escarpment. The Roaring River, the Fisher River, and the Ararat River, all tributaries of the Yadkin River in North Carolina, were selected (Figure 21). Parameters were calculated in ~0.7 km increments, beginning at the headwaters and continuing to the Yadkin River. Each point represents the cumulative effect of the entire upstream area. Plotted against total channel length, these two parameters show how each drainage basin changes with distance from the escarpment (Figure 22).

The transect of boxes shows the concentration of rugged topography at the escarpment (Figure 20). Each profile shows average slope and total relief peaking within a narrow zone, and hypsometric integral peaking on the upland, just above the escarpment. With increasing distance from the escarpment, however, these parameters gradually decrease. Slight variations from this steady decay are due to the presence of small hills and interfluves encountered near the base of the escarpment. Interestingly, the

distance required for these values to attain the nominal values of the Piedmont is greater than the apparent width of the escarpment (Figures 11, 12, 20). This may indicate a transitional zone between the escarpment and the Piedmont. In addition, the Brevard fault zone appears to have no consistent effect on any of the values.

The drainage basin transects show a general increase in both magnitude density and drainage density with downstream distance (Figure 22). Significant fluctuations occur in the first 15-18 km of each profile, where the total basin area is still relatively small and thus the average parameters are very sensitive to the addition of tributary basins. This is somewhat of a surprise, however, as one would expect all headwater basins that rise along the escarpment to exhibit a greater similarity. The oscillations stop at nearly the same downstream distance from each basin's headwaters, regardless of basin area, location, or nearby scarp morphology. For example, the Ararat River basin is located where the escarpment is sharp, yet its basin parameters settle into a discernable trend at nearly same position as in the Roaring River basin along the wide southern escarpment zone (Figures 11, 22). Only isolated deviations occur further downstream where major tributaries join the main channel. Once these fluctuations cease, magnitude density and drainage density increase steadily away from escarpment. These values do not reach the nominal Piedmont averages observed in basins 1-3 (Figures 11, 17). This is at least partly due to the effect of the escarpment zone is cumulatively integrated into the basin-wide averages. Unfortunately, it is difficult to separate out this cumulative signal. Despite differences in basin geometry and basin area, the three basin curves require nearly identical distances before attaining a constant value.

2.5 Discussion

Topography records the sum of erosional processes that have acted upon a landscape over time. Topographic parameters can be used to make inferences about the relative distribution of erosion between Piedmont, upland, and escarpment domains. Using previously established relationships between topographic parameters and erosion rates, I infer the relative landscape age and the magnitude of denudation for each domain and, where possible, the amount of divide migration that may have occurred. These

inferences can then be compared to the predictions made by the hypotheses for the origin of the Blue Ridge Escarpment.

2.5.1 Topographic subsets

The small topographic subsets were chosen to represent the lowest relief surfaces along the interfluves of the upland and Piedmont. These surfaces best represent what were considered peneplains in previous studies (e.g. Davis, 1903; Johnson, 1933). By comparing their topography, we test whether these visually-similar surfaces are essentially the same or topographically dissimilar. We can also explore what any differences might imply about relative erosion kinematics. Topographic ruggedness (i.e. average slope, relief) and elevation distribution (i.e. hypsometry) generally reflect the erosional intensity and topographic maturity of a landscape and are thus useful for contrasting the magnitude of denudation or landscape age of the upland and Piedmont. These may thus provide clues about the origin the escarpment.

Relief and slope exhibit the most consistent relationship with aspects of landscape evolution. Numerous studies have found a positive correlation between relief and denudation rate (e.g. Schumm, 1963; Ahnert, 1970), relief and structural rock uplift (e.g. Hurtrez et al., 1999), and slope and long-term exhumation rates (Burbank et al., 1996; Blythe et al., 2000; Spotila et al., in press). Theoretical erosion laws also show a positive correlation between rates of individual erosional processes and slope. Diffusive hillslope erosion (e.g. Gilbert, 1909; Culling, 1960; Roering et al., 2001), fluvial sediment transport (Gilbert, 1914), bedrock incision (e.g. Whipple and Tucker, 1999), and glacial erosion (e.g. Paterson, 1981) all increase with slope. Relief is also affected by other factors such as lithologic resistance or climate, and can thus be used only as a general proxy for erosion rate when other influences are accounted for.

Because relief and slope are greater on the upland, we infer that erosion rates are greater there than on the Piedmont. Greater slope may mean that fluvial and hillslope processes are more active on the upland, if lithologic and climatic influences are ignored. Higher relief at all wavelengths also shows that erosional intensity is likely greater on the upland. Note that the greater relief at long lengthscales may also represent another aspect of topographic development. It has noted that the correlation between relief and uplift

(erosion) rate is weak at lengthscales greater than 0.6 km (Hurtrez et al., 1999). The higher relief at long wavelengths on the upland may thus represent structural controls. This may imply the upland has experienced recent rejuvenation (incision) and thus has a younger landscape age relative to the Piedmont. Conversely, the greater elevation difference between resistant and non-resistant lithologies may mean that the upland has undergone a longer period of differential erosion, giving it an older landscape age. The difference between these lies in whether the excess relief is due to incised canyons or positive relief forms associated with etchplanation. Examination of other topographic parameters is required before relative landscape age can be inferred.

Hypsometry has been used as a proxy for landscape age and may provide clues to the magnitude of denudation. Strahler (1952) inferred a relationship between the shape of area-altitude plots and basin maturity. Youthful or rejuvenated landscapes exhibit a high, convex curve while mature areas possess more sweeping, S-shaped curves. The monadnock, or peneplain stage, is represented by a low, concave profile. Hypsometric integral has also been tied to erosion rate. Empirical studies have found that basins with high erosion rates often possess high hypsometric integrals (Ohmori, 1993; Hurtrez et al., 1999a). Landscape evolution models have also predicted a positive correlation between hypsometric integral and erosion rate (e.g. Lifton and Chase, 1992). However, applying hypsometry to interpreting erosional kinematics requires caution. Scale dependence, the competition of hillslope and fluvial processes, and influence of rock resistance (e.g. Hurtrez et al., 1999; Willgoose and Hancock, 1998; Strahler, 1952; Lifton and Chase, 1992) affect hypsometry and may cause deviations from the general relationship. For example, Strahler (1952) found that smaller basins, where hillslope processes are more important, exhibited an inverse relationship between hypsometric integral and relief (a proxy for erosion rate). A similar inverse relationship was found between hypsometric integral and uplift rates in square topographic boxes in the San Gabriel Mountains in southern California (Lifton and Chase, 1992), although this correlation arises partly from an unintentional bias due to the selection of subsets that included portions of very low-relief alluvial surfaces.

Hypsometric curves from both upland and Piedmont subsets would be classified as mature or monadnock type using the framework put forth by Strahler (1952). These

curves and the associated hypsometric integrals also show consistent differences, clustering in two groups by domain. Using the interpretation of Strahler (1952), the subsets of the Piedmont are less mature and possess a higher erosion rate than their upland counterparts. These subsets, however, do not encompass complete basins. Situated in interfluve areas, the subsets only represent the lowest-relief, most stable portions of each domain. These results might not be directly comparable to those from moderately-sized drainage basins, as used by Strahler (1952), Hurtrez et al. (1999a), and others. Because hypsometry from these square subsets may not relate to maturity, it is better use the results to compare similar landscape position by domain. For example, the high hypsometric integrals and curves from the Piedmont indicate that at the interfluves, the land primarily consists of rolling hilltops, broken only occasionally by weakly-incised channels. In contrast, hypsometric integrals are lower in the more rugged interfluve areas of the upland, because the total elevation range is greater due to more deeply incised streams and because of isolated hills that stand higher than the adjacent interfluves.

Although hypsometry cannot be used as a direct proxy for erosion rate or landscape age, it has importance for the erosional kinematics of the two domains. This relationship is conveyed in the consistent variations between the upland and Piedmont. With few exceptions, the hypsometric curves of each domain cluster together, implying that the erosional history experienced by the interfluves of each has been self-similar but distinct with respect to one another. Hypsometry brings out distinctions between these two visually-similar surfaces, implying that the upland and Piedmont do not make up a formerly continuous erosional surface, as argued by several of the hypotheses for the origin of the escarpment. This would only be possible if significant erosional modification took place subsequent to their separation.

2.5.2 Basins

The basins selected to represent the drainage evolution of each domain show marked differences in both topographic expression and drainage network parameterization. These differences may have importance for the interpretation of erosional history in each domain. As stated above, denudation magnitude and rates have are linked to relief and hypsometry. In addition to these parameters, drainage density,

which is correlated with a number of controls (including uplift, precipitation, lithology, and time), sinuosity, which is linked to stream discharge and sediment load, and bifurcation ratios, which may indicate the degree of basin integration, are considered. By comparing basin parameters from the upland and Piedmont with relationships found in other studies, I hope to find clues to the development of these domains with respect to time.

Basin relief is strongly related to regional topography. Unlike the topographic subsets, we cannot filter out the areas of anomalously high relief from intact basins. These positive relief features increase the elevation range considerably, although they contribute little area to the basin. Basin relief is useful, however, in demonstrating the uniqueness of the upland and Piedmont domains. The strong grouping of relief values (i.e. all upland basins are higher relief than Piedmont basins) hints that the upland basins are eroding more quickly and that the basins of each domains have experienced different erosional histories. Because basin relief may be strongly affected by geologic structure, however, it is of limited value for interpreting landscape evolution.

Hypsometry differs much less systematically among upland and Piedmont basins than for the square topographic subsets. However, reliable comparisons with established relationships between hypsometry and erosion rate or maturity require basinal area-altitude distribution. Analysis of basin hypsometry may thus be useful. As with the topographic subsets, the hypsometric curves from all six basins are equivalent to Strahler's (1952) mature or graded designations. The range of hypsometric integrals (.26 to .56) from the six basins also correspond to values from mature basins. Unlike the subsets, however, hypsometric curves are generally higher in the upland basins. This may indicate that the upland basins are less mature and have younger landscape ages than the Piedmont basins. This interpretation is consistent with Strahler (1952), field observations of Schumm (1956), and with the topographic evolution found in channel network growth models (Willgoose et al., 1991a/b). Higher upland integrals may also indicate higher erosional intensity. This interpretation is based on the positive correlation between uplift/erosion rate and hypsometry found in field studies (e.g. Ohmori, 1993; Hurtrez et al., 1999a) and in landscape evolution models (e.g. Lifton and Chase, 1992).

However, these interpretations are weakened by complications concerning the meaning of hypsometry. For example, hypsometry may be scale dependent. Hurtrez et al. (1999b) found an empirical relationship between drainage area and hypsometry that was consistent with results from a precipitation-erosion model and associated physical experiments. Differently shaped hypsometric curves were produced simply by changing basin size or geometry. This dependence is caused by the relative importance of hillslope processes (resulting in high, convex hypsometric curves) and fluvial processes (resulting in S-shaped or concave curves) (Hurtrez et al., 1999b). Smaller basins typically have higher curves because hillslope processes play a much greater role in their topographic evolution. Because the selected drainage basins on the upland and Piedmont are roughly similar in size, competition between hillslope and fluvial processes may not be a big factor in controlling curve shape. For example, Basins 1 and 6 are somewhat larger than the others, yet their hypsometric curves are not significantly different from the rest (Figures 15b, 16). However, basin shape could be important. Basins 4 and 5 are significantly more elongate than the rest and display curves that are somewhat lower than the third upland basin (Basin 6). Elongate basin geometries are sometimes associated with low, "monadnock" type curves (Hurtrez et al., 1999b). Another complication may be lithologic contrasts. Although bedrock of similar lithology is found in all six basins, it is unclear how subtle differences in resistance may affect hypsometry (Strahler, 1952; Lifton and chase, 1992). Due to these apparent complications and the overlap between the hypsometric curves of the upland and Piedmont basins, it seems that solid conclusions concerning the relative erosion rates and topographic maturity or landscape age of these basins cannot be reached. At best, I can only speculate that the upland basins experience a higher erosional intensity and are less mature or more recently rejuvenated than their Piedmont counterparts.

Aspects of basin network geometry may also be important. Drainage density is consistently higher for Piedmont basins. Because drainage density is affected by numerous variables, however, it is difficult to conclude what it means in terms of geomorphic history. A discussion concerning possible relationships between drainage density and erosion rate, erosional process type (i.e. diffusive hillslope versus fluvial), relief and slope, climate, lithology, and time is warranted.

There is indication that drainage density may be positively correlated with relief and erosion rate (e.g. Oguchi, 1997). For example, flume studies (e.g. Mosley, 1972; Schumm, 1987) and an empirical study of badland topography in small (<1 km^2) basins (Schumm, 1956) revealed an association between drainage density and erosion rate. Rinaldo et al. (1995) found a correlation between drainage density and erosion rate based on landscape evolution models. Willgoose et al. (1991b) used changes in basin relief to create variations in erosion rate on channel network development models and found that drops in base-level resulted in incision and headward growth of channels. Thus, increasing erosion rates lead to increases in drainage density. These empirical and modeling studies, however, represent only specialized cases. A universal correlation between drainage density and erosional intensity has yet to be established. For example, Hurtrez et al. (1999a) showed no correlation between drainage density and erosion rate in 17 rapidly uplifting basins in the Siwalik Hills, Nepal. Other indications show that drainage density may be most heavily influenced by competition between erosional processes.

Drainage density is linked to the relative proportion of a basin dominated by diffusive hillslope erosion (i.e. no channels) rather than fluvial transport. For example, the landscape evolution model of Tucker and Slingerland (1997) showed that drainage density increases when hillslopes become channelized and a shift is made from hillslope processes to fluvial processes. In contrast, when relief is increased, diffusive hillslope processes dominate a larger proportion of basin area, limiting channelization and thereby decreasing drainage density. Tucker and Bras (1998) investigated threshold-driven hillslope processes and their effect on drainage density. For example, where landslides dominate there is a negative correlation between drainage density and relief. Similarly, a negative relationship between drainage density and relief is found where saturated overland flow controls hillslope processes. Areas where these hillslope processes are dominant are commonly found in particular climates and possess a certain substrate character. Thus, climate has an influence on drainage density. In humid, vegetated regions with thick soils (i.e. high soil transmissivity), diffusive hillslope transport will be important and may increase with relief, resulting in a negative correlation between relief and drainage density (Chorley, 1957; Carlston, 1963; Kirkby, 1987; Tucker and Bras,

1998). In this case, the role of vegetation is intuitive. Dependent upon climate, vegetation can shield soil and rock from erosion and helps to increase soil production rates. In arid regions, however, there is less vegetation and thinner soil, making diffusive transport unimportant. In these regions, higher relief equates to higher fluvial transport power, increasing drainage density (Chorley, 1957; Gregory and Gardner, 1975; Moglen et al., 1998). In other studies, Kirkby (1987) suggested that drainage density is independent of relief in arid areas, while Melton (1958) thought that drainage density increased with total precipitation in all circumstances.

Other influences on drainage density include lithology and time. Strahler (1957) pointed out that, where tectonic uplift rates are uniform, areas of less resistant rock will have higher drainage densities because channelization occurs easier. This can be seen in locations underlain by shale, where drainage pattern is more dissected and a greater abundance of blind hollows exists than in areas underlain by sandstone. Time can also play a role in drainage development. Through time, overland flow integrates into channels, thereby increasing total channel length per area through headward growth (Horton, 1945). Modeling has also demonstrated that drainage density increases as basins evolve (e.g. Willgoose et al., 1991b). Drainage density increases linearly at first, but drainage growth rate decays as source areas become smaller (i.e. headwater regions become fully channelized), eventually reaching an ultimate value. Drainage growth declines and halts because hillslope processes can keep pace with channel initiation at the channel source areas (i.e. the interfluves).

Because the southern Appalachians are humid and well-vegetated and because both the upland and Piedmont have thick soil cover (Dietrich, 1959), the above reasoning predicts that drainage density should decrease with relief. Fluvial processes may play a greater role in the erosion of the lower relief Piedmont, thus explaining its higher drainage density. Similarly, the higher slopes of the upland may be more conducive to diffusive processes such as creep. The effect of erosional process and its relationship with relief may thus be responsible for observed drainage density variations, rather than differences in erosion rate and landscape age. However, other important factors may be a difference in the erosivity of upland and Piedmont climate. Intense precipitation is often brought to the Piedmont by hurricanes and tropical storms. These systems often stall

against the Appalachians and inundate regions adjacent to the Blue Ridge, as happened in Nelson and Madison Counties when Hurricane Camille moved north through Virginia in 1969, locally dropping ~30" of rain (Whittecar and Duffy, 1992). This more intense precipitation could be partly responsible for higher drainage density in the Piedmont.

Several other drainage parameters are closely linked to drainage density. For example, magnitude density follows the same pattern as drainage density and is strongly controlled by the number of 1st order streams. I therefore consider these indexes to convey the same information. Stream number ratio and length ratio of upland and Piedmont basins are nearly indistinguishable. Like magnitude density, both are strongly controlled by the number and length of 1st order streams. Because upland and Piedmont values are so similar, I infer that the influence of 1st order streams on other measurements (e.g. drainage density) are nearly identical.

Bifurcation ratios are also used to quantify stream network integration, which may have important implications for basin maturity and relative age. In general, there is a geometric relationship between the quantity of streams in one stream order and the quantity of streams in the next higher order (Horton, 1945). This type of relationship is also found in stream length and basin area; thus, bifurcation ratios follow the pattern of drainage density. Any deviation from this relationship may indicate that recent adjustment has taken place. For example, an increase in relief (due to rejuvenation or uplift) will result in the growth of new 1st order streams and an increase in bifurcation ratio. Using rainfall events as a proxy for time, Parker (1977) showed that bifurcation ratios, after an initial period of instability, increased with time. Network growth modeling has shown a similar relationship between time and bifurcation ratio (Willgoose, 1991b). Other studies, however, have shown some doubt about the utility of bifurcation ratios. Strahler (1957; 1952) argued that bifurcation ratio is controlled by process and is generally a constant for any fluvial network. Kirchner (1993) argued that any random basin geometry could also produce significant variations in bifurcation ratio that could be misinterpreted to represent maturity.

Bifurcation ratios thus provide only minor insight into the differences in landscape age between the upland and Piedmont basins. The higher Piedmont ratios indicate the basins have more low order streams that do not combine to form higher order

channels. Using the lines of reason described above, this may indicate that greater time (and thus greater opportunity) for 1st order channel initiation has occurred. More likely, however, it represents a lower threshold for channel head initiation than is present in upland basins, perhaps the result of climate or differences in erodibility. Overall, bifurcation ratio is not necessarily a good indicator of maturity or landscape age.

A final parameter that may help to highlight the differences in erosional kinematics between the upland and Piedmont is stream sinuosity. Although low-order streams in both domains possess similar sinuosity, the upland basins contain much more sinuous higher-order streams. Two lines of thought determine what the significance of this difference. Generally, sinuosity is simply regarded as a function of topography. In this case, the difference in sinuosity is due to the differences between upland and Piedmont topography. Another idea is that upland meandering is a feature of relict drainage patterns. Because meanders tend to develop in streams that are at or near grade and not incising, this difference could indicate that a shorter period of time has passed since Piedmont streams have stabilized or become graded. With more time, these streams may begin to develop greater sinuosity. This is consistent with a younger landscape age for the inner Piedmont. On the upland, the meandering stream courses are entrenched. This indicates that, although they were once graded, stream conditions have changed and incision has resulted. Implications for these possibly relict meanders are explored in more detail in Chapter 3.

2.5.3 Topographic Transects

Comparison of the Blue Ridge upland and Piedmont has hinted that each geomorphic domain has developed differently. Examination of the topographic changes across the escarpment itself may add further clues to its origin. The box and incremental drainage transects show important variations in several topographic parameters at and away from the escarpment. These results are discussed in light of the understanding of what parameters mean as developed in the previous section. Interesting results arise from each of these exercises.

Relief and slope peak along the box profiles where the escarpment is crossed (Figure 20). These parameters share positive correlations with erosion rate (Hurtrez et al,

1999; Ahnert, 1970; Ohmori, 1993), indicating that erosion is most intense at the escarpment. This is not only intuitive but also consistent with Hack's (1973) assessment of stream-gradient index in the region, which showed a locus of high values on the escarpment. Hypsometric integrals also peak at the escarpment, showing a positive correlation with relief. This could indicate higher erosional intensity at the escarpment (Ohmori, 1993; Hurtrez et al., 1999a). Hypsometry may also have implications for landscape and basin maturity, as discussed above. The high hypsometric integrals at the escarpment are consistent with it being an immature or youthful landform, using the interpretations of Strahler (1952). However, the link between hypsometry and maturity is a tenuous one and may be a factor of landscape position. In both box profiles, the hypsometric integral may be high where the subset is dominated by a hilltop and low in the adjacent valleys. Perhaps most important in the box profiles is the distance over which slope and relief values, and, to a lesser extent, hypsometric integral, decay with increasing distance from the escarpment. The escarpment is quite sharp (< 3 km wide) where these profiles cross, yet it requires 10-25 km for values to settle into the Piedmont average (Figure 19). This is consistent with the idea that the escarpment represents an area of concentrated erosional intensity that has migrated to the west like a wave, leaving behind transitional topography that has not yet settled into the typical character found elsewhere in the Piedmont.

Similar interpretations can be made from the drainage basin transects. Drainage density and magnitude density follow similar patterns and are both extremely low at the escarpment. This is consistent with the idea that the escarpment is eroding more effectively via saturated overland flow or landslides rather than fluvial processes. This is expected in high-relief topography in humid, vegetated regions (Chorley, 1957; Carlston, 1963; Kirkby, 1987; Tucker and Bras, 1998). In each of the profiles, there is also a zone of fluctuation in both drainage density and magnitude density out to ~15 km from the divide. This zone represents the transitional area between a landscape dominated by hillslope processes to one governed by fluvial processes. This matches the observation from the box transects that the innermost Piedmont consists of transitional topography that may denote escarpment retreat. Note, however, that drainage density and magnitude density are cumulative along the channel course (i.e., each data point is calculated from

the total channel length and area upstream of it). The low values at the escarpment may thus dilute the typical Piedmont values for some distance, leading to an exaggeration of the width of the transition zone.

2.6 Summary

Topographic analyses provide some clues for interpreting the geomorphic history of the upland, Piedmont, and Blue Ridge Escarpment. Comparison of the upland and Piedmont domains, which share similar gentle topography characteristic of "erosional surfaces" or "peneplains," reveals important distinctions that suggest somewhat different erosional kinematics. Topographic subsets and basins are more similar within each domain than they are between domains, indicating either independent geomorphic evolution or that a significant amount of time has passed (allowing for modification) since they were connected. Higher relief, slope, and basin-wide hypsometric integral indicate that modern erosional intensity should be greater along the upland. At the same time, the sinuosity of high order streams and the greater long-wavelength relief, which is due to the greater erosion of geologic structures, suggest that the upland has a greater landscape age. However, based on the degree of stream incision, there may have been some amount of rejuvenation of the upland landscape. If the upland does have an older landscape age, it seems that signs of this will not last much longer. Greater relief, steeper hillslopes, and recent incision indicate the upland is increasingly being eroded. Conversely, topographic parameters from the Piedmont suggest it is a young landscape currently experiencing little erosion. However, hints exist, such as isolated monadnocks, that indicate the Piedmont once possessed a much more varied topography and that it has since been reduced to the form it now is.

In contrast, the differences between other topographic parameters probably represent different processes and their functional response to boundary conditions in the upland and Piedmont. For example, drainage density and bifurcation ratios may be higher in Piedmont basins due to lower relief, greater importance of fluvial processes, or perhaps greater climate erosivity. Any combination of these factors may lower the threshold for channel initiation on the Piedmont. Because such complex relationships exist, it is important to use caution when using these parameters to make interpretations.

The topographic transects across the escarpment suggest that a transition zone exists along the innermost Piedmont. The decay in slope, hypsometric integral, drainage density, and magnitude density away from the escarpment represent a transition from hillslope processes to fluvial processes. Because this shift takes place over a distance greater than the escarpment zone itself, it may indicate that a northwest-propagating wave of erosion passed as the escarpment retreated. This represents migration of the asymmetric divide, which is predicted by several of the hypotheses.

Based on these results, the field of hypotheses on the origin of the escarpment can be narrowed. Models that require the upland and Piedmont to have developed as one surface that was later separated (e.g. recent faulting; Figure 6) are not favorable. Models in which the Piedmont and upland share the same erosional and exhumational intensity (e.g. local geodynamic uplift; Figure 4) or in which the Piedmont erodes much more rapidly than the upland (e.g. lithologic differences; Figure 3) are also less favorable. In addition, the lack of effect on topographic transects across the escarpment by the Brevard fault zone discourages origins due to near-field faulting (e.g., Figure 6) as well as lithologic differences (e.g., Figure 3), given that the Brevard is the primary lithologic contact in the vicinity. The models which predict escarpment migration and differences in landscape age between the upland and Piedmont appear more likely. A plausible scenario is one in which intense erosion at the escarpment results in divide (and escarpment) migration to the northwest. Areas in the Piedmont recently passed by this wave of erosion are left with few topographic features and young landscape ages. The Blue Ridge upland, with an older landscape age, is being gradually reduced by the erosional wave

However, since the meaning of topographic parameters can be ambiguous, the inferences for erosional kinematics and the origin of the escarpment are speculative. Many parameters are related in a complex way to erosional process and can be positively or negatively correlated to one another or to erosional kinematics of a landscape, depending on independent variables (e.g. climate). Answering the questions of relative landscape age, the effect of basin maturity, erosional intensity, or denudational magnitude is thus difficult at best.

Topography cannot provide information enough to fully interpret the evolution of the region containing the Blue Ridge Escarpment even when the latest data and tools are used. This fact makes older interpretations of the region more impressive since workers lacked many of tools we have today. It also makes the older interpretations more suspect. While topographic analysis provides some clues to the origin of the escarpment, other techniques are required before any conclusions are drawn.

Chapter 2 – Figure and Table Captions

Figure Captions

Figure 9 - Slope map of study region, created from USGS 30-m DEMs using Microdem. The scale at lower left is in degree. The red outline indicates region of upland sampled for Table 1 and Figure 10.

Figure 10 – Elevation distribution of upland, Piedmont, and north and south escarpment zones, created from USGS 90-m DEMs using Microdem. Concentration represents the number of cells. Elevation is in meters.

Figure 11 – Location map for topographic subsets, drainage basin comparisons, topographic box profile transects, and river transect basins. Base map was created from 90-m DEMs using Rivertools 2.0. Elevations are represented in a color scheme from dark green (~200 m) to red (~1500 m).

Figure 12 – Plot of topographic parameters for upland and Piedmont subsets, extracted by Microdem using USGS 30-m resolution DEMs. Average domain values are in bold. Refer to Table 3 for parameter definitions.

Figure 13 – Topographic profiles and profile locations, created from USGS 30- DEMs using Microdem. Note the choppier, lower-relief topography of the Piedmont.

Figure 14 - Hypsometric curves of the topographic subsets, extracted from 30-m DEMs using Microdem. Note the general clustering by domain.

Figure 15a – Piedmont drainage basins, created using RiverTools. Elevation is represented by a color scheme in which green covers the lowest elevations and red the highest elevations. Actual elevation range is different for each drainage basin, as well as in Figure 11. Refer to Figure 11 for locations, Figure 17 for basin relief.

Figure 15b – Upland drainage basins, created using RiverTools. Elevation is represented by a color scheme in which green covers the lowest elevations and red the highest elevations. Actual elevation range is different for each drainage basin, as well as in Figure 11. Refer to Figure 11 for locations, Figure 17 for basin relief.

Figure 16 – Hypsometric curves from three upland and three Piedmont basins. Hypsometric integrals for each basin are shown in upper right. Created from USGS 30-m DEMs using Microdem.

Figure 17 – Plot of topographic parameters for upland and Piedmont basins. Extracted from 30-m DEMs using RiverTools.

Figure 18 – Sinuosity for all streams in upland and Piedmont basins. Extracted from 30-m DEMs using RiverTools. Note that upland basins are consistently more sinuous than Piedmont basins among the 6^{th} to 8^{th} order streams.

Figure 19 – Example and location of topographic box transects. Each 25 km^2 subset is centered at the junction of the previous and subsequent subset box. Relief, Slope, and HI are measured over each box. Created from 30-m DEMs using Microdem. Elevation scale is in meters.

Figure 20 – Plots of topographic box transect parameters Extracted using Microdem. Locations of transects are shown in Figure 11.

Figure 21 – Piedmont basins bounding the Blue Ridge Escarpment, used to compare basin drainage density and magnitude density along main channels draining the escarpment. Elevation scale as in Figure 15. Locations are shown in Figure 11. Created using RiverTools.

Figure 22 – Plots of drainage density and magnitude density from incremental basin transect. Note the fluctuations over the first ~15 km of each transect. This plot is cumulative from headwaters (left) to trunk stream (right).

Table Captions

Table 2 – General topographic values for upland, Piedmont, and north and south escarpment zones. Extracted from USGS 90-m DEMs. "Average Relief" values are visually extracted from a relief map calculated from 90-m DEMs and thus represent the highest values of relief over ~100 m.

Table 3 – Drainage basin parameter list with definitions.

Figure 9

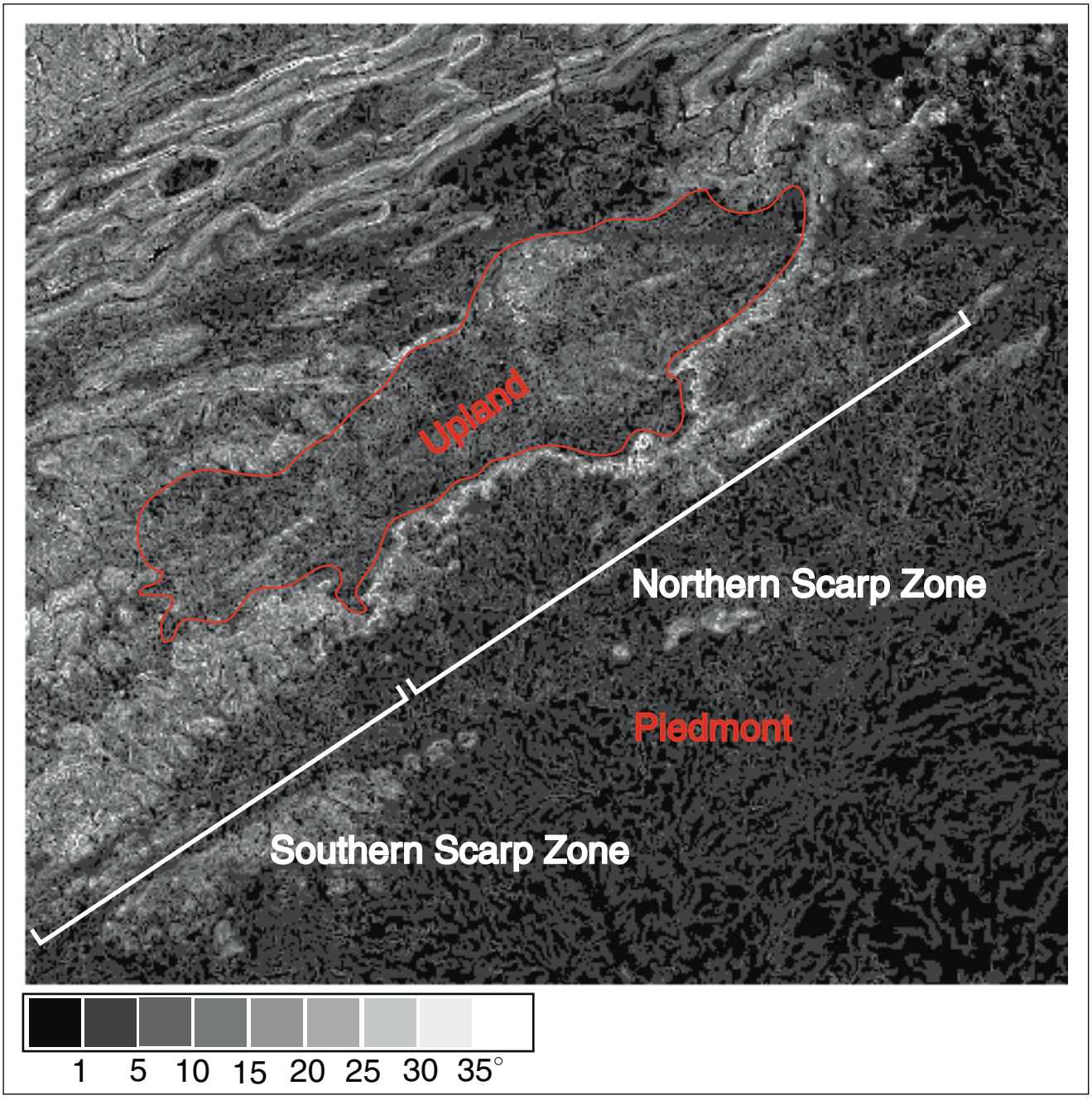
Upland
Northern Scarp Zone
Piedmont
Southern Scarp Zone
1 5 10 15 20 25 30 35°

Figure 10

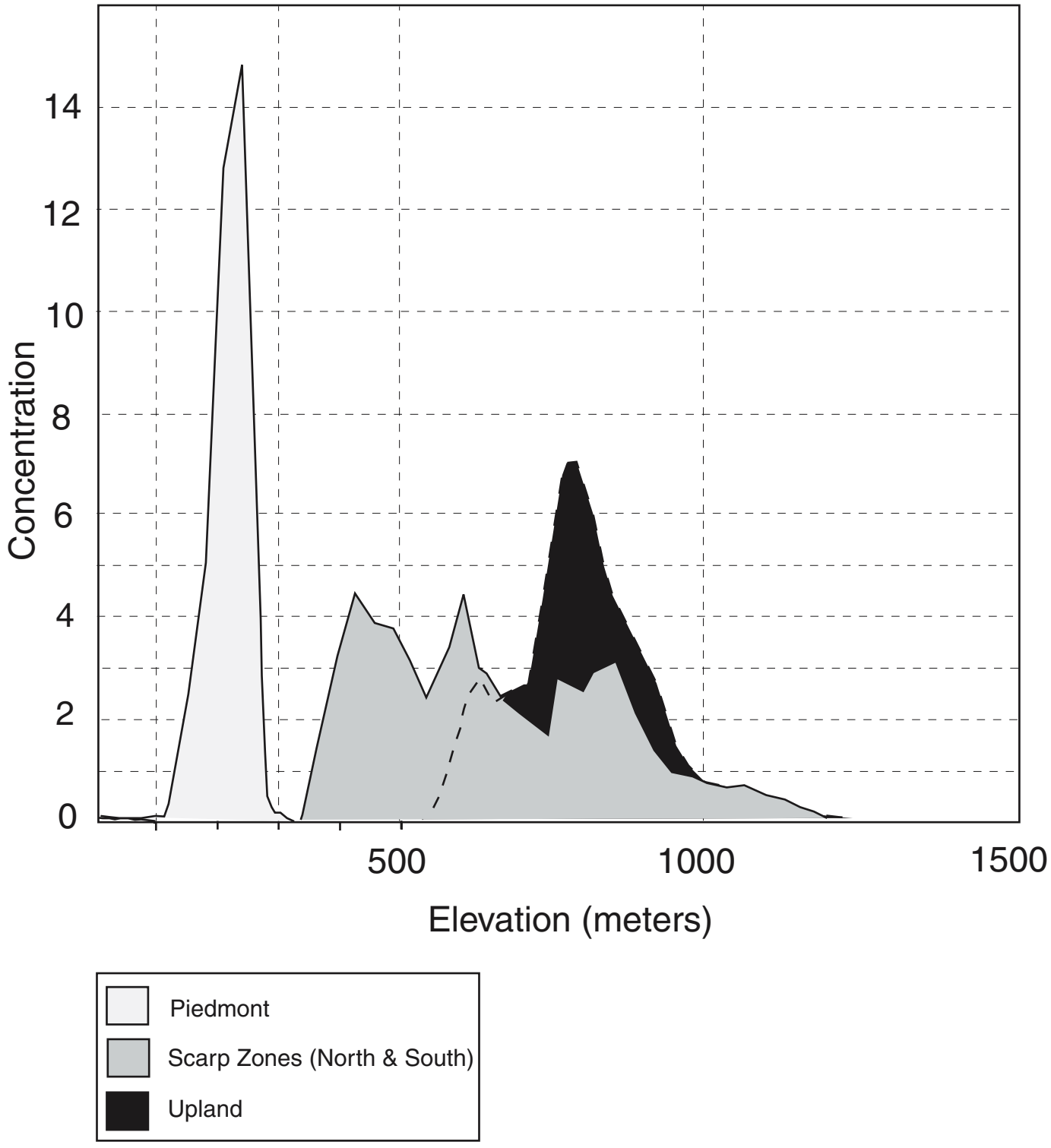
14
12
10
8
6
4
2
0
Concentration
500
1000
1500
Elevation (meters)
Piedmont
Scarp Zones (North & South)
Upland

Figure 11

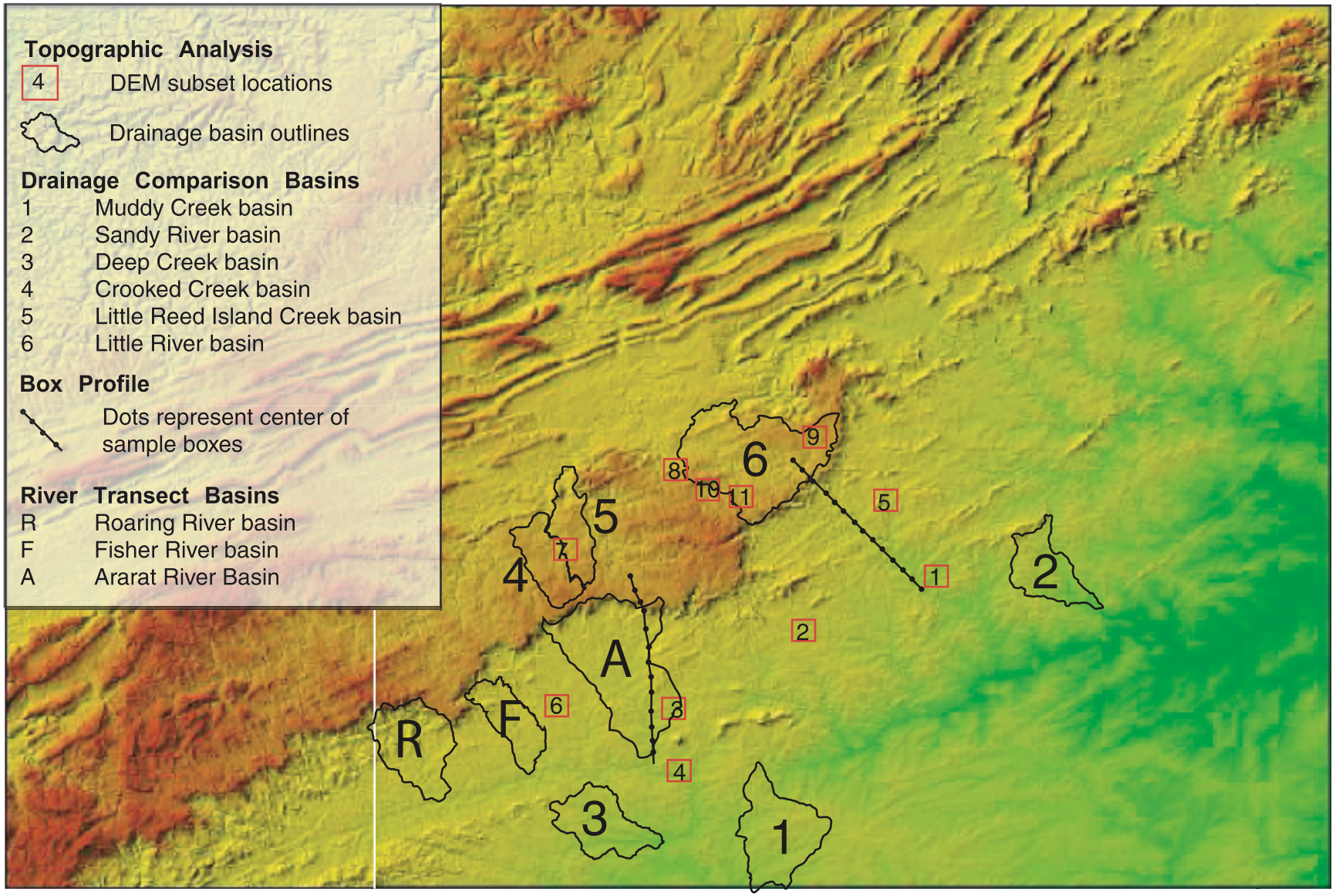
Topographic Analysis
4 DEM subset locations
Drainage basin outlines
Drainage Comparison Basins
1 Muddy Creek basin
2 Sandy River basin
3 Deep Creek basin
4 Crooked Creek basin
5 Little Reed Island Creek basin
6 Little River basin
Box Profile
Dots represent center of sample boxes
River Transect Basins
R Roaring River basin
F Fisher River basin
A Ararat River Basin
6
5
4
A
R
F
3
1
2
9
8
10
11
7
5
1
2
6
3
4

Figure 12

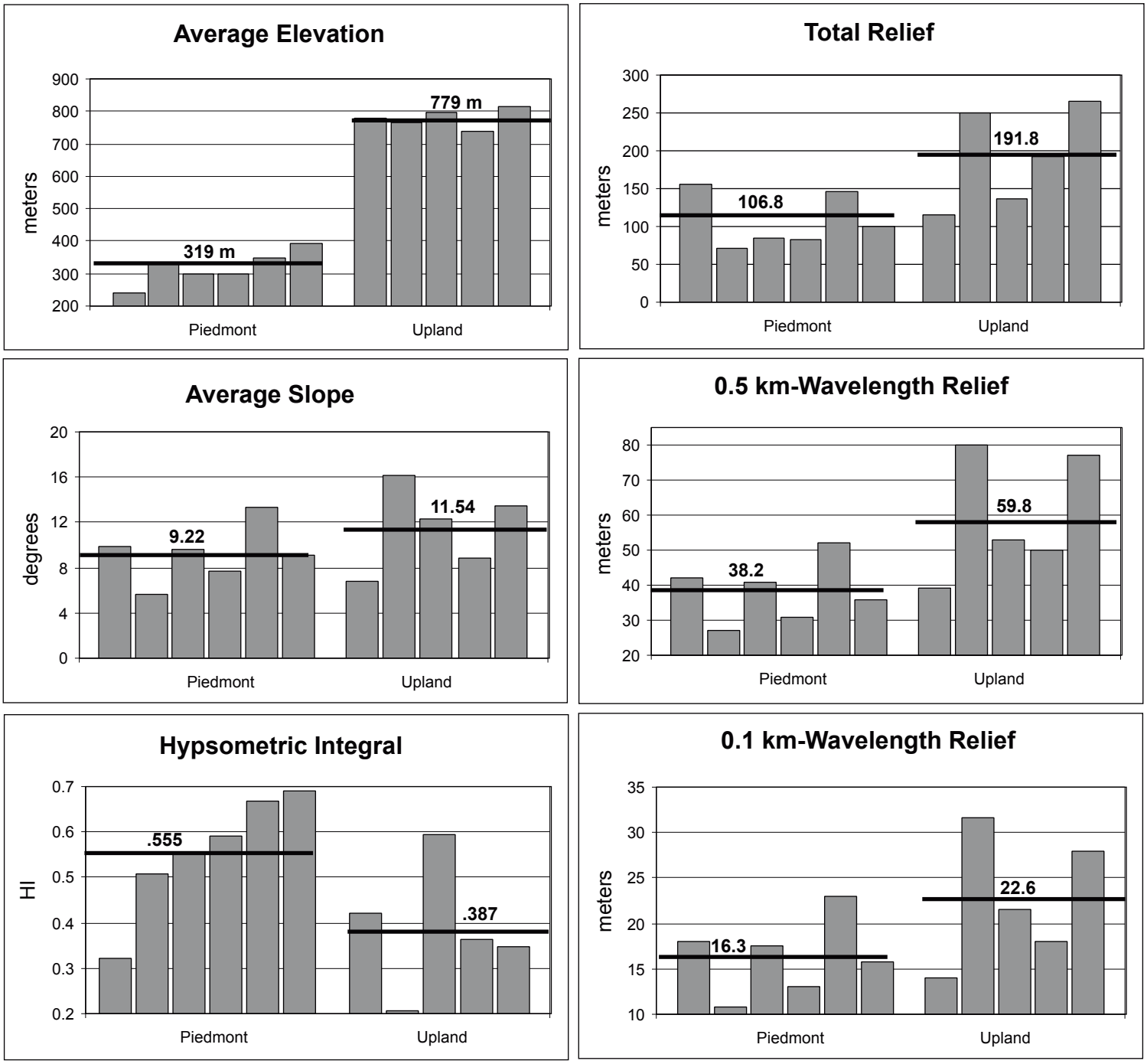
Average Elevation
meters
900
800
700
600
500
400
300
200
319 m
779 m
Piedmont
Upland
Total Relief
meters
300
250
200
150
100
50
0
106.8
191.8
Piedmont
Upland
Average Slope
degrees
20
16
12
8
4
0
9.22
11.54
Piedmont
Upland
0.5 km-Wavelength Relief
meters
80
70
60
50
40
30
20
38.2
59.8
Piedmont
Upland
Hypsometric Integral
HI
0.7
0.6
0.5
0.4
0.3
0.2
.555
.387
Piedmont
Upland
0.1 km-Wavelength Relief
meters
35
30
25
20
15
10
16.3
22.6
Piedmont
Upland

Figure 13

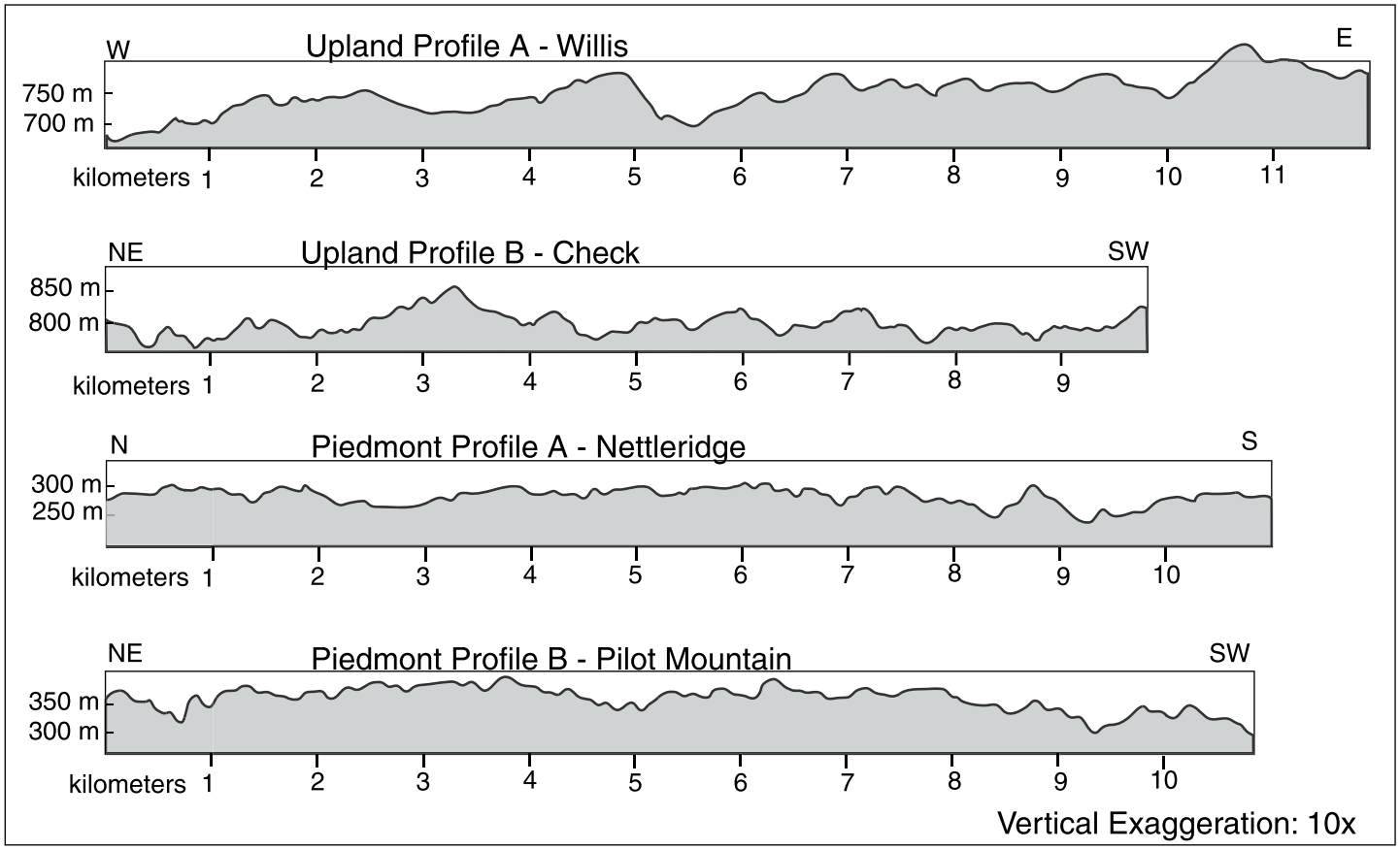
W
Upland Profile A - Willis
E
750 m
700 m
kilometers 1 2 3 4 5 6 7 8 9 10 11
NE
Upland Profile B - Check
SW
850 m
800 m
kilometers 1 2 3 4 5 6 7 8 9
N
Piedmont Profile A - Nettleridge
S
300 m
250 m
kilometers 1 2 3 4 5 6 7 8 9 10
NE
Piedmont Profile B - Pilot Mountain
SW
350 m
300 m
kilometers 1 2 3 4 5 6 7 8 9 10
Vertical Exaggeration: 10x

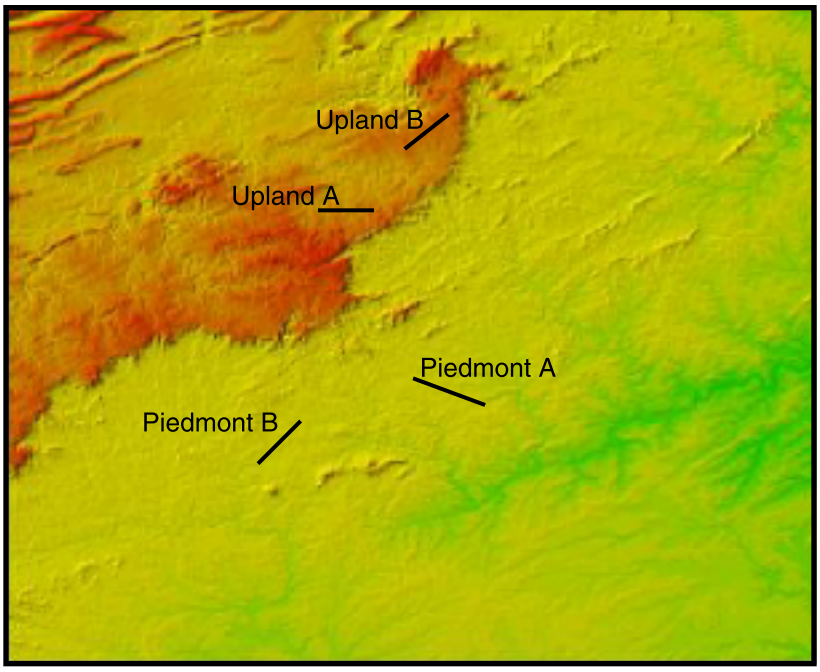
Upland B
Upland A
Piedmont A
Piedmont B

Figure 14

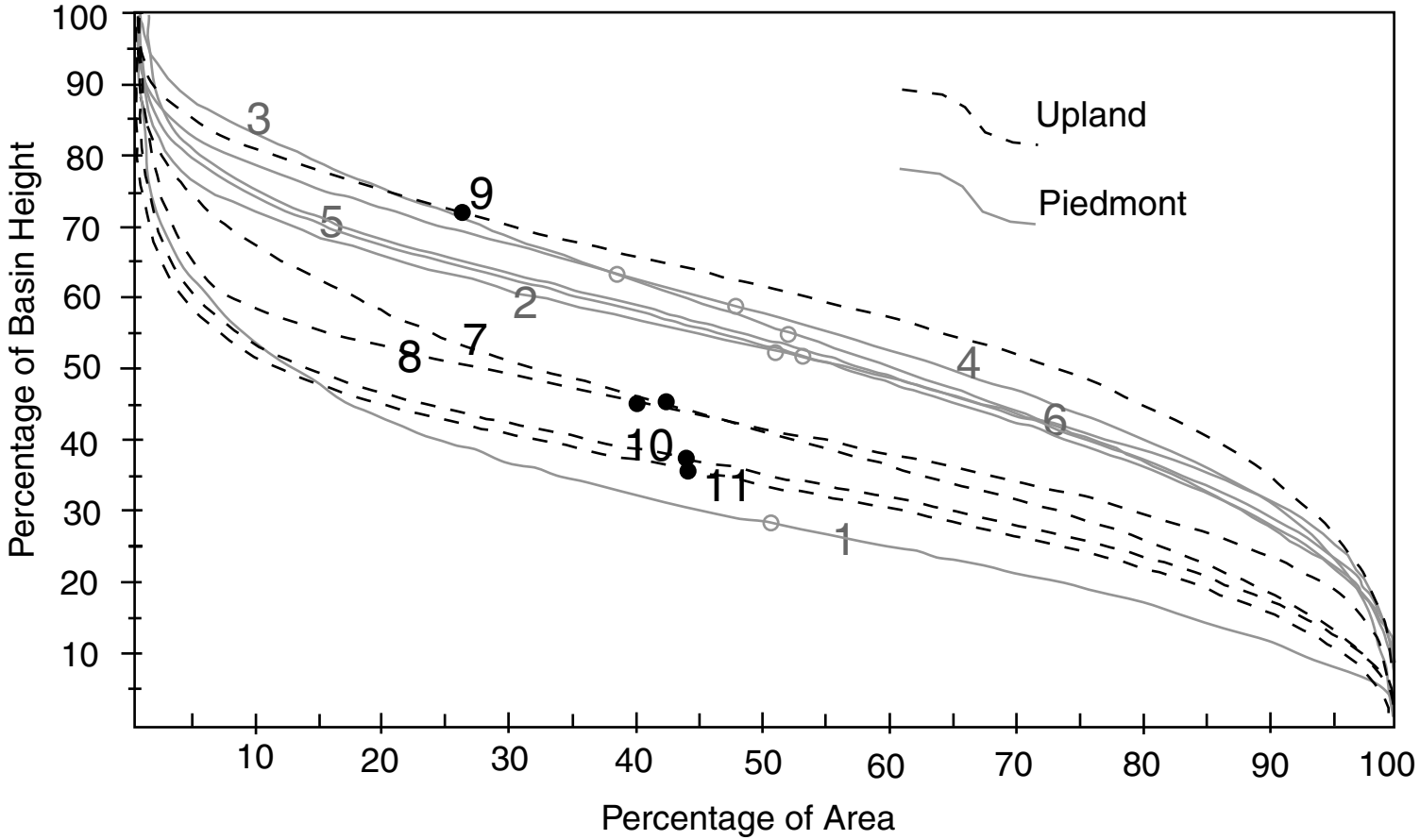
Percentage of Basin Height
Percentage of Area
Upland
Piedmont
100
90
80
70
60
50
40
30
20
10
10
20
30
40
50
60
70
80
90
100
1
2
3
4
5
6
7
8
9
10
11

Figure 15a

Basin 1 - Muddy Creek

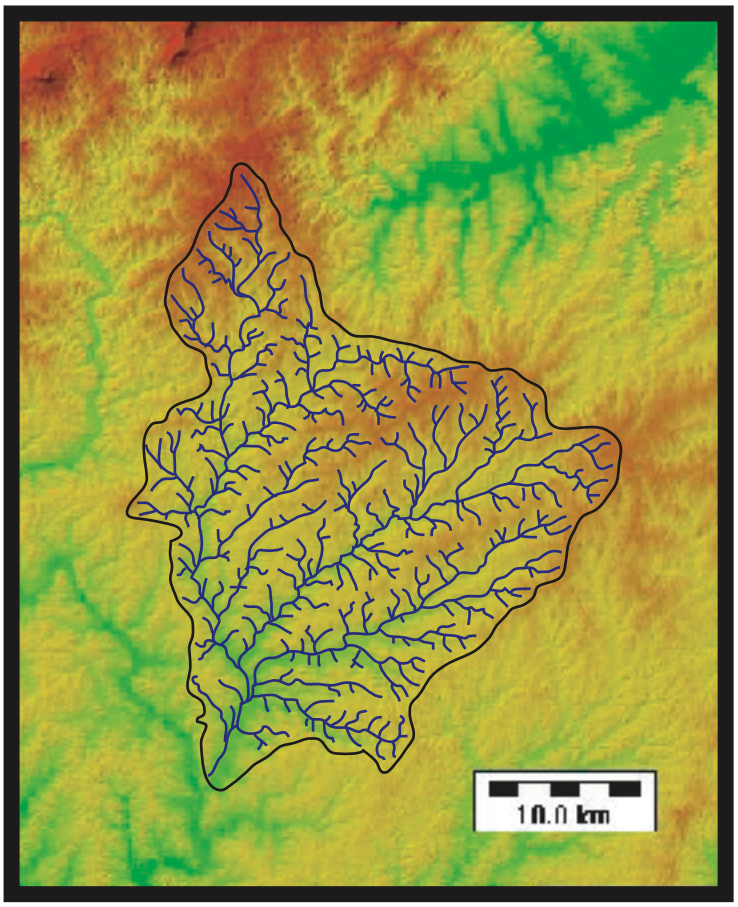

Basin 2 - Sandy River

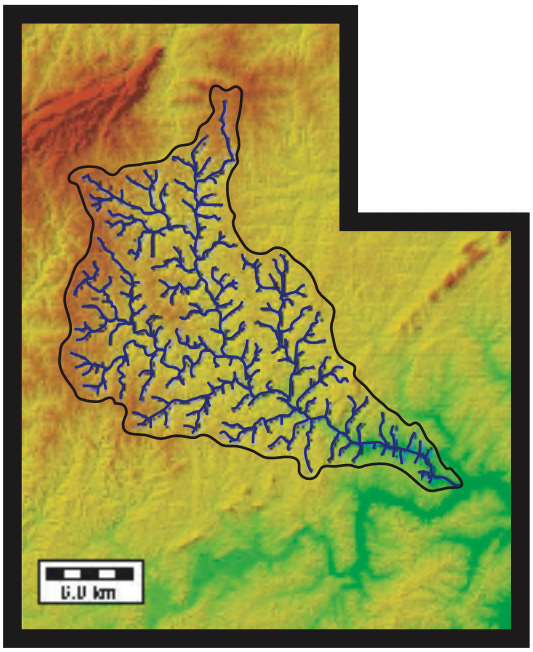

Basin 3 - Deep Creek

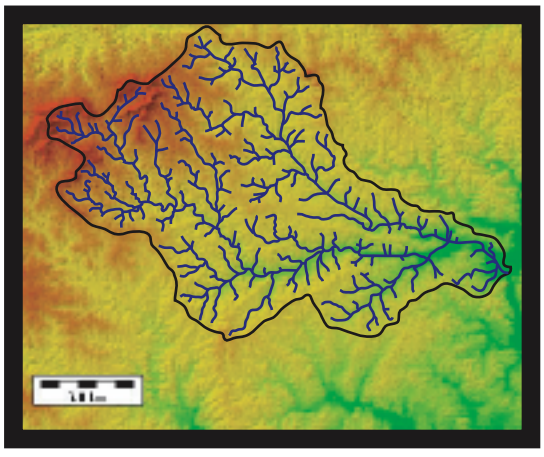

Figure 15b

Basin 4 - Crooked Creek

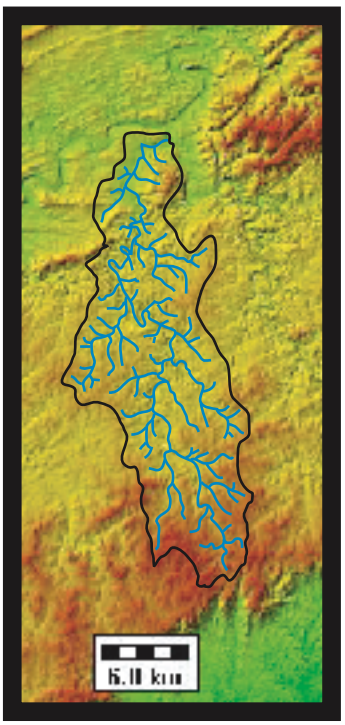

Basin 5 - Little Reed Island Creek

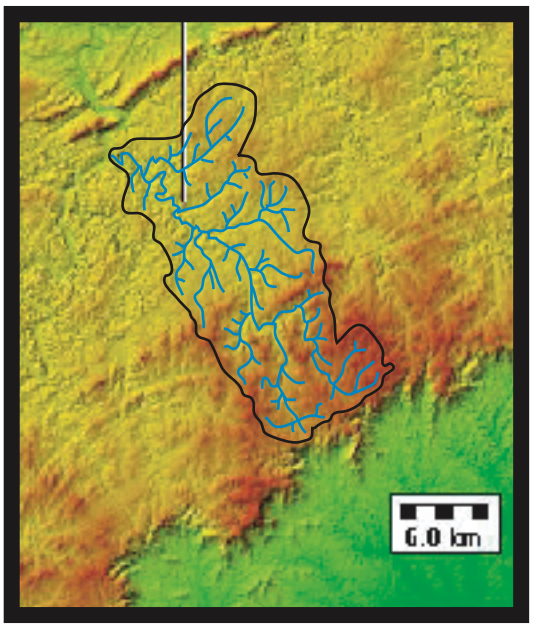

Basin 6 - Little River

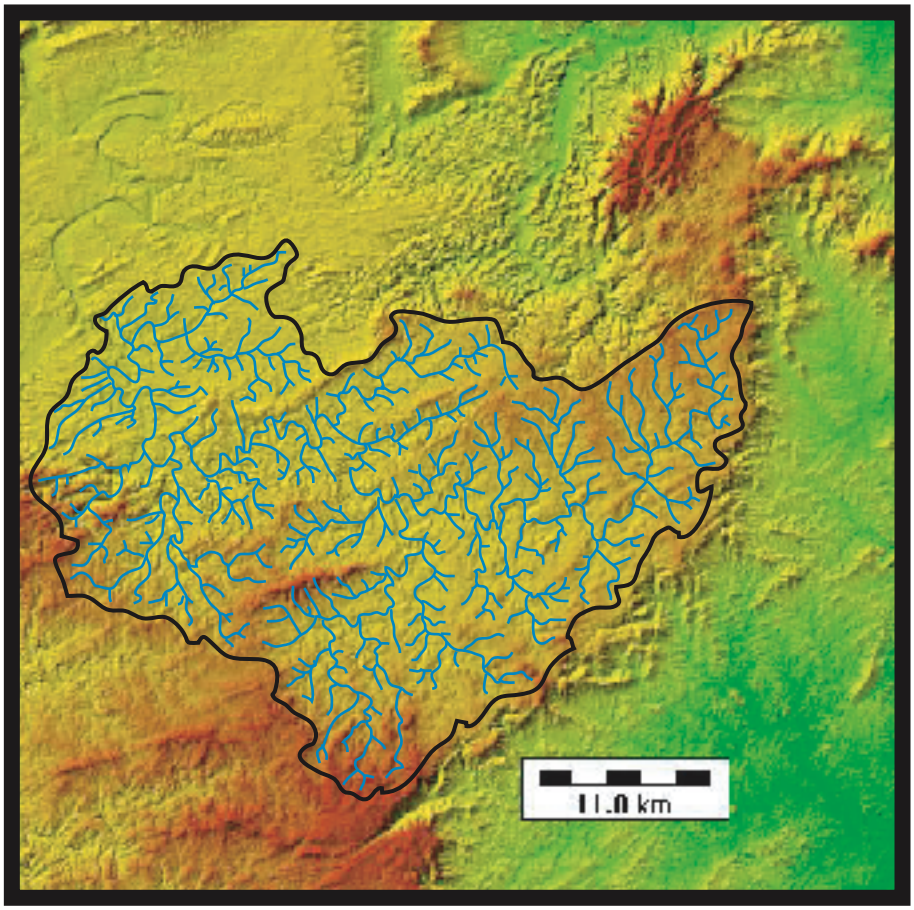

Figure 16

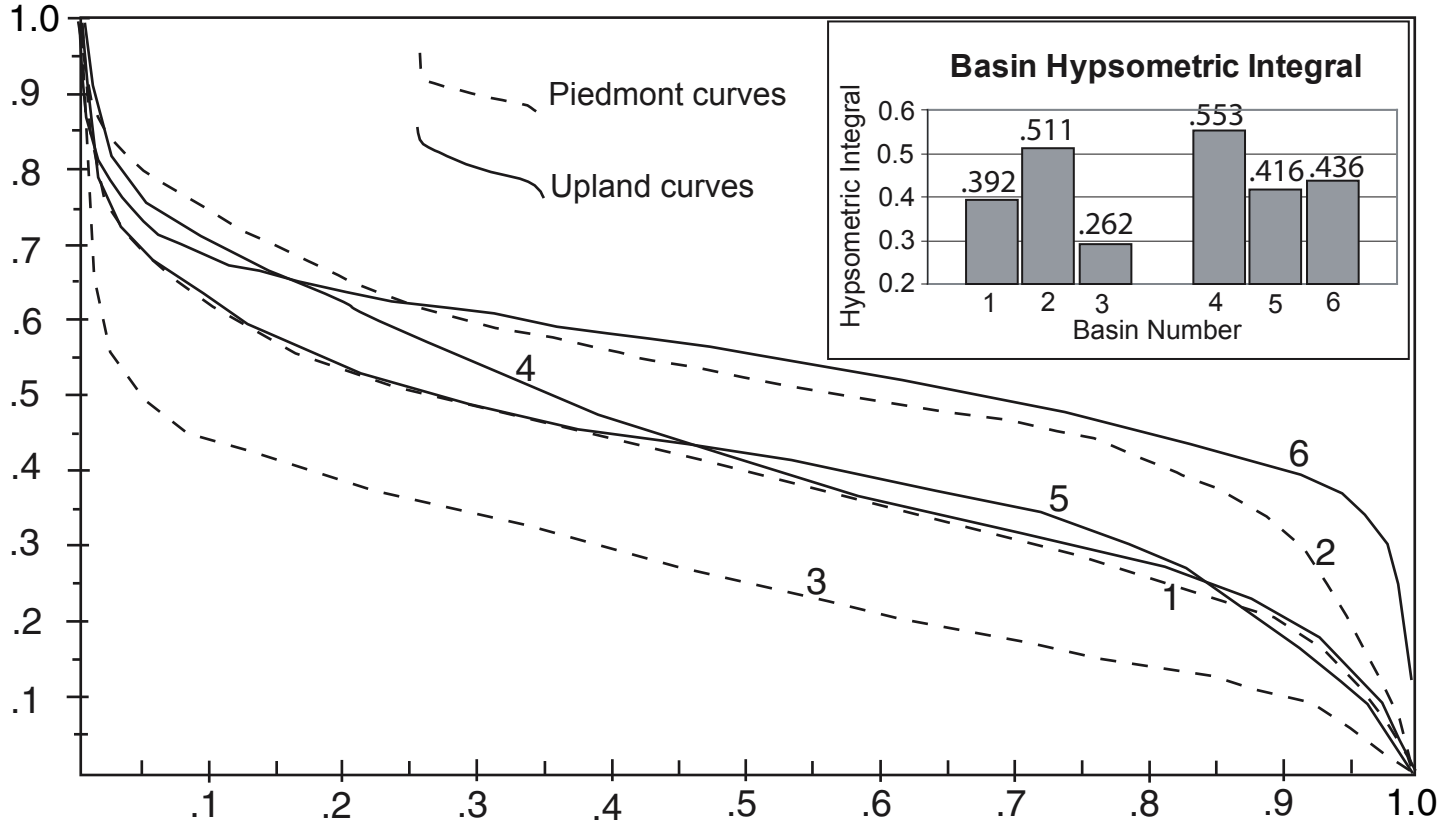
1.0
.9
.8
.7
.6
.5
.4
.3
.2
.1
.1
.2
.3
.4
.5
.6
.7
.8
.9
1.0
Piedmont curves
Upland curves
1
2
3
4
5
6
Basin Hypsometric Integral
Hypsometric Integral
0.6
0.5
0.4
0.3
0.2
.392
.511
.262
.553
.416
.436
1
2
3
4
5
6
Basin Number

Figure 17

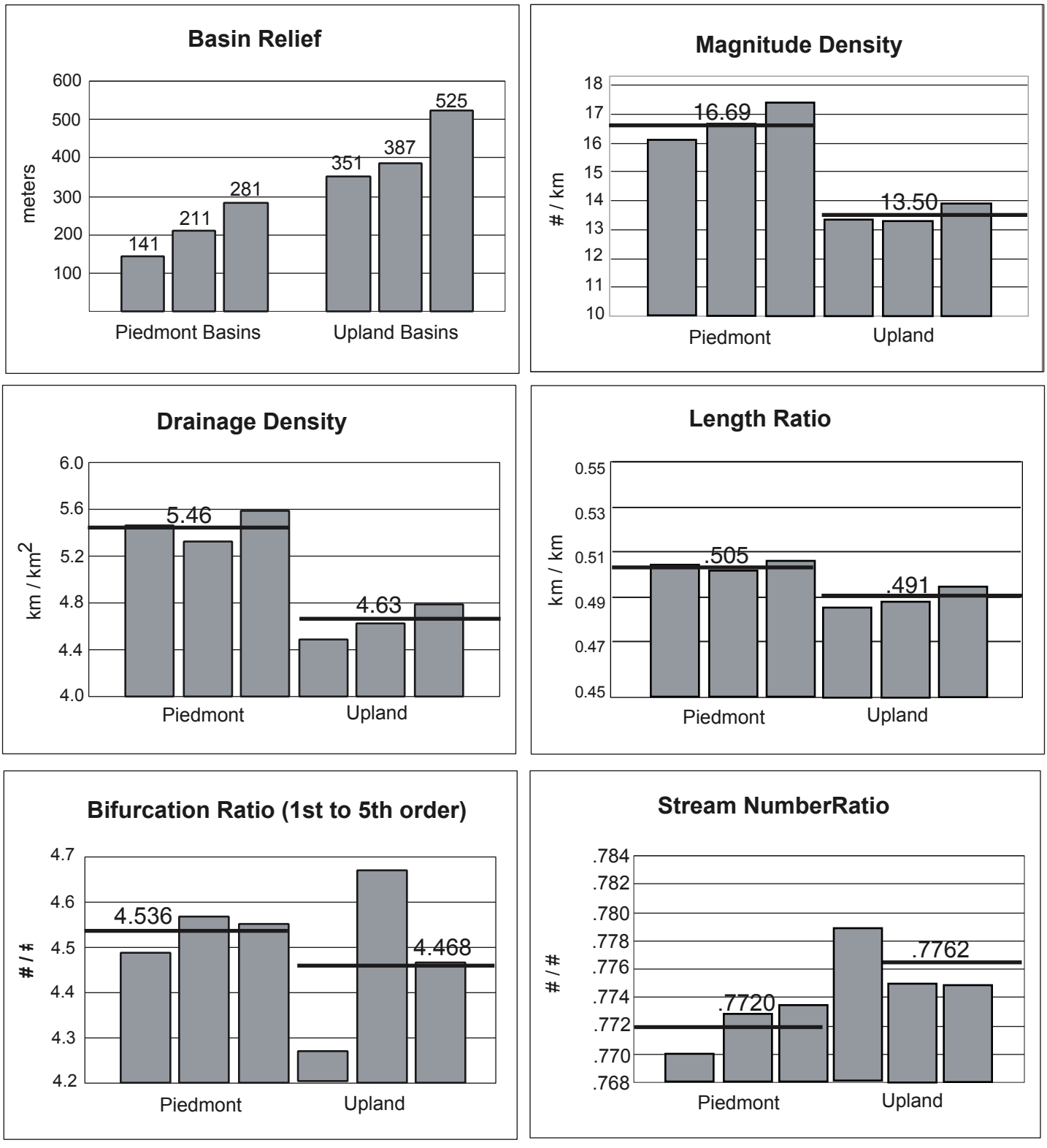
Basin Relief
meters
600
500
400
300
200
100
141
211
281
351
387
525
Piedmont Basins
Upland Basins
Magnitude Density
/ km
18
17
16
15
14
13
12
11
10
16.69
13.50
Piedmont
Upland
Drainage Density
km / km2
6.0
5.6
5.2
4.8
4.4
4.0
5.46
4.63
Piedmont
Upland
Length Ratio
km / km
0.55
0.53
0.51
0.49
0.47
0.45
.505
.491
Piedmont
Upland
Bifurcation Ratio (1st to 5th order)
/
4.7
4.6
4.5
4.4
4.3
4.2
4.536
4.468
Piedmont
Upland
Stream NumberRatio
/
.784
.782
.780
.778
.776
.774
.772
.770
.768
.7720
.7762
Piedmont
Upland

Figure 18

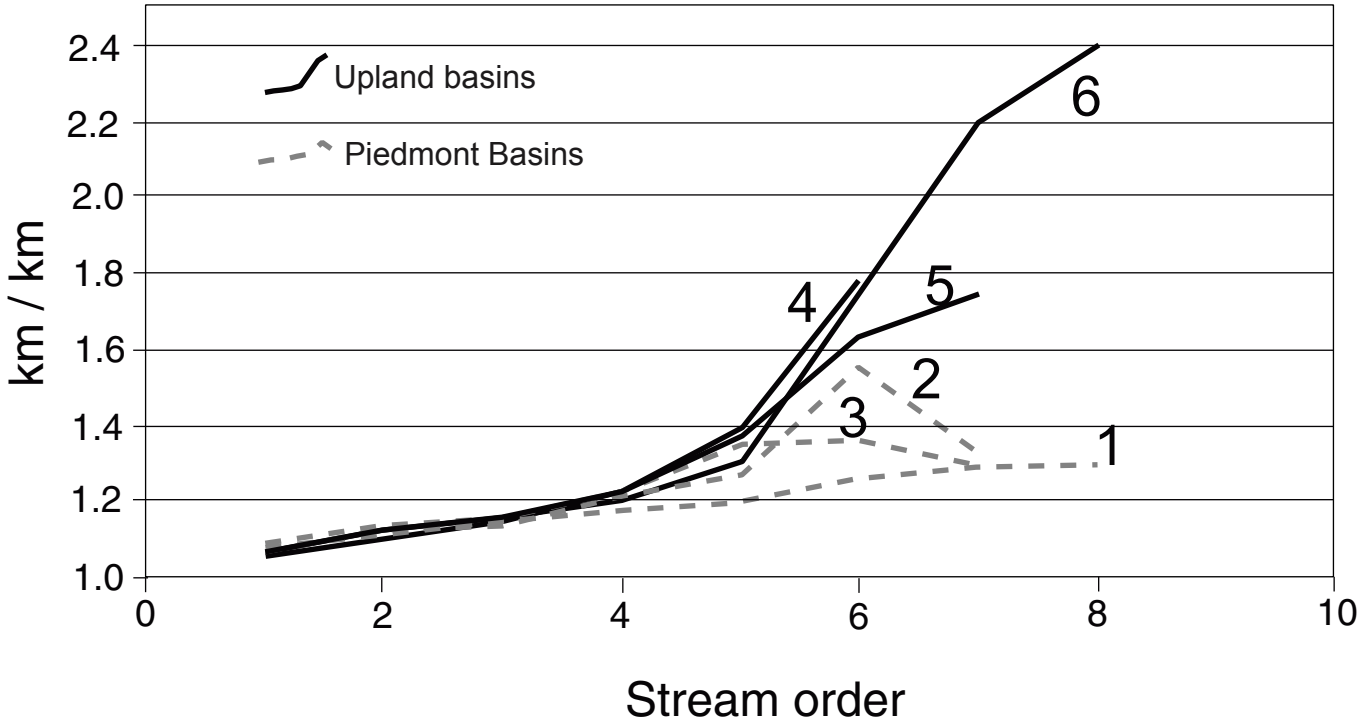

1	Muddy Creek
2	Sandy River
3	Deep Creek
4	Crooked Creek
5	Little Reed Island Creek
6	Little River

Average Sinuosity for >4th order streams:

Upland: 1.7
Piedmont: 1.4

Figure 19

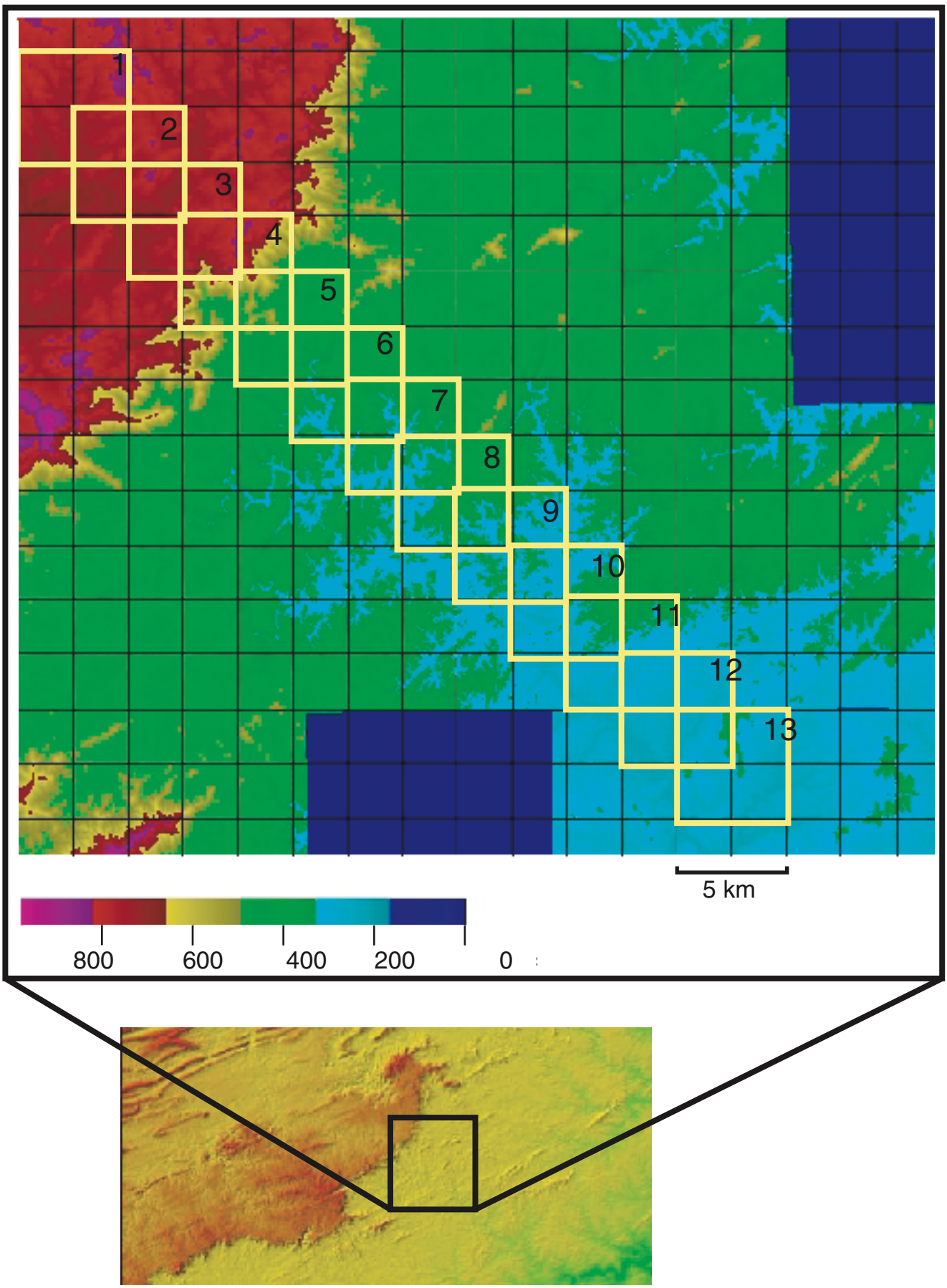

Figure 20

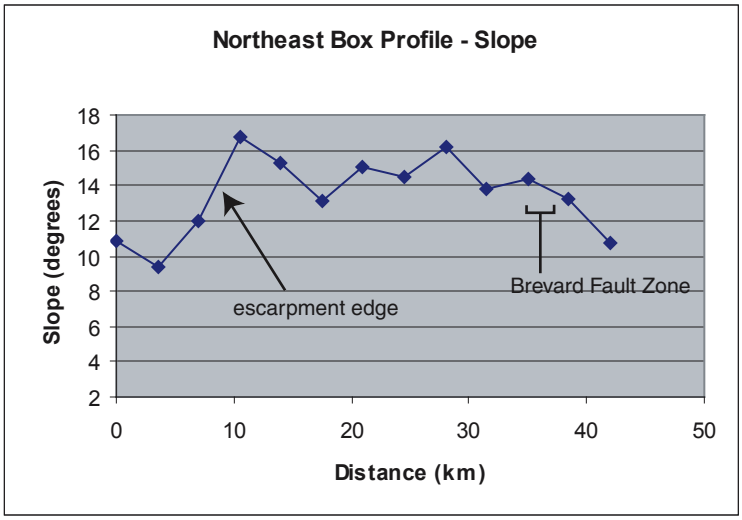
Northeast Box Profile - Slope
Slope (degrees)
Distance (km)
escarpment edge
Brevard Fault Zone

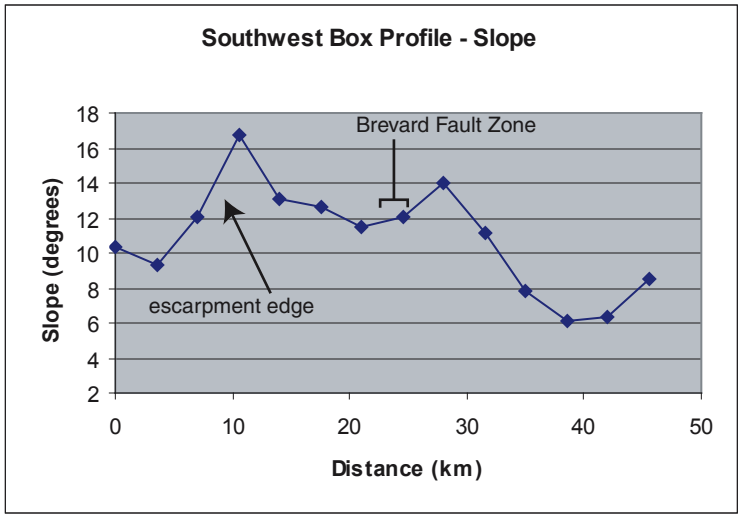
Southwest Box Profile - Slope
Slope (degrees)
Distance (km)
Brevard Fault Zone
escarpment edge

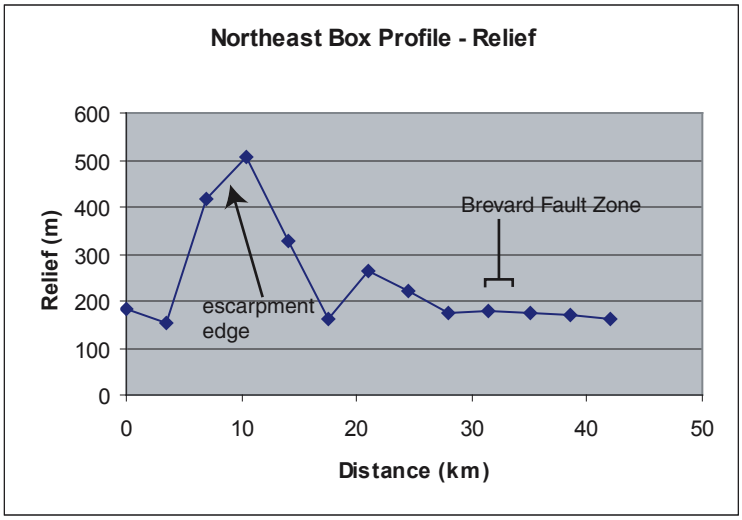
Northeast Box Profile - Relief
Relief (m)
Distance (km)
Brevard Fault Zone
escarpment edge

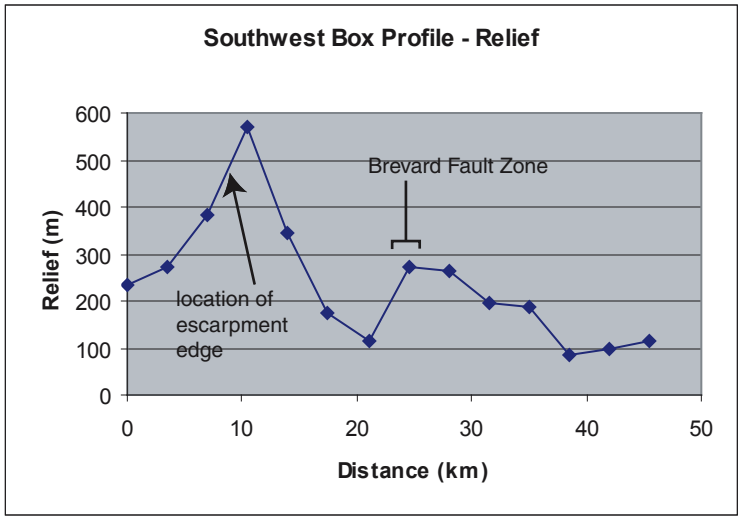
Southwest Box Profile - Relief
Relief (m)
Distance (km)
Brevard Fault Zone
location of escarpment edge

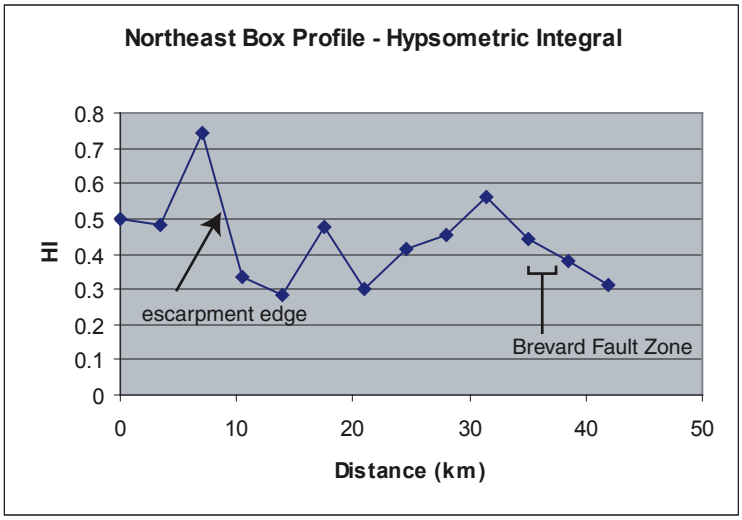
Northeast Box Profile - Hypsometric Integral
HI
Distance (km)
escarpment edge
Brevard Fault Zone

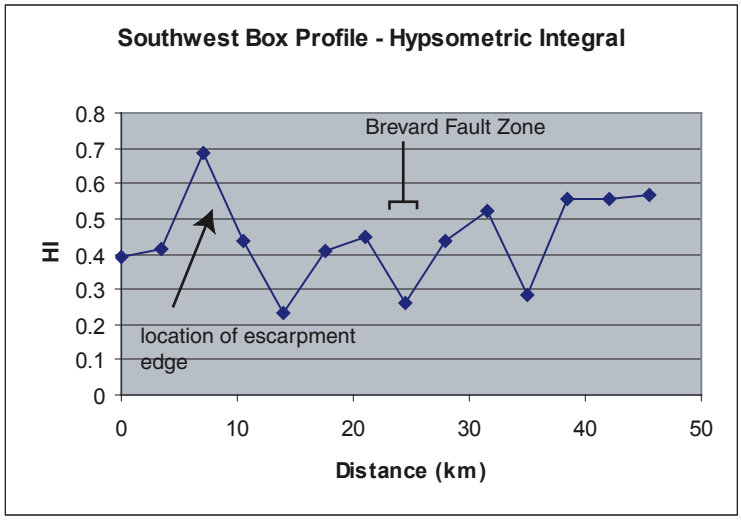
Southwest Box Profile - Hypsometric Integral
HI
Distance (km)
Brevard Fault Zone
location of escarpment edge

Figure 21

Fisher River Basin

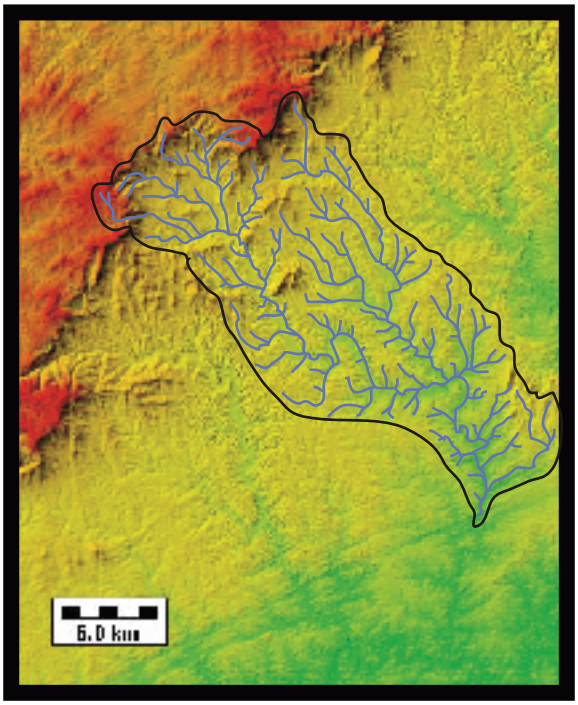

Ararat River Basin

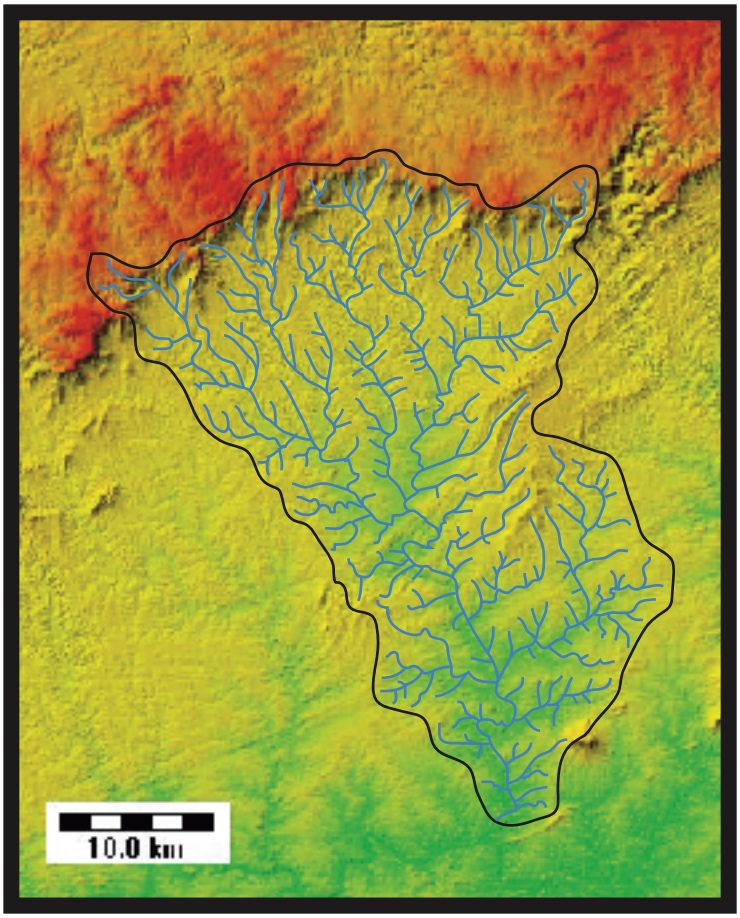

Roaring River Basin

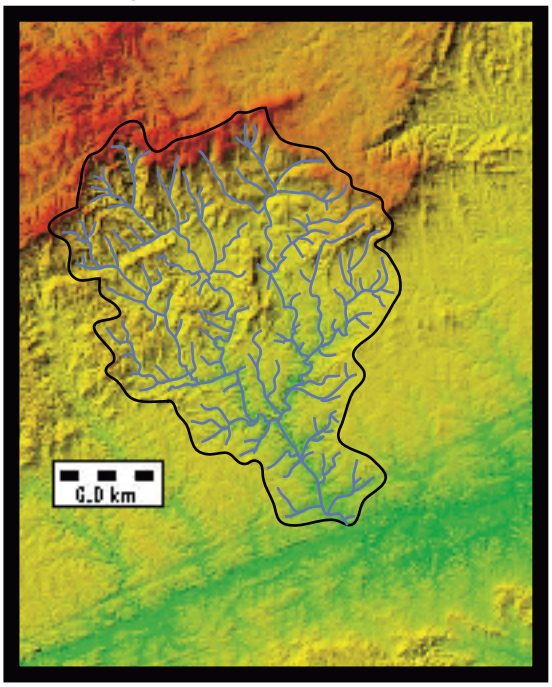

Figure 22

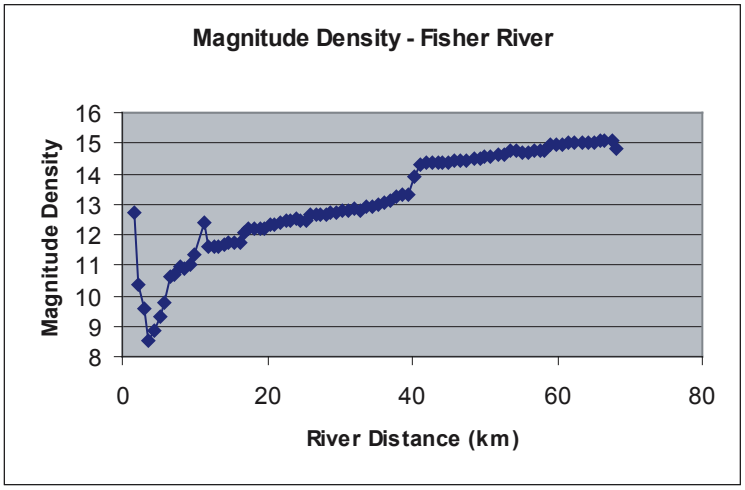
Magnitude Density - Fisher River
Magnitude Density
16
15
14
13
12
11
10
9
8
0
20
40
60
80
River Distance (km)

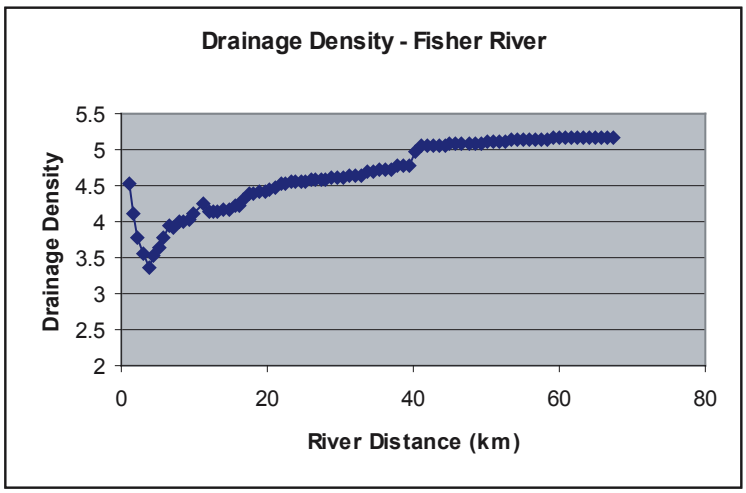
Drainage Density - Fisher River
Drainage Density
5.5
5
4.5
4
3.5
3
2.5
2
0
20
40
60
80
River Distance (km)

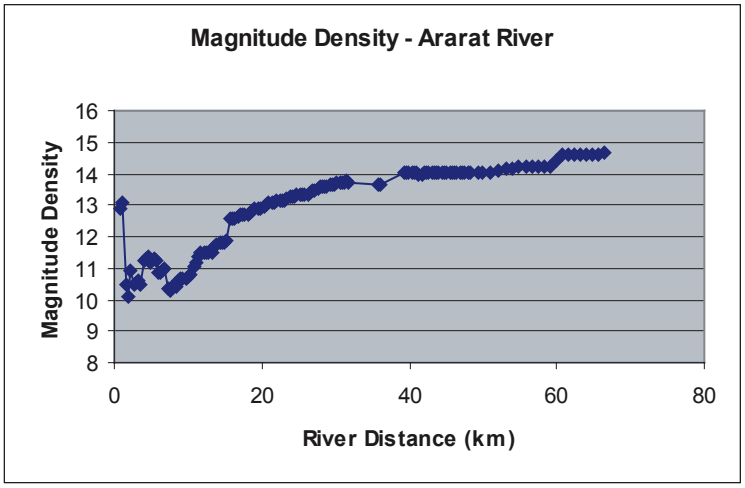
Magnitude Density - Ararat River
Magnitude Density
16
15
14
13
12
11
10
9
8
0
20
40
60
80
River Distance (km)

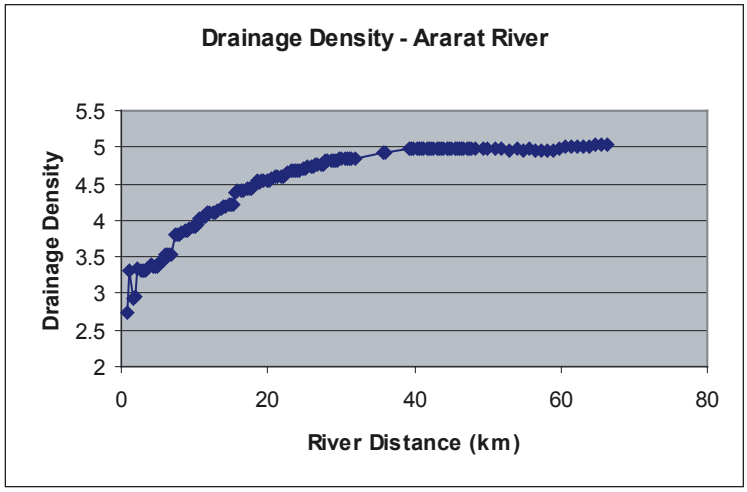
Drainage Density - Ararat River
Drainage Density
5.5
5
4.5
4
3.5
3
2.5
2
0
20
40
60
80
River Distance (km)

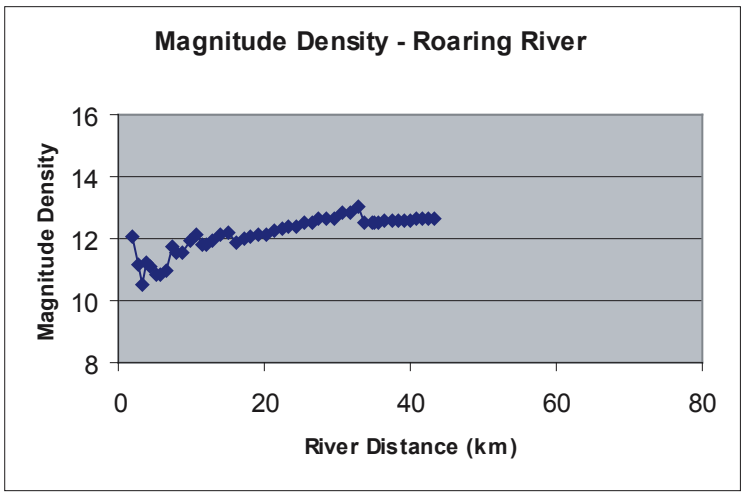
Magnitude Density - Roaring River
Magnitude Density
16
14
12
10
8
0
20
40
60
80
River Distance (km)

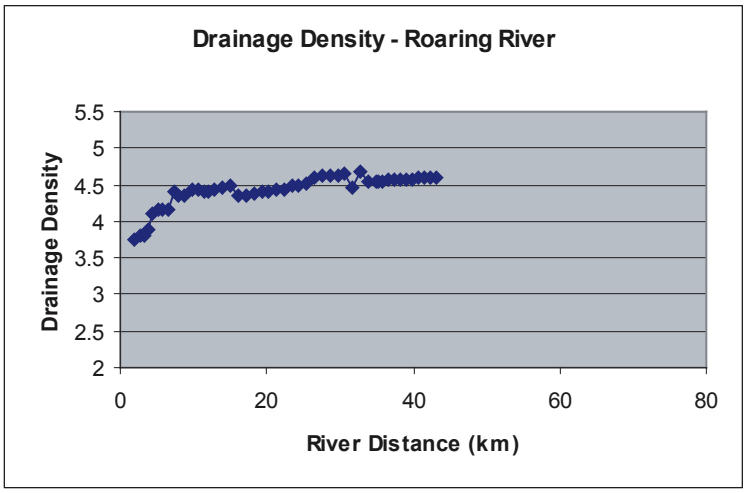
Drainage Density - Roaring River
Drainage Density
5.5
5
4.5
4
3.5
3
2.5
2
0
20
40
60
80
River Distance (km)

Table 2

	Average Elevation (m)	Average Slope (°)	Total Relief (m)
Upland	803	7.7	90
Piedmont	223	1.7	22
North Scarp Zone	647	13.2	140
South Scarp Zone	667	13.6	132

Table 3

Parameter	Definition	Units
Drainage Density	Total length of streams / area	km / km^2
Magnitude	# of 1^{st} order streams	#
Magnitude Density	# of 1^{st} order streams / area	# / km^2
Length Ratio	total length of 1^{st} order streams / total length of all higher order streams	km / km
Stream Number Ratio	# of 1^{st} order streams / total # of all higher order streams	# / #
Sinuosity by Stream Order	sinuosity (channel length / valley length) according to stream order	km / km
Bifurcation Ratio	average increase coefficient in the # of streams with each step in decreasing stream order	# / #

Chapter 3: Evidence for Escarpment Migration Based on the Fluvial Geomorphology of Upland Basins

3.1 Introduction

Topographic analysis is useful for constraining some aspects of the erosional kinematics of the Blue Ridge Escarpment, but does not conclusively demonstrate that the escarpment has migrated nor does it provide data on how fast or how far it may have migrated. Escarpment retreat requires migration of the asymmetric drainage divide and signs of this migration may be preserved in upland drainage basins. I have looked for such evidence in the form of relict terraces, clast shape and provenance, and morphologic evidence of stream capture along the drainage divide. Although these results are reconnaissance in nature, they support the idea of significant escarpment retreat.

3.2 Fluvial Terraces atop the Divide

Because the Blue Ridge Escarpment corresponds with an asymmetric drainage divide, previous workers have sought evidence for divide migration. Wright (1927) noted a number of localities near Hillsville, Virginia, where quartz-rich gravels up to several inches in diameter occur. The lithology of these cobbles argued against a local provenance. Though deeply pitted and often broken, the cobbles appeared to have been rounded through fluvial processes (Wright, 1927). The elevation of these localities ranged from 850 m to nearly 980 m and were only a short distance from the edge of the escarpment. Dietrich (1957) reported similar deposits northwest of Floyd, Virginia. Conducting roundness measurements and more detailed provenance studies on clasts from these deposits could help make a stronger case for or against divide migration.

3.2.1 Terrace Locations

Reconnaissance fieldwork in Floyd County, Virginia, which is bounded on the east by the Blue Ridge Escarpment, revealed several sites where rounded, weathered cobbles of varying lithology were concentrated and exposed. These sites are located in two small stream basins (< 1 km^2) that drain the upland side of the escarpment (Figure 23). Only Site 2 lies near a perennial stream. The main valleys of the small basins seem too wide for the small streams currently occupying them, suggesting their headwaters

have been truncated (i.e. beheaded). The cobbles may thus have been deposited when the stream possessed greater power and have subsequently been stranded due to reduction in stream competence.

Site 1 is comprised of two roadcuts near the Blue Ridge Parkway. The larger location is a linear deposit of clasts of varying lithology exposed in a small roadcut near the Blue Ridge Parkway (Figure 23). The smaller location is similar in all respects to the larger except in size. The straight-line distance from the larger deposit to the escarpment edge is ~400 m. No sizeable channels or streams drain the area upstream of this terrace. The soil of this deposit is very red and no bedrock is exposed along the ~30-meter-long, two-meter-high roadcut. Cobbles found in this deposit are quartz-rich, which may indicate that all other lithologies are absent due to prolonged weathering. Along with the redness of the soil, this indicates that that the site is quite old. Most cobbles in this terrace are small (<5 cm in diameter) but rounded. Clasts generally have only one or two angular edges, and it is possible to reconstruct rounded clasts by piecing together fragments. Although the cobbles are not very large, their form and the semi-linear shape of the deposit suggest a fluvial origin.

Site 2 is located southeast of Site 1, along an unnamed channel flowing through a pasture ~200 m from the edge of the escarpment. A rounded but weathered cobble of coarse-grained amphibolite was found here, along with other quartz-rich cobbles. The cobbles are well-rounded (Figure 24). The degree of rounding suggests a fluvial origin, although the amphibolite sample is very pitted due the weathering of less resistant mineral phases.

Site 3 is located in the same small basin southeast of where the amphibolite cobble was found. The site is a small, rocky stream that rises from a spring <100 m from a very abrupt interfluve at the escarpment. This stream flows over a large assortment of rounded cobbles (mostly quartz-rich and muscovite-bearing) and is the site from which most of the samples were recovered. The cobbles ranged from ~3 cm to >20 cm in diameter and were well rounded. A selection can be seen in Figure 24.

3.2.2 Clast Provenance

Lithology is important for determining the source area of these cobbles. A clast lithology different from underlying bedrock indicates some degree of fluvial transport. If a specific cobble lithology can be linked to a unique source, the transport distance can be established (e.g. Sadler and Reeder, 1983).

The bedrock underlying all three cobble locations is the pre-Cambrian Ashe Formation (Espenshade et al., 1975). This unit is predominantly a mica- and quartz-rich gneiss, although layers of phyllite may also be found. Amphibolite bodies are also generally found in this unit (Espenshade et al., 1975). Minor amounts of quartz-rich gneissic conglomerate is also found ~20 km southwest of the terrace sites. The Ashe Formation as well as the overlying Alligator Back Formation commonly contain large (~ 1 m thick) quartz veins. Because the resistance to weathering of the quartz is so great, these veins are readily mapped by visually tracing quartz fragments in fields and pastureland. Outcrops of quartz veins are readily found in the vicinity of the three sites.

The cobbles from terraces atop the escarpment are predominantly quartz. Of those collected, three consist of vein quartz, which is recognized by large grains, some of which display crystal faces. Four others are conglomeratic quartzite, recognized by the granular quartz grains 2-4 mm in diameter. The grains appear to be somewhat melded together, indicating some metamorphism has occurred. One cobble contains mica in addition to quartz and is probably derived from a quartz-rich layer from the schist found throughout the study area. Similar descriptions of cobbles are given by other workers (Wright, 1927; Dietrich, 1957). The last cobble is the amphibolite from Site 2. Very coarse-grained (2-6 mm) and consisting of ~80% amphibole, this cobble is distinct from anything else found in the vicinity of the cobble locations. Although the clast was significantly weathered, its core was fresh and the original petrology could be discerned. This allowed visual comparison with possible source outcrops of amphibolite found elsewhere.

Only the amphibolite and conglomerate clasts are exotic and may be tied to specific bedrock sources that do not exist in the immediate vicinity of the terrace deposits. Amphibolite bodies are found in both the upland and Piedmont and follow the regional structural fabric, trending northeast-southwest. The nearest mapped unit is ~6

km to the east on the Piedmont side of the escarpment, at an elevation ~350 m lower than the terraces. The closest amphibolite body in the upland is ~10 km south along the escarpment, but occurs in a different drainage basin. In order for the amphibolite clast to be sourced from this or any other upland outcrop, the regional drainage pattern would have to be nearly opposite its present-day geometry. It is more likely that this clast was transported from a source in the east prior to divide migration. Extending the current upland drainage pattern into the Piedmont by moving the divide and escarpment to the east is more plausible. The clast, however, cannot be linked to a specific body of amphibolite, given the general variability in grain size and accessory mineralogy in amphibolite throughout the area.

The conglomeratic quartzite is also not found in the vicinity of the terraces. The closest outcrop of similar lithology is in the Lynchburg Group, ~7 km east of the divide. Mapping has also revealed similar lithology in Unicoi Formation, ~20 km southwest of the terrace locations (Henika et al., 2000). It is likely that the protoliths of these units were deposited at the same time and in the same environment but have been juxtaposed by Paleozoic faulting. The lithology of both outcrops matches the lithology of the conglomerate clasts. They are very pure, slightly metamorphosed conglomerates characterized by ~1-5 mm quartz grains. A Piedmont source is more favorable because all that is required is replacing portions of the upland that may have been eroded away as the divide and escarpment have migrated eastward. An upland source would require complete drainage rearrangement and a more distant source.

The amphibolite and conglomerate clasts require transport and, although provenance is not unique, there is a strong case for considerable transport from the east. This strongly suggests drainage divide migration. Dietrich (1959) reported another exotic clast lithology which I did not observe, but which would strengthen the argument for transport from the east. Diabase clasts were recognized on the upland adjacent to the divide. Dietrich (1959) described the lithology of these cobbles as “similar to Triassic diabase.” Diabase is found in the Triassic basins (the closest of which is the Dan River Basin, ~60 km to the east) as well as in dikes found throughout the Piedmont. Field mapping on the upland has revealed no such features, although magnetic surveys have located one possible diabase dike in the headwater region of the South Fork of the

Roanoke River, 20 km southwest of Roanoke, Virginia (B. Henika, pers. comm.). The absence of diabase outcrops on the upland requires the diabase cobbles to have been deposited prior to substantial divide migration.

A Piedmont origin is favored for deposits from Site 1, 2, and 3 because the relative abundance of exotic lithologies, especially amphibolite and diabase, and because such a source area requires less upland drainage network rearrangement.

3.2.3 Clast Roundness

Clast roundness is a function of the duration of sediment transport processes such as abrasion and particle collision, and can therefore serve as a proxy of fluvial transport distance. Numerous workers have correlated roundness with downstream distance from a source area (e.g. Mills, 1978; Sadler and Reeder, 1983). By assessing the roundness of stranded cobbles atop the escarpment and comparing them with previously calibrated roundness-transport distance functions, it may be possible to constrain the minimum distance of divide migration.

I use the Cailleux index method (Cailleux, 1947) to represent roundness of quartzite cobbles recovered from Site 3. In this technique, a circle is fitted to the sharpest corner on a traced outline of a the maximum projection of a cobble. The index is defined as the circle diameter (in mm) divided by the length of the longest axis of the clast (in mm). This is a modification of the original formula (after Mills, 1978), to allow comparison with results from other studies.

Indices from the five quartz clasts from Site 3 ranged from 0.203 to 0.340. Matching these results to those from Miocene-age, fluvially transported quartz clasts in the San Bernardino Mountains (Sadler and Reeder, 1983) gives a transport distance for each cobble ranging from ~6 km to ~21 km (Figure 25). Because the source outcrop for each cobble may not have been at the divide, 21 km is the minimum channel distance lost by the upland drainage basin.

Other indices exist and different results may be found using these measurement methods. the review of Mills (1978) reports that, while the rounding of quartz clasts appears to systematically increase with downstream distance in any one study, a compilation of results from many studies shows that factors other than transport distance

must play a role in rounding. Still, comparison with the San Bernardino study provides a evidence that some amount of migration has occurred.

3.2.4 Implications

Cobble provenance and roundness make a strong case for significant distances of fluvial transport. The presence of terrace deposits within ~400 m of the divide indicates that the streams that formed them drained a significantly larger upstream area than presently exists. In addition, cobbles of exotic lithology recovered from these deposits show that material was probably transported from source areas east of the asymmetric divide. The maximum value from roundness-transport distance relationships of quartz-rich cobbles from Site 3 was ~20 km. This represents a minimum of ~20 km of channel distance lost to basin capture and suggests that the divide and escarpment have migrated tens of kilometers. Based on this evidence, incremental drainage capture by Atlantic streams is a likely mechanism driving divide migration. Evidence of such capture may exist elsewhere along the escarpment.

3.3 Capture of Upland Streams

3.3.1 Introduction

Because the Blue Ridge Escarpment is associated with an asymmetric divide, a necessary implication of escarpment retreat is divide migration from east to west. This migration can be considered a result of stream piracy, in which Piedmont streams gain drainage area at the expense of upland basins. The steady decline in basin area for these upland streams should leave a measurable mark on network geometry, given the critical importance of drainage area on fluvial processes (e.g. Leopold and Maddock, 1953; Hack, 1973; Whipple and Tucker, 1999). Below I describe both new and previously explored evidence for drainage capture at the divide. I then explore just how much area upland basins may have lost by investigating their meander-drainage area relationships.

3.3.2 Evidence of Capture: Morphology of Upland Basins

Perhaps the best case for stream capture along the divide can be made for the Dan River. Hack (1982) hypothesized that the Meadows of Dan area had been captured from

the Big Reed Island Creek basin by Atlantic streams (Figure 26). The Meadows of Dan is located on a promontory of the Blue Ridge upland that juts southeastward into the Piedmont. The Dan River drains ~100 km^2 of the upland before flowing across the escarpment. Much of the upland area has not yet been incised, although the knickpoint where the river flows across the escarpment marks the head of a ~400-meter-deep gorge. Hack (1982) argued that the Dan River captured part of the upland based in its longitudinal profile and variation in stream-length gradient index along its course. Dietrich (1970) also proposed that the Dan River had beheaded Big Reed Island Creek via headward erosion. But the Dan River, although the most significant, is not the only example of channel beheading and basin capture along the escarpment.

The Roanoke River pierces the Blue Ridge province northeast of the Blue Ridge Escarpment at Roanoke, Virginia, and is another good example of basin capture along the escarpment. Upstream, its two branches drain the Valley and Ridge between the New River basin and the James River Basin (Figure 2). Tributaries of the South Branch of the Roanoke River have captured portions of the Blue Ridge upland by eroding headwardly from the north and east (Dietrich, 1959). The headwater area of the Flat Run/Goose Creek basin contains topography similar to that of the Meadows of Dan, with rolling hills typical of the upland. Downstream, however, the escarpment is marked by a sharp change in stream gradient. The drainage pattern in the vicinity resembles the gorge-type escarpment described by Weissel and Seidl (1997). Because the Roanoke River and its tributaries are eroding into the Blue Ridge upland from the north and northeast (i.e. perpendicular to the regional northwest drainage direction), they can more effectively capture New River streams. As a result, these capture events here involve sizeable drainage areas, rather than the piecemeal captures typical along the asymmetric divide to the southwest. There is also evidence that the groundwater flow of the New River upland has already been partially captured by the North Fork of the Roanoke River (Waller, 1971). Thus, drainage capture is more effective and evident along the northern edge of the divide.

Other examples of upland stream capture include the headwater streams of the Ararat River and Smith River (Hack, 1982). Examples of capture by the gradual removal of headwaters (i.e. channel beheading) are common along the escarpment in North

Carolina. For example, the main valley of Mulberry Creek, an upland stream draining to the New River in Ashe County, leads directly to the escarpment and ends at Mulberry Gap (Number 1, Figure 27). The valley is relatively wide and appears oversized for its headwater area. The adjacent upland basin, Peak Creek, begins just as abruptly at the divide (Number 2, Figure 27). Another example is Chestnut Creek, south of Galax, Virginia. The headwaters of this stream drain a small upland promontory abutted on the north and south by Atlantic drainages that have created embayments in the escarpment. The beheading of these drainages can be easily imagined when inspected with aerial photographs. In some locations, it is also possible to identify upland streams that may soon be beheaded. The South Fork of the New River near Glendale Springs, North Carolina, meanders within 3.5 km of the divide (Number 3, Figure 27). Given time, tributaries of Reddies River, the adjacent Atlantic-draining stream, will catastrophically capture >500 km^2 of drainage area from the New River basin.

3.3.3 Meander-Drainage Area Relationship of Upland Streams

In addition to direct morphologic evidence of drainage capture or divide migration, it may also be possible to infer it by identifying misfit streams in the upland. Misfit streams are those which display characteristics typically observed along streams of higher order or of large drainage area. Given that relationships can be calibrated between drainage area (or distance downstream) and clast size, channel width or meander wavelength, it may be possible to demonstrate that upland basins were once much larger.

The wavelength of river meanders is generally related to stream discharge (Friedkin, 1945; Carlston, 1965), which in turn can be related to drainage basin area (Hack, 1957). Knowing these relationships, it may be possible to estimate the total drainage area required for the meander wavelength of present-day upland streams. If substantially greater than present drainage area, this may require significant divide migration. It may even be possible to estimate the magnitude of this migration based on the calibrated relationships. It is worth noting that most of the meanders in upland basins are entrenched. The streams may have been alluvial and were probably free to meander in the past and their geometries prior to incision may be preserved in the entrenched meandering they currently display.

I explored the possibility that upland meanders may be underfit using previously calibrated relationship between meander wavelength and discharge. Carlston (1965) found a correlation between discharge and "free meander" wavelength. He defined a free meander as, "one developed in alluvium and free to erode laterally, unrestrained by valley walls, and with waveforms not materially distorted by inhomogeneities in the alluvium." This relationship between wavelength and discharge is: $L_m = 106.1 \times Q_m^{0.46}$, where L_m is the wavelength of the meander (crest to crest) in feet and Q_m is the mean annual discharge (Carlston, 1965). In addition to Carlston's (1965) relationship, other indices exist that relate meander geometry to river width. Although I do not use any such relationships, they may provide interesting results if calibrated to different upland streams and compared to streams in the Piedmont.

I first used Carlston's relationship to estimate whether the wavelengths of meanders of the lower Little River (Figure 28) are in proportion with historical mean annual discharge. If the predicted discharge is approximately similar to the present-day value and precipitation-runoff has been approximately uniform, there would be no indication of divide migration. If the predicted discharge is much greater, it would indicate a history of much greater precipitation or a previously larger drainage area, according to the drainage area-discharge relationship of Hack (1957). There is a significant caveat to the use of meander geometry as a sign of basin enlargement. The Little River is a bedrock stream and Carlston's equation was formulated using alluvial streams. His relationships therefore may not be completely valid. However, if the difference is significant, I believe the difference would be mainly the result of a change in basin size.

The Little River contains very sinuous reaches directly upstream from its confluence with the New River. Its mean annual discharge at Graysontown, Virginia (the last gaging station before confluence with the New River) is 364 cubic feet per second (cfs) (USGS Streamflow Data; 1929-1999). The present-day drainage basin upstream of the Graysontown gaging station is ~300 sq. mi. (~770 km^2). Meanders along the lower reaches are entrenched in bedrock and are irregular, often forming peninsulas with pinched necks (Figure 28). I measured the wavelengths of eight meanders from the Radford and Galax USGS 1:100,000 series topographic maps. The average meander

wavelength is 4690' (~1430 m). Using Carlston's (1965) relationship, the discharge for a river with meanders of this wavelength should be ~3800 cfs. This is ten times greater than mean annual discharge over the past 70 years, implying either tremendously higher precipitation in the past or significant drainage area reduction since meander formation. Although it is not possible to determine what role climate would have played (which could be significant) and I do not believe that this comparison demonstrates the actual magnitude of drainage basin reduction along the upland, it is consistent with significant divide migration.

3.3.4 Summary

The evidence for stream piracy and basin capture along all points of the Blue Ridge Escarpment is strong. There are two methods by which capture takes place. The more common (but less effective) method is by headward migration. An Atlantic stream rising at a low point in the divide gradually erodes headwardly, taking over drainage area from an upland stream piecemeal. The more effective basin capture, typified by the Dan River and Roanoke River captures, takes over very large portions of upland basins in a very short geologic time. As captures occur, the divide, and thus escarpment, migrate to the north and west.

Relict meandering in upland basins also show indirectly that divide migration has occurred. The wavelength of meanders on the westward-draining Little River are too large to be caused by the present-day stream. If drainage capture has occurred, the discharge of the Little River has declined. The preserved meanders represent a time when the drainage basin was much larger.

3.4 Implications

Field evidence in the form of terrace deposits and allochthonous cobbles supports the idea of a larger or more complex upland drainage network. Upland headwaters are characterized by overly wide valleys with ephemeral streams containing clasts that have probably been transported a greater distance than allowed by present location. Cases of channel beheadings and basin capture also argue that drainage capture is common along the escarpment. The underfit meanders of the Little River further reveal that the mean

annual discharge of upland streams may have been much greater in the past, due to a substantially greater drainage area. Although each of these observations may only hint at some degree divide migration, the argument for divide migration via upland basin capture by Atlantic streams is made much more convincing when they are considered in conjunction.

Despite the fact that much of the work has been reconnaissance in nature and that there is plenty of opportunity for future study, the results suggest that the drainage divide between the Atlantic Ocean and Gulf of Mexico has migrated to the north and west by a significant amount, perhaps on the order of tens of kilometers. This narrows the field of hypotheses for the origin and evolution of the escarpment. Hypotheses that do not include some amount of divide migration are discouraged by the likelihood that the divide has retreated. The final task is to compare the remaining hypotheses to exhumation patterns based on low-temperature thermochronometry.

Chapter 3 – Figure and Table Captions

Figure Captions

Figure 23 - location of fluvial terraces and cobble deposits in Floyd County, Virginia. Maps on right side are from USGS 1:24000-series Callaway quadrangle (elevations are in feet). On location map (created in RiverTools), dotted lines represent approximate locations of nearby amphibolite bodies.

Figure 24 - Cobbles recovered from the Blue Ridge upland.

Top – cobbles recovered from Site 3. Lithologies are: A) vein quartz, B) conglomeratic quartzite, C) vein quartz, D) conglomeratic quartzite, E) conglomeratic quartzite.

Middle – Amphibolite cobble recovered from Site 2. It was broken after recovery

Bottom - Broken coarse-grained quartz cobble recovered from Site 1. The shape (well-rounded with one or more broken sides) is typical of cobbles found at Site 1.

Figure 25 – Roundness-Transport distance plot calibrated for quartz clasts from the San Bernardino Mountains (after Sadler and Reeder, 1983). Roundness values (Table 4) for this study are plotted as gray triangles.

Figure 26 – Map of Meadows of Dan area, created from USGS 30-m DEMs using RiverTools. Elevation scale is as in Figure 15. Nearly 100 km of upland has been capture from Big Reed Island Creek basin by the Dan River Basin. The Dan River has partially incised the upland, created the ~400-m-deep Dan River Gorge (south-central on map)

Figure 27 – Map of Basin captures and channel beheadings in North Carolina, created from 30-m DEMs using RiverTools. Elevation scale is as in Figure 15.

#1 is the beheaded channel of Peak Creek.

#2 marks the beheaded channel of Roan Creek

#3 marks the separation (<3 km) of the South Fork of the New River (west) from the Reddies River. Headwater channels of the Reddies River will eventually capture all of the upper New River basin.

Figure 28 - Map of lower Little River, near confluence with New River. Created from USGS 30-m DEMs using Rivertools. Meanders shown were measured on USGS

1:100,000-series maps. The meander wavelength appears to be too large for the present-day mean annual discharge of the Little River.

Table Caption

Table 4 – Cobble statistics. All five cobbles measured were recovered from Site 3.

Figure 23

location map

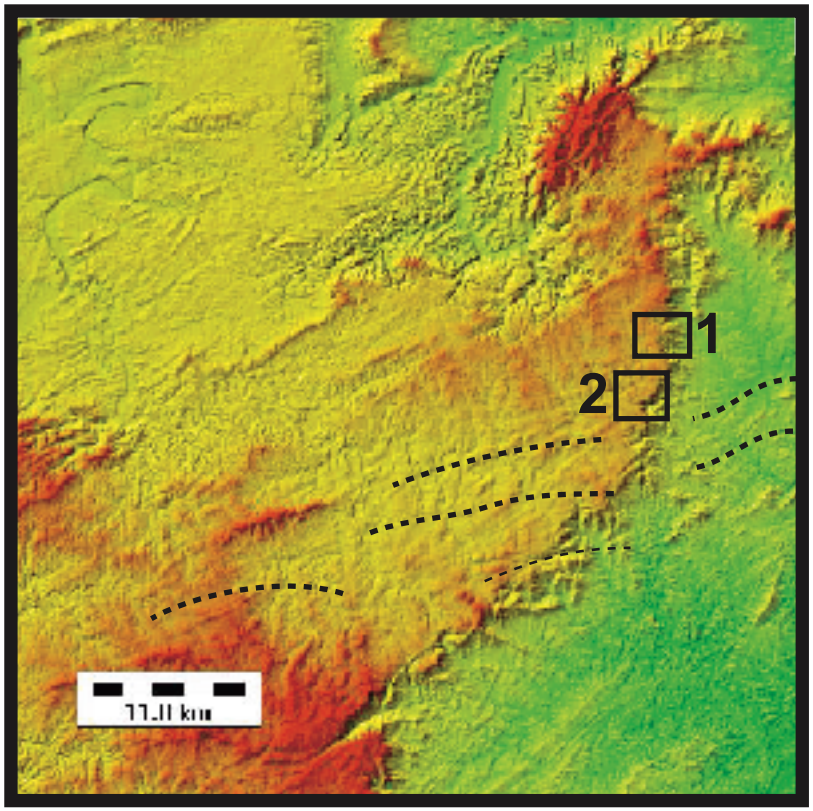

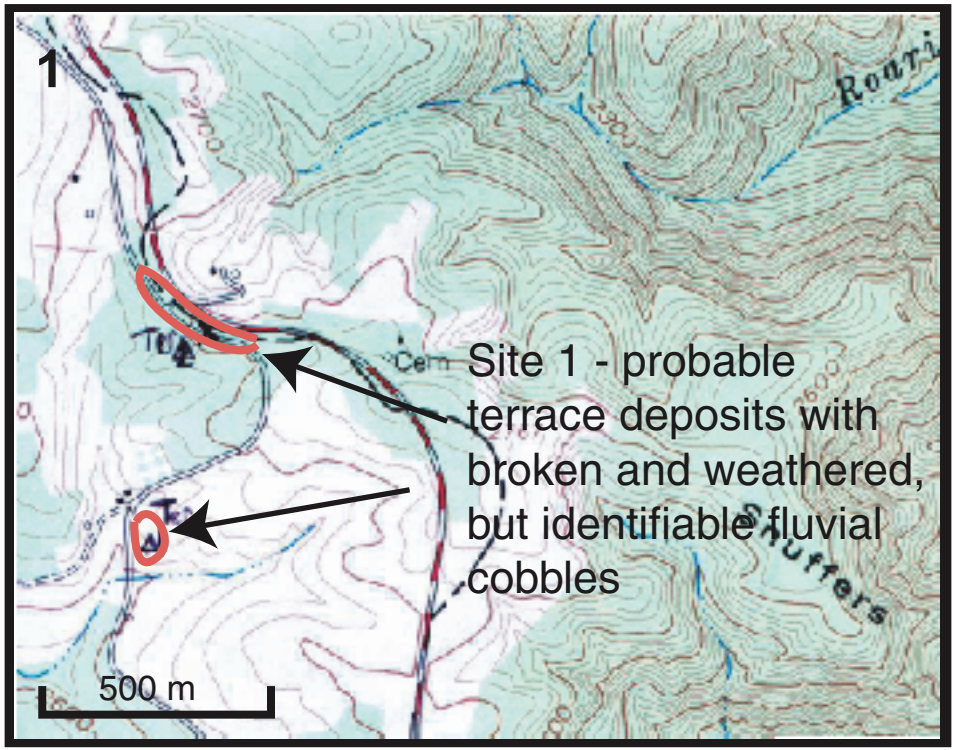

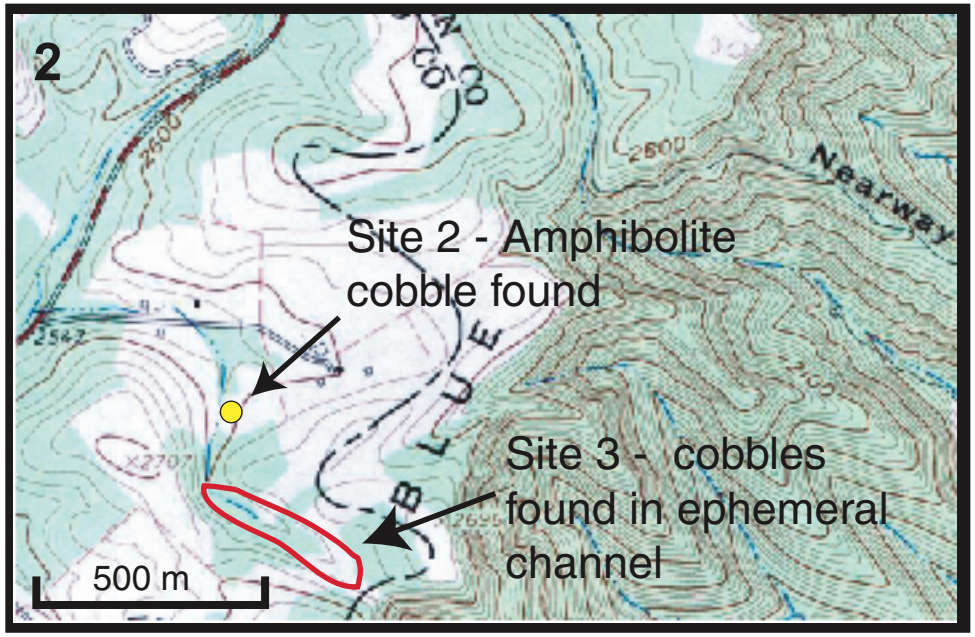

Figure 24

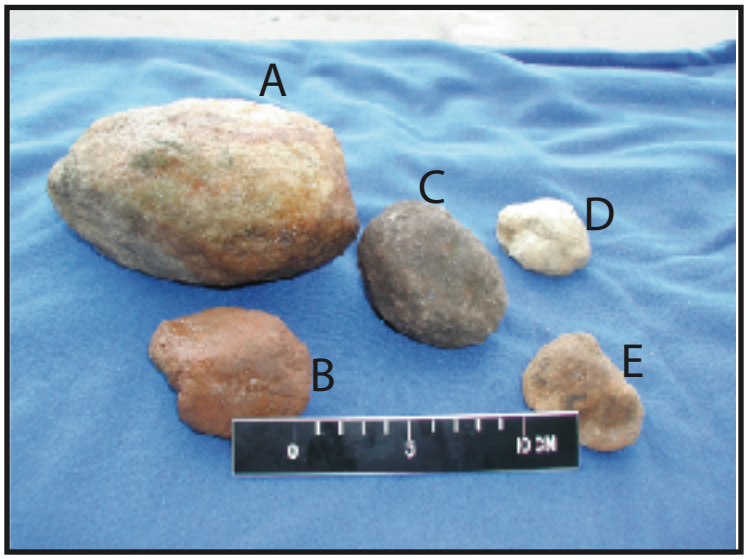

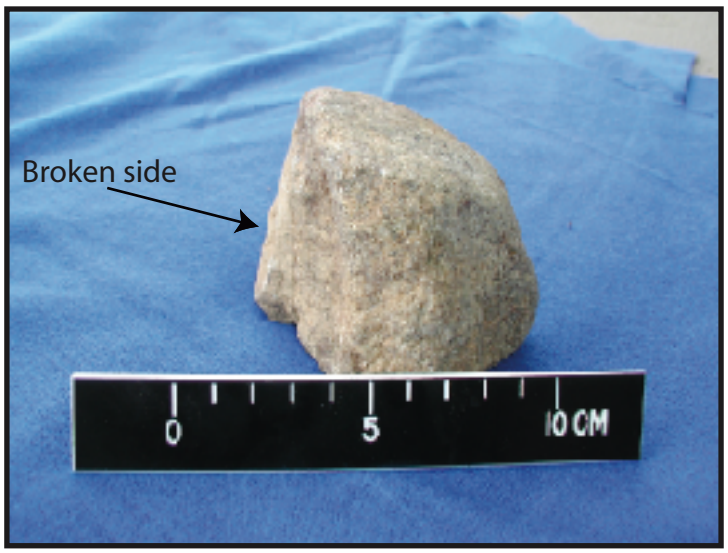

Figure 25

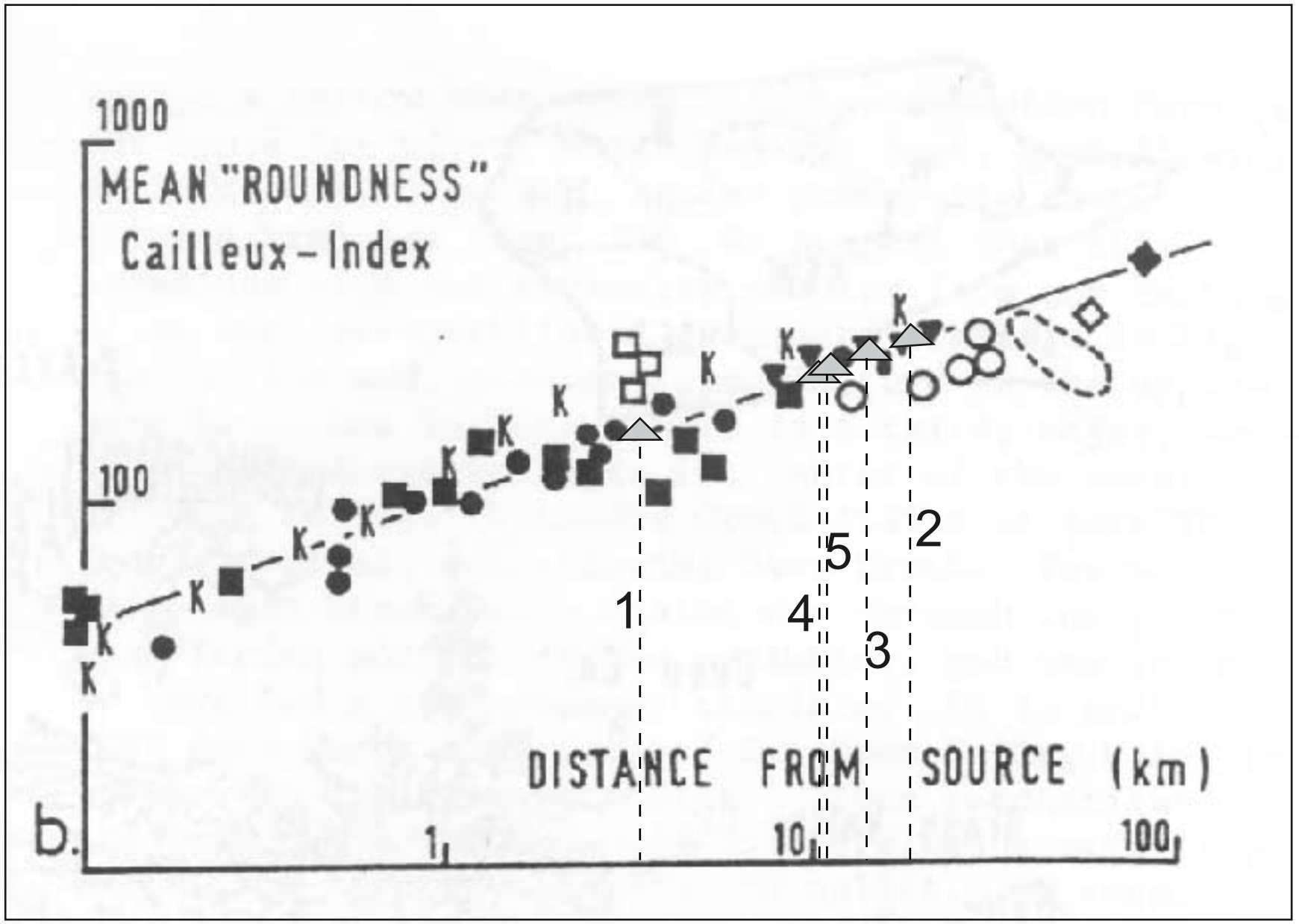
1000
MEAN "ROUNDNESS"
Cailleux-Index
100
K
1
2
3
4
5
DISTANCE FROM SOURCE (km)
b.
1
10
100

Figure 26

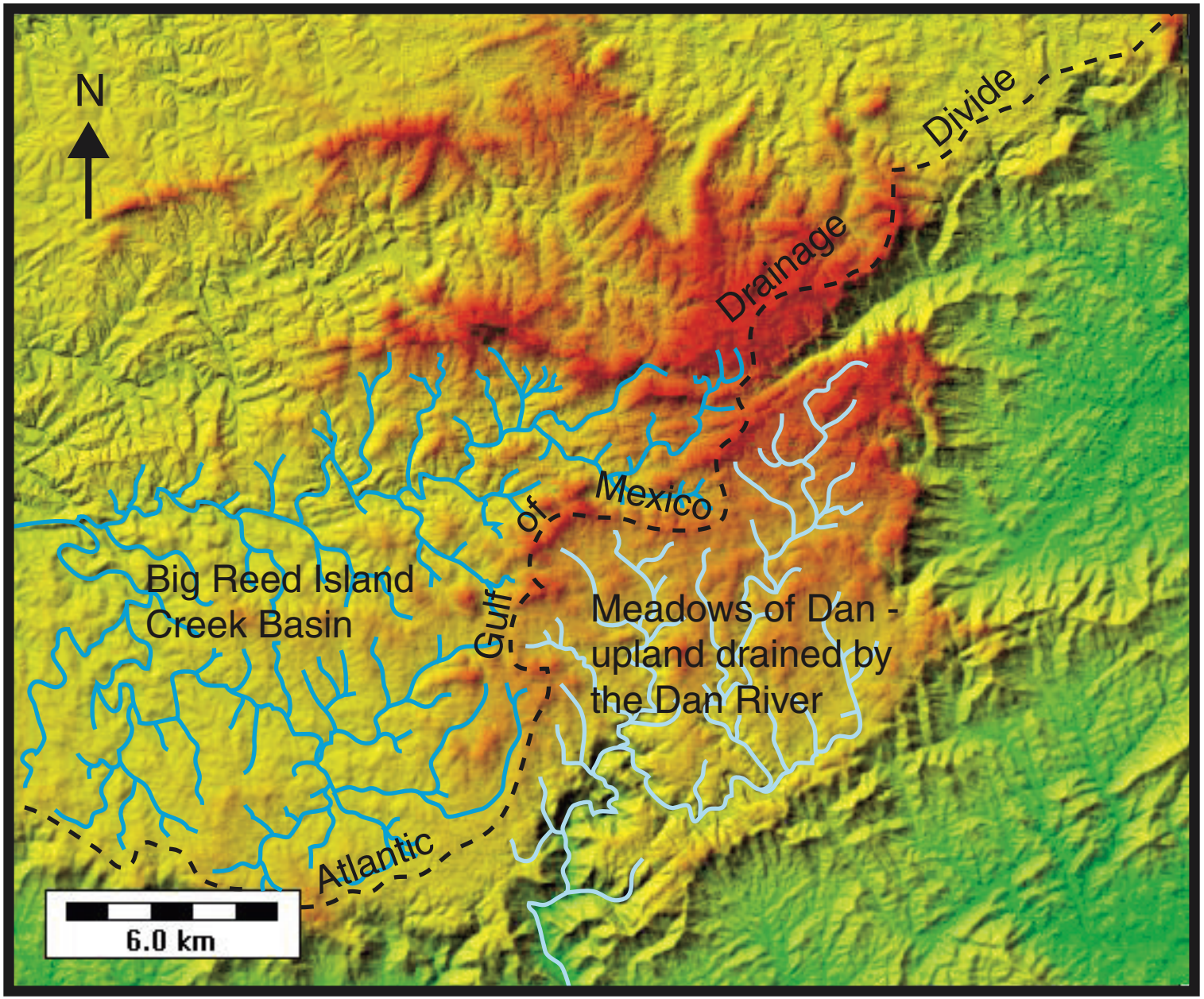
N
Divide
Drainage
Gulf of Mexico
Big Reed Island Creek Basin
Meadows of Dan - upland drained by the Dan River
Atlantic
6.0 km

Figure 27

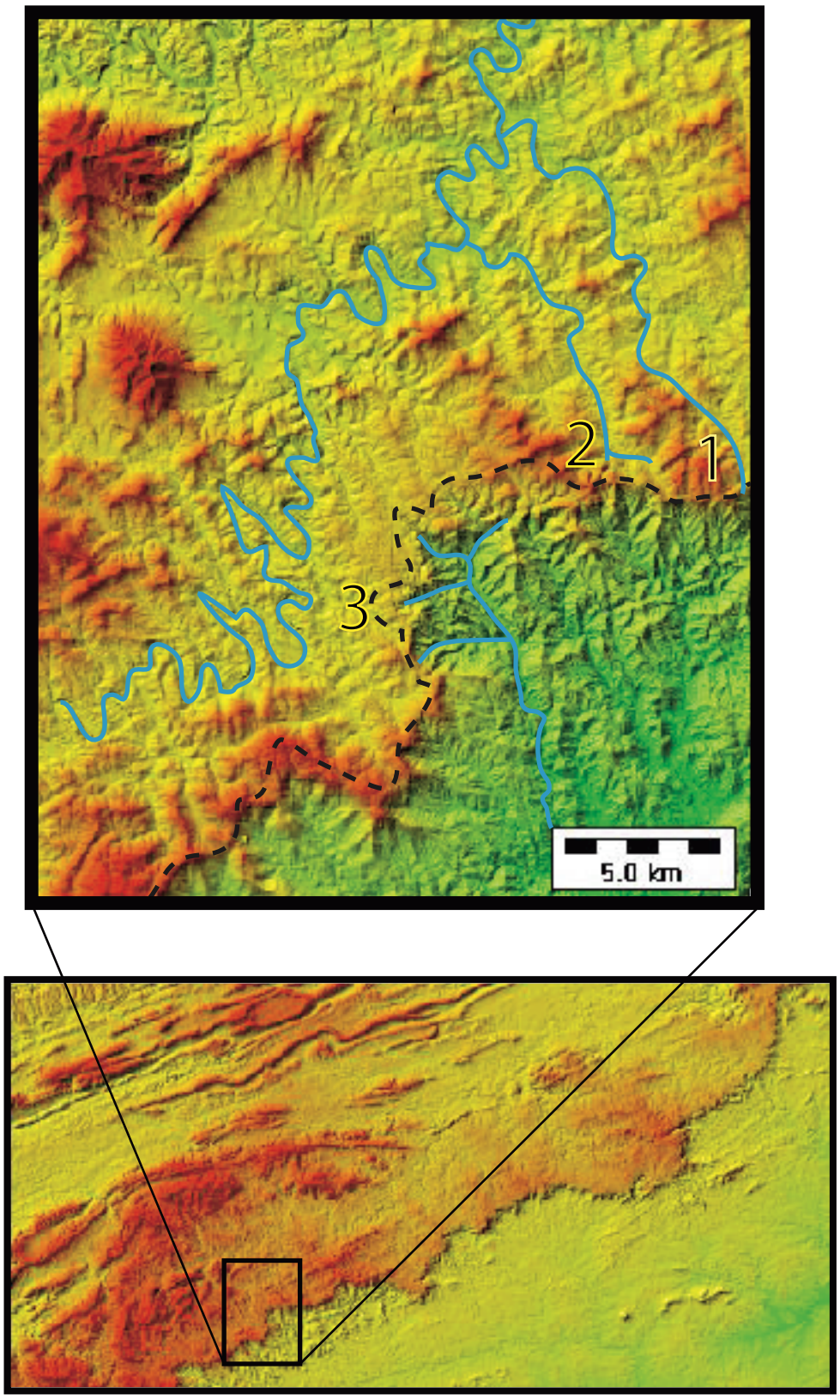

Figure 28

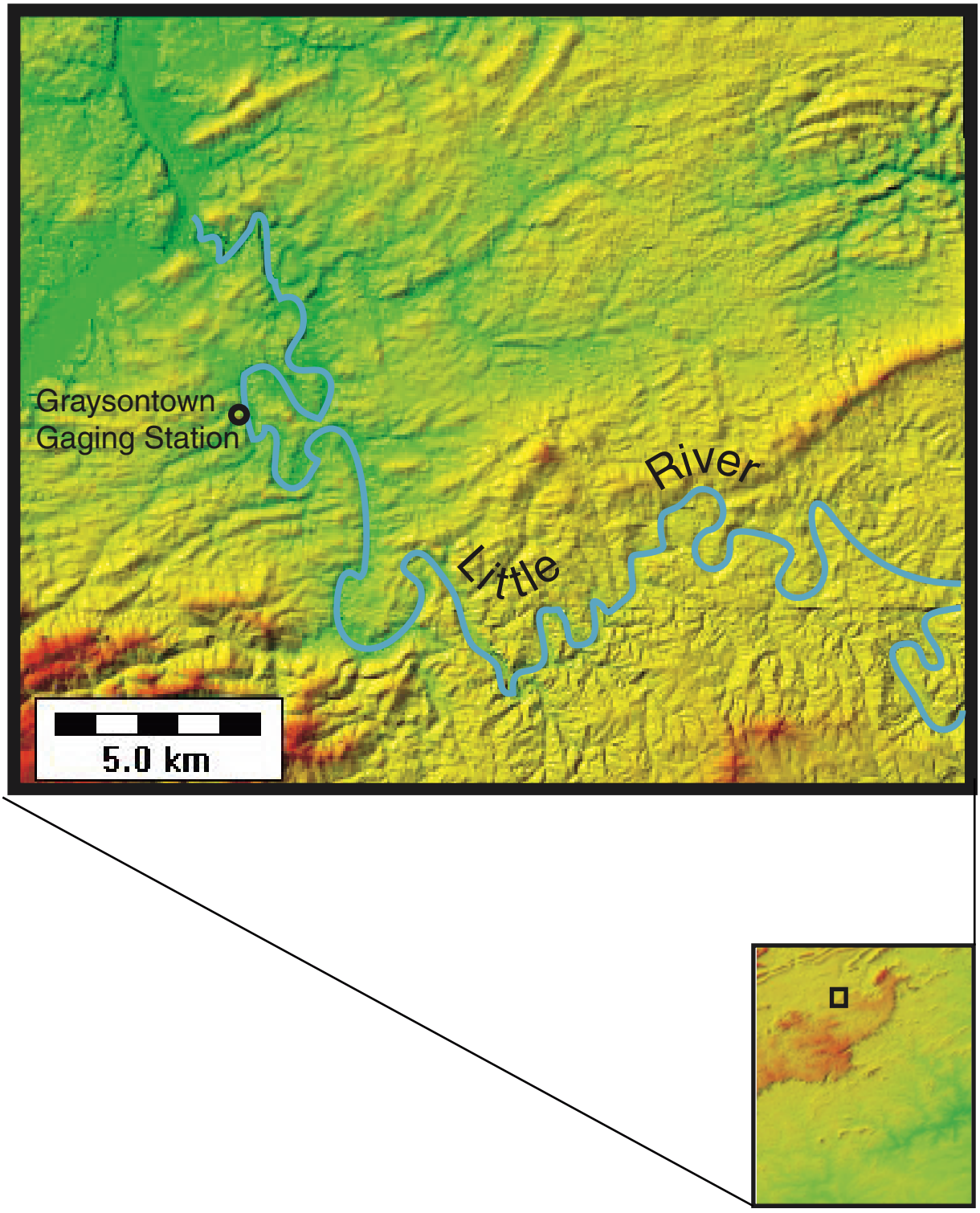

Table 4

Cobble Number	Diameter of sharpest corner (mm)	Longest Axis (mm)	modified Cailleux Index	estimated distance traveled (km)
1	41	201.5	0.203474	5.8
2	29	85.3	0.339977	21.1
3	20	63	0.31746	17.7
4	23.5	92.5	0.264865	11.3
5	17.3	64	0.270313	11.9

Chapter 4 – Constraints on exhumation using (U-Th)/He thermochronometry

4.1 Introduction

The various hypotheses discussed earlier for the origin of the Blue Ridge Escarpment make predictions about the magnitude and spatial distribution of exhumation experienced by the Piedmont and upland domains. However, topographic analyses can only be used to infer relative landscape age or recent erosional intensity and cannot provide estimates of total denudation. Likewise, fluvial geomorphology provides clues to the basin evolution of the Piedmont and upland domains and therefore to escarpment migration, but reveals nothing about exhumation patterns. To measure exhumation, a low-temperature thermochronometer is required.

(U-Th)/He thermochronometry is based on radiogenic production and thermal diffusion of ^{4}He in the mineral apatite (Zeitler et al., 1987; Lippolt et al., 1994; Wolf et al., 1996; Warnock et al., 1997; Farley, 2000). Helium is produced in situ by the radioactive decay of uranium and thorium series nuclides and remains trapped in apatite until diffused away. Because this thermally-controlled diffusion is sensitive to low temperatures, (U-Th)/He ages constrain the recent cooling history of samples. Closure temperature for helium in apatite is quite low (~70ºC for a 10ºC/Myr cooling rate; Wolf et al., 1996; Farley et al., 2000), so that helium ages record the cooling associated with exhumation from shallow crustal depths (~1-3 km for typical geothermal gradients).

Although the idea of using radiogenic helium as a dating technique was first proposed by Ernest Rutherford (1905), initial results were unreliable (c.f. Wolf et al., 1996). Recent interest in (U-Th)/He dating has come about due to improved technology for measuring helium, uranium, and thorium (e.g. Wolf et al., 1996; House et al., 1998, Farley, 2000). In addition, the principles involved have become better understood through recent experimentation. For example, Farley et al. (1996) developed corrections (the F_T correction) for the loss of helium due to long stopping distances of alpha ejection. Improved understanding has increased the value of helium dating. For example, helium ages can be used to deduce detailed thermal histories for crustal sections by numerically solving the diffusion/production equation, rather than simply interpreting them using assumed closure temperature (Wolf et al., 1998). This can account for the time a rock has spent in the zone of partial retention, a temperature window (~40-90º C) in which

helium diffuses at variable rates from apatite. Although apatite has the lowest temperature sensitivity and is most useful for geomorphic studies, other mineral phases can be dated by this technique as well (e.g. Reiners and Farley, 2000).

(U-Th)/He dating of apatite has been used to study the evolution of landscapes in tectonically active mountain belts. House et al. (1998) applied this technique in a uniform elevation transect along the strike of the Sierra Nevada in California and found that the oldest helium ages correspond with the location of major river valleys. Models of the variation in cooling history associated with variable geothermal gradients between valleys and interfluves suggest that aspects of the Sierra Nevada topography may have originated in the early Cenozoic. In another study, Farley et al. (2001) dated rocks along a transect parallel to the strike of the Coast Mountains of British Columbia to investigate regional exhumation history. The results suggest that the topography of the Coast Mountains has been affected by intense erosion by continental and alpine glaciation within the last 2.5 Ma (Farley et al., 2001). In another example, (U-Th)/He proved instrumental in reconstructing the Neogene uplift history of the San Bernardino Mountains of southern California (Spotila et al., 1998). This study demonstrated that two adjacent fault blocks experienced very different uplift histories due to their location along the San Andreas fault zone. These studies demonstrate the potential of the (U-Th)/He technique in geomorphic studies and provide a framework for using the technique to constrain the exhumation experienced in the vicinity of the Blue Ridge Escarpment.

By dating samples along two transects perpendicular to the escarpment, I have tried to constrain the amount of exhumation at different positions along the upland, Piedmont and escarpment zone. The resulting exhumation pattern helps to further test whether the upland and Piedmont surfaces share similar exhumation histories, whether regional fault structures juxtapose rocks of different cooling history (and could therefore have played a role in shaping modern topography), and whether significant divide migration has taken place. Helium dating thus provides important constraints that bear directly on predictions of each hypothesis for escarpment origin.

4.2 Methods

Samples were collected along two transects trending approximately perpendicular to the Blue Ridge Escarpment. Each transect, separated from one another by ~30 km, was ~90 km long and extended ~70 km southeast of the escarpment into the Piedmont. Forty-four samples of mixed lithology (including felsic gneisses, mica schists, granitic intrusions) were collected at ~10-15 km intervals along these transects (Figure 29; Table 5). Of these, 27 samples were selected for mineral separation and processed by *Donelick Analytical, Inc.* for apatite content. The remainder were deemed too weathered, fine-grained, or schistose to yield quality apatite. Of the processed samples, 15 contained apatite grains of suitable quality for (U-Th)/He dating.

Apatite U-Th/He age determinations require several analytical measurements. Approximately 10-20 grains are selected from the apatite fraction of each sample, based on their crystal form, size, and clarity. Each grain is examined under cross polarized light to identify the presence of small birefringent inclusions. Grains with such inclusions are not acceptable for dating. In order to correct for the loss of helium due to alpha election, F_T corrections must be made according to the size and shape of individual crystals (Farley et al., 1996). Helium is extracted from apatite by holding the crystals at 900º C in a high vacuum furnace for ~30 minutes. Helium abundance is measured through isotope dilution by spiking with a known amount of ^{3}He and quadrupole mass spectrometry. Uranium and thorium contents are then measured on the same aliquots of apatite following HNO_3 dissolution and ^{235}U and ^{230}Th spiking, by isotopic dilution with inductively-coupled plasma mass spectrometry (ICP-MS). (U-Th)/He age is calculated using the formula:

$$\#\,He = [(8)\,(Ab)\,(\#^{238}U)\,(e^{\lambda t}-1) + (7)\,(Ab)\,(\#^{235}U)\,(e^{\lambda t}-1) + (6)\,(Ab)\,(\#^{232}Th)\,(e^{\lambda t}-1)]$$

where, Ab = natural abundance of each respective isotope, λ = decay constant of each respective isotope, t = (U-Th)/He age, and # = number of atom of each isotope in sample. The integers represent the number of alpha particles emitted during the decay series of each isotope. The uncorrected age is divided by the calculated F_T value (derived from grain volume and shape measurements) in order to get a true helium age.

All but one of the (U-Th)/He ages in this study were measured at Washington State University by Dr. P. Reiners (now at Yale University). Analytical uncertainties for these ages are ~6%, based on comparison with the reproducibility of Durango fluoroapatite and other standards. One reported age (GB21-1) was measured in the new helium dating facility at Virginia Tech. The same analytical techniques were employed, although U/Th were measured by ICP-MS by *Activation Laboratories Ltd.* (Ancaster, Ontario). Although the Virginia Tech facility has measured Durango fluoroapatite to within ~5% of its known age with ~5% (1σ) reproducibility, additional work is required to fully characterize the performance of this new facility. The uncertainty of the GB21-1 age may thus be higher (~10%, 2σ) than the ages measured at Washington State University. For interpretation, however, I treat this age the same as the others.

In some cases, the accuracy of (U-Th)/He ages can be far worse than reported analytical reproducibility, due to the presence of U-Th-bearing inclusions in the apatite grains. One sample (GB4) produced an anomalously old age of 281 Ma (Table 6). The source of this sample is granite from the Alleghanian (~360 Ma; Sinha, pers. comm.) Mt. Airy pluton in North Carolina. Visual inspection of apatite from this sample revealed that ~90% of the grains contained birefringent inclusions and other defects. Although the most pure grains were selected for dating, it is possible that sub-microscopic U- or Th-bearing inclusions may have resulted in an anomalously old age. To test this, I examined eight apparently inclusion-free apatite crystals using scanning electron microscopy. Within some grains, very small (<3 microns) zircon inclusions were found (Figure 31). It is impossible to know whether the dated grains contained any micro-inclusions, but it seems likely given its old age. The 281 Ma age for GB4 is thus excluded from the following interpretations.

4.3 Results

A total of thirteen dates have been measured so far from nine samples (Table 6, Figure 29). The ages range from 89 Ma to 197 Ma, excluding the anomalously old age from GB4. Samples that were dated multiple times reproduced reasonably well, with the greatest difference being ~16% (Table 6). In addition, sample GB21, dated at the

Virginia Tech facility, overlapped with the age of the nearest sample dated at Washington State University (GB2, Table 6).

The most apparent trend in the distribution of ages is in the dichotomy between the upland and Piedmont (Figure 32). The average upland age is ~177 Ma, while the average Piedmont age is ~116 Ma. A secondary trend is found in the distribution of Piedmont ages. Despite a change in elevation of only 200 m, ages appear to become younger with increasing distance from the escarpment to ~20 km distance, at which point ages begin to increase with distance (Figure 30). Ages along the northern transect also appear to be slightly younger than their counterparts to the southwest (Figure 30).

The fact that clear trends have emerged with minimal data is very important for this study. These trends in age distribution may be important in interpreting exhumation patterns and may bear on the origin of the escarpment. This pattern is discussed in the following section. Although these early trends are discussed here, additional ages will be required for a more rigorous analysis.

4.4 Interpretations

The age dichotomy between the upland and Piedmont has important implications. The difference implies that the two domains have experienced not only different topographic development but different exhumation histories. Based on this pattern, it is unlikely that the upland and Piedmont are an offset surface with the same origin. In addition, these ages show no clear relationship to the location of major faults. Normal-sense motion along the Bowens Creek-Brevard Fault zone cannot explain the age difference between the upland and Piedmont because the sense of displacement implied by the age dichotomy is reversed. Reverse faulting along this southeast-dipping fault could account for the age distribution observed, but this would have created a northwest-facing escarpment rather than the existing landform (Figure 33). Other Piedmont faults, such as the Danville Basin border fault or the Shacktown fault, also appear to have no effect on the (U-Th)/He ages (Figure 30).

One possible explanation for the age difference of the two domains may simply be their elevation difference. If the isochrons are flat along the length of the transects, the average age difference (~61 Ma) and the vertical separation (~500 m) of the upland and

Piedmont would translate to an elevation/age gradient of 0.0082 mm/yr (Figure 34). Such a gradient could only be produced by very slow exhumation or crustal stasis in the helium partial retention zone. If a reasonable closure temperature and geothermal gradient are assumed (see Table 7), an exhumation rate of 0.0082 mm/yr would require 366 Myr to reach the present age difference between the upland and Piedmont. This is at odds with previous thermochronometric studies conducted nearby. For example, Ar/Ar dating on hornblende and biotite show that gniesses and granites of the eastern Piedmont were still well above 200ºC only two hundred million years ago (Gates and Glover, 1988). In addition, sphene and zircon fission track ages (T_c > 200º C) from the Piedmont northeast of Washington (Kohn et al., 1993) and apatite fission track ages (T_c ~105ºC) from the Valley and Ridge near Radford, VA (Roden, 1991) are both ~150-200 Ma. These studies show that cooling history of rocks from adjacent areas are inconsistent with such a slow exhumation rate. It therefore seems unlikely that the (U-Th)/He age pattern represents a simple age-elevation distribution exposed by erosion of rock with flat isochrons.

Another possible explanation for this age distribution is that the isochrons are bent. Ideally, this would be tested by suites of (U-Th)/He dates spanning vertical crustal sections, but the subdued topography of the study area precludes this. It is possible, however, to estimate the shapes of isochrons by calculating exhumation rates for each location. Assuming a geothermal gradient of 20ºC/km (from Geothermal Data – Virginia Tech Regional Geophysics Laboratory, http://rglsun1.geol.vt.edu/va.html) and a closure temperature of ~65ºC for helium in apatite (Wolf et al., 1996; Warnock et al, 1997), ages on the upland and Piedmont can be translated into long-term exhumation rates (Table 7). The average calculated rates for the upland and Piedmont, 0.017 mm/yr and 0.026 mm/yr respectively, are comparable to other estimates of regional denudation rate for the Appalachians (Pavich and Obermeier, 1985; Gardner and Sevon, 1989; Granger and Kirchner, 1995). With these rates, I can estimate the shapes of isochrons along the transects.

At the slow average exhumation rate for the upland, it would take 177 Myr (i.e. the average age) to bring rocks from their closure depth to their present position at the surface. In a similar period, the higher exhumation rates estimated for the Piedmont

would result in a greater magnitude of exhumation. For example, at the location of GB3 (119 Ma), an inferred exhumation rate of 0.025 mm/yr would correspond to a total exhumation of 4.46 km over 177 Myr. While ~3 km of this would have brought the rocks from closure depth to the surface, an additional 1.46 km of exhumation would have occurred. This difference positions the inferred 177 Ma isochron high above the present Piedmont surface. Using this approach, the position of the 177 Ma isochron can be inferred along the transects, showing a large bulge over the Piedmont (Figure 35).

The inferred locus of exhumation southeast of the escarpment along the inner Piedmont may explain the age difference between the upland and Piedmont and has important implications for escarpment development. The non-uniform distribution of exhumation implies that northwesterly divide and escarpment migration has occurred. This matches the predictions made by three hypotheses for escarpment genesis (Figures 5,7,8). Helium ages are thus very useful, as the exhumation patterns they constrain illustrate kinematic erosional patterns that are not apparent with topography alone. However, caveats to this interpretation must be made. First, additional ages must be measured along the transects to better constrain the apparent pattern. Second, rather than assuming a closure temperature and inferring long-term average exhumation rates, it would be more robust to model the thermal history of samples using numerical solution to the helium production-diffusion equation (e.g. Wolf et al., 1998). By incorporating other thermochronometric data into these models, it may also be possible to examine what effect variable geothermal gradients may have had. Geothermal gradients in the region are sure to have varied over the past 200 Myr and were sure to have been higher than 20ºC/km in the Mesozoic. Future work may further constrain the pattern of exhumation across the region.

Chapter 4 – Figure and Table Captions

Figure Captions

Figure 29 – Sample location map. Map created from USGS 30-m DEMs using Microdem. Yellow triangles are dated samples. Blue triangles are processed, ubt undated samples. Major geologic structures are also shown.

Figure 30 – Location map with ages. Map created from USGS 30-m DEMs using Microdem. Sample ages are given in millions of years (Ma). Samples with replicate ages display two ages. Sample GB4 (281 Ma) is shown in red because of it's erroneous age and is not included in exhumation calculations. The topographic profile (A-A') used in Figure 35 is also shown.

Figure 31 – Scanning Electron Microscope image of Zircon inclusion in Apatite grain (Sample GB4). Mineral identity is confirmed by EDS. Line drawing of apatite grain shows location of zircon inclusion.

Figure 32 – Age-Elevation plot of samples. Sample GB 4 is not included.

Figure 33 – Hypothetical scenario required if (U-Th)/He age distribution were the result of flat isochrons and near-field faulting. The result would be a northwest-facing escarpment.

Figure 34 – Topographic profile across escarpment with flat isochrons. If elevation difference is solely responsible for age distribution, it would require ~366 Ma to excavate 3 km of Piedmont. This is too long a time and too slow an exhumation rate when compared to other thermochronometers.

Figure 35 – Reconstruction of isochrons illustrating the increased exhumation across the Piedmont. The approximate position of the average upland isochron (177 Ma) is projected over the Piedmont by assuming a closure temperature of 65ºC and a geothermal gradient of 20ºC/km. Double lines represent conservative 2σ error associated with (U-Th)/He technique. The area between the 177 Ma isochron and the ground surface is the amount of exhumed material since 177 Myr. The maximum slope of the of projected isochron is ~3.5º over ~35 km. The location of this bulge is consistent with the idea of divide and escarpment migration. The location of the transect is shown on Figure 30. The lower profile (no vertical exaggeration) shows only a slight bulge in exhumation.

Table Captions

Table 5 – Sample list with location and description of each dated sample.

Table 6 – Dated samples with thermochronometric measurements and age data. Correction factor (Ft) from Farley (1996). U, Th, He abundances used to calculated raw age.

Table 7 – Age, exhumation rate, and exhumation magnitude for each dated sample. Exhumation rates and magnitude are calculated using the conditions shown below table.

Figure 29

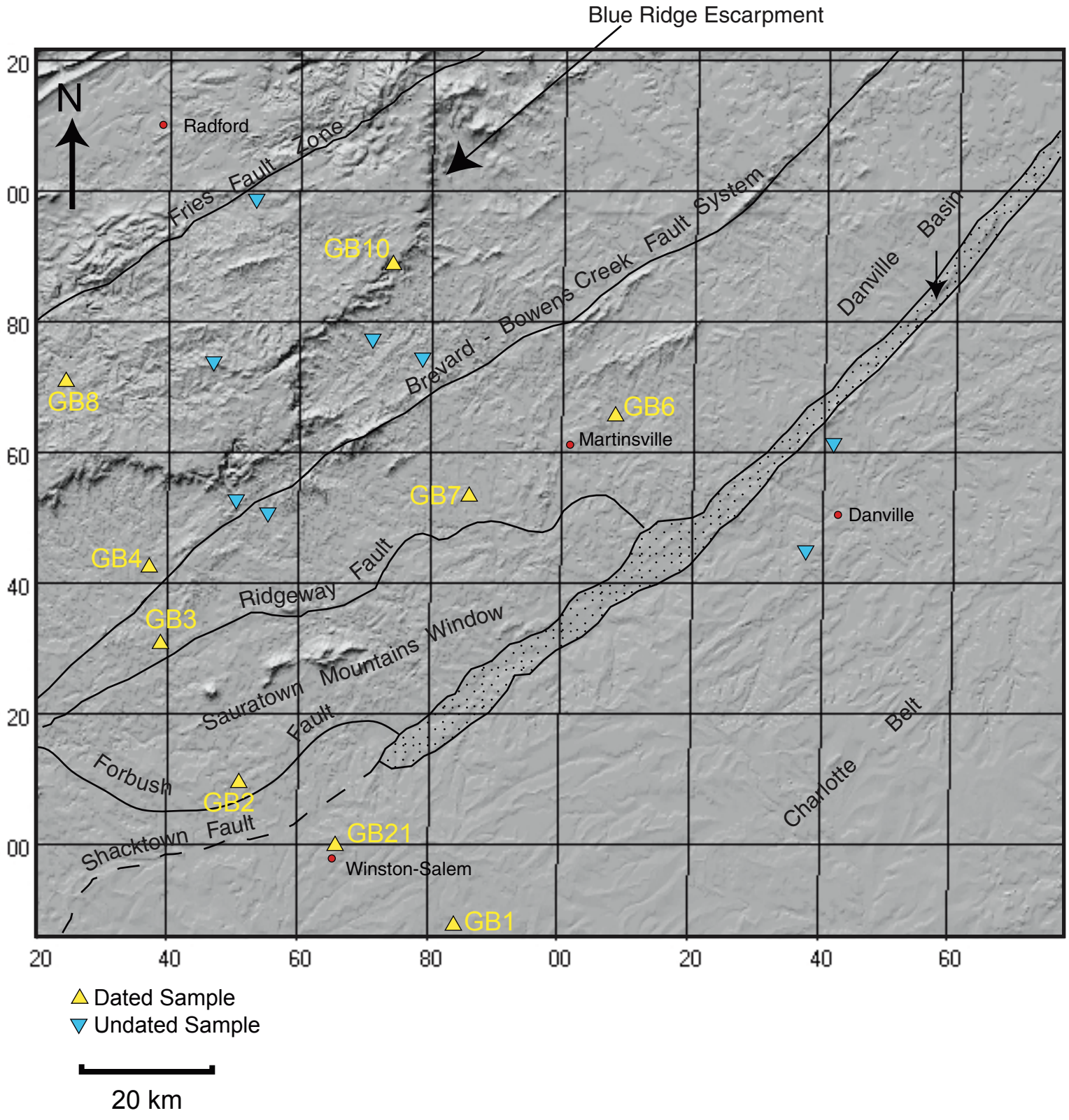
Blue Ridge Escarpment
N
Radford
Fries Fault Zone
Brevard - Bowens Creek Fault System
Danville Basin
GB10
GB8
GB6
Martinsville
GB7
Danville
GB4
Ridgeway Fault
GB3
Sauratown Mountains Window
Fault
Forbush
GB2
Shacktown Fault
GB21
Winston-Salem
GB1
Charlotte Belt
20
00
80
60
40
20
00
20
40
60
80
00
20
40
60
Dated Sample
Undated Sample
20 km

Figure 30

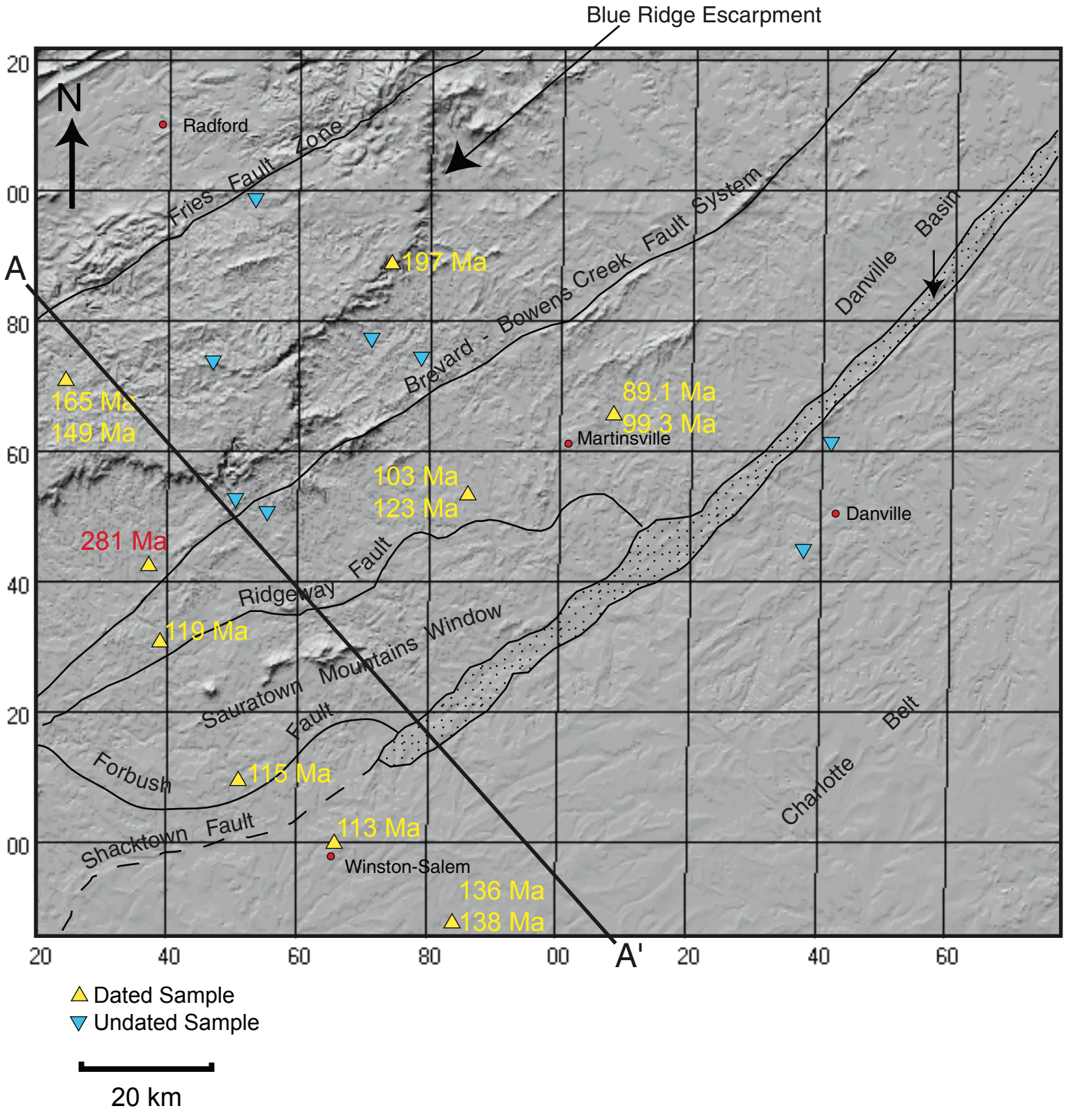
Blue Ridge Escarpment
N
Radford
Fries Fault Zone
Brevard - Bowens Creek Fault System
Danville Basin
A
197 Ma
165 Ma
149 Ma
89.1 Ma
99.3 Ma
Martinsville
103 Ma
123 Ma
Danville
281 Ma
Ridgeway Fault
119 Ma
Sauratown Mountains Window
Fault
Forbush
115 Ma
Charlotte Belt
Shacktown Fault
113 Ma
Winston-Salem
136 Ma
138 Ma
A'
20
00
80
60
40
20
00
20
40
60
80
00
20
40
60
Dated Sample
Undated Sample
20 km

Figure 31

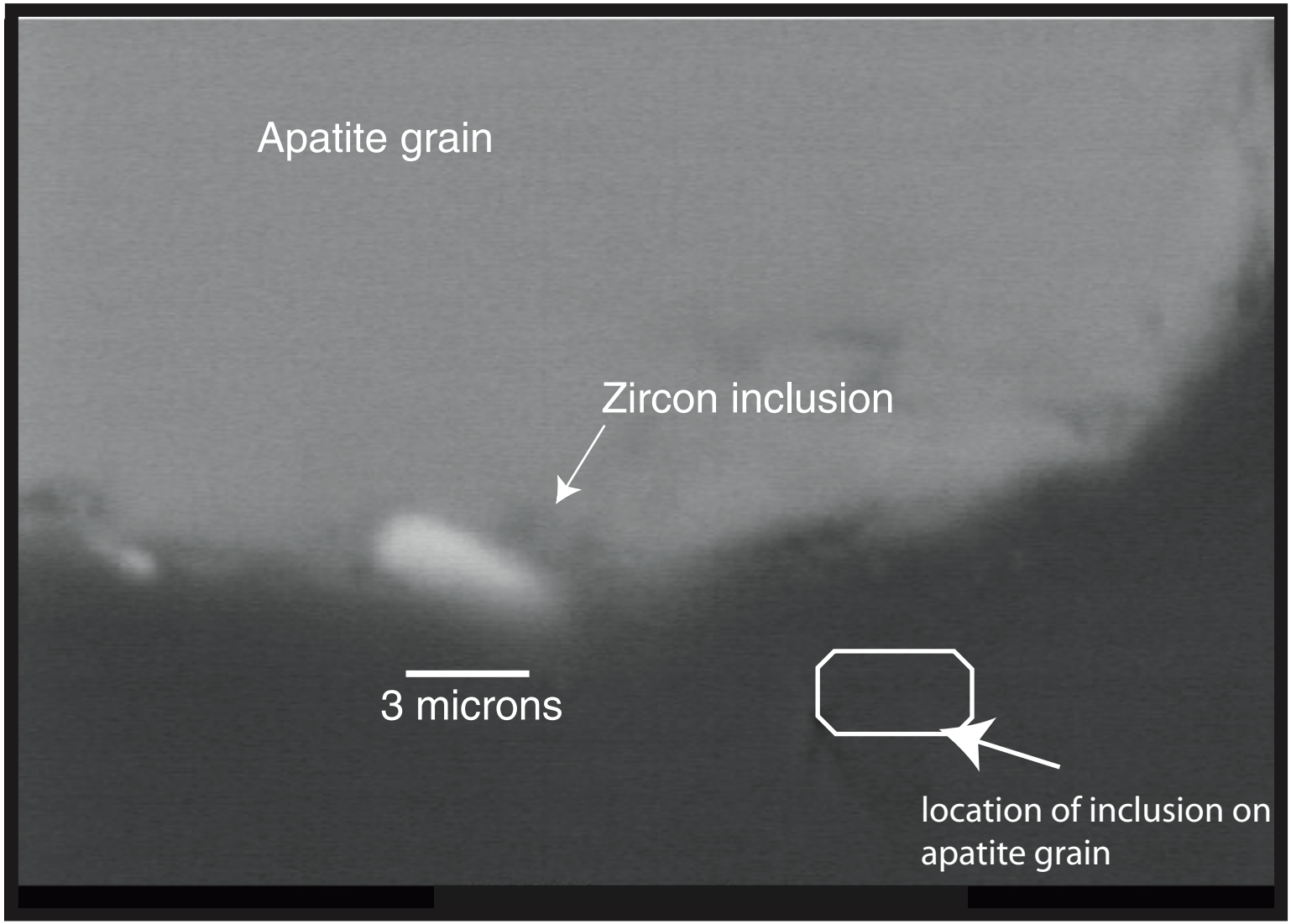
Apatite grain
Zircon inclusion
3 microns
location of inclusion on
apatite grain

Figure 32

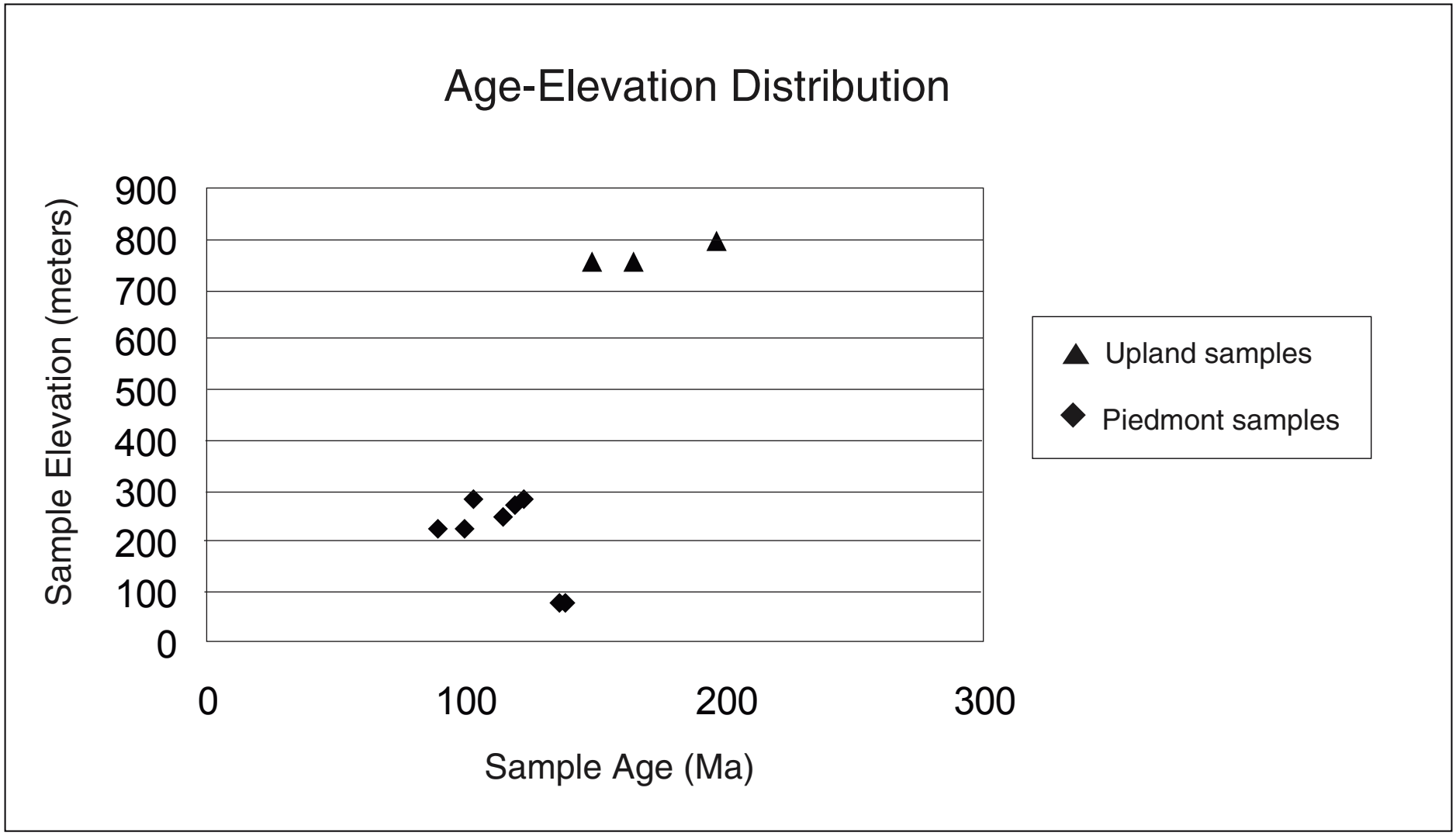
Age-Elevation Distribution
Sample Elevation (meters)
900
800
700
600
500
400
300
200
100
0
0
100
200
300
Sample Age (Ma)
Upland samples
Piedmont samples

Figure 33

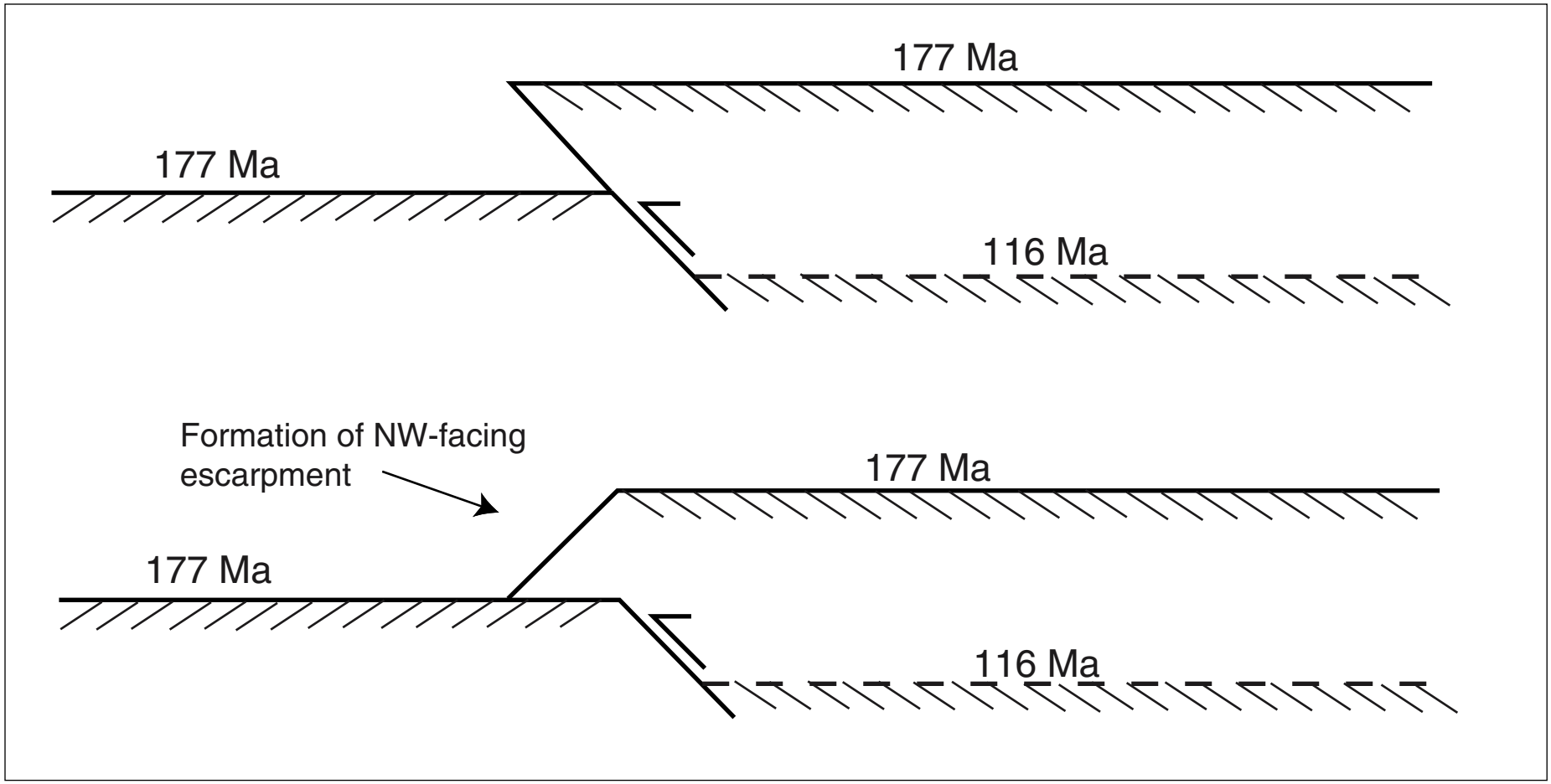
177 Ma
177 Ma
116 Ma
Formation of NW-facing
escarpment
177 Ma
177 Ma
116 Ma

Figure 34

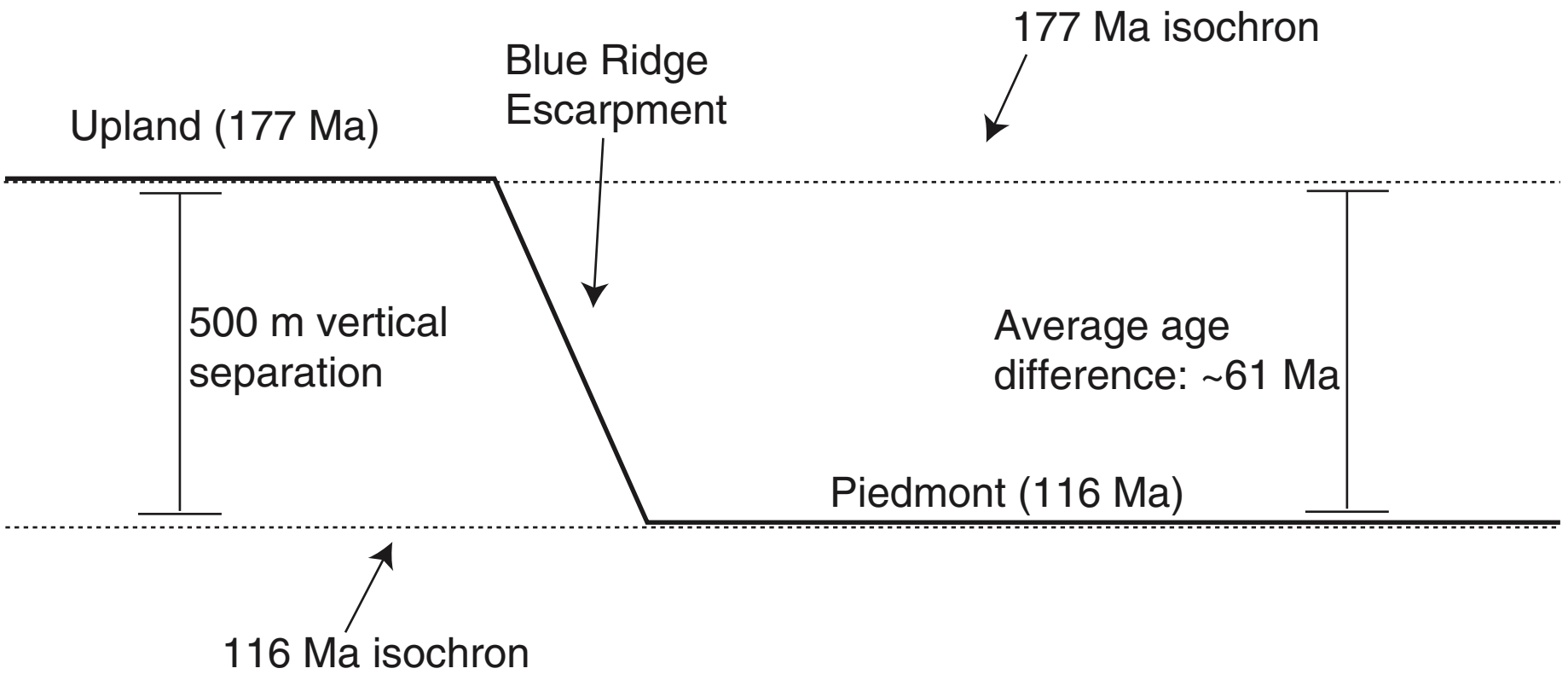

500 m / 61 Ma = 0.0082 mm/yr

It would require ~366 Myr from the time the upland reached closure depth until the present in order to attain this age difference, assuming flat isochrons. This length of time is too long and the exhumation rate too slow.

Figure 35

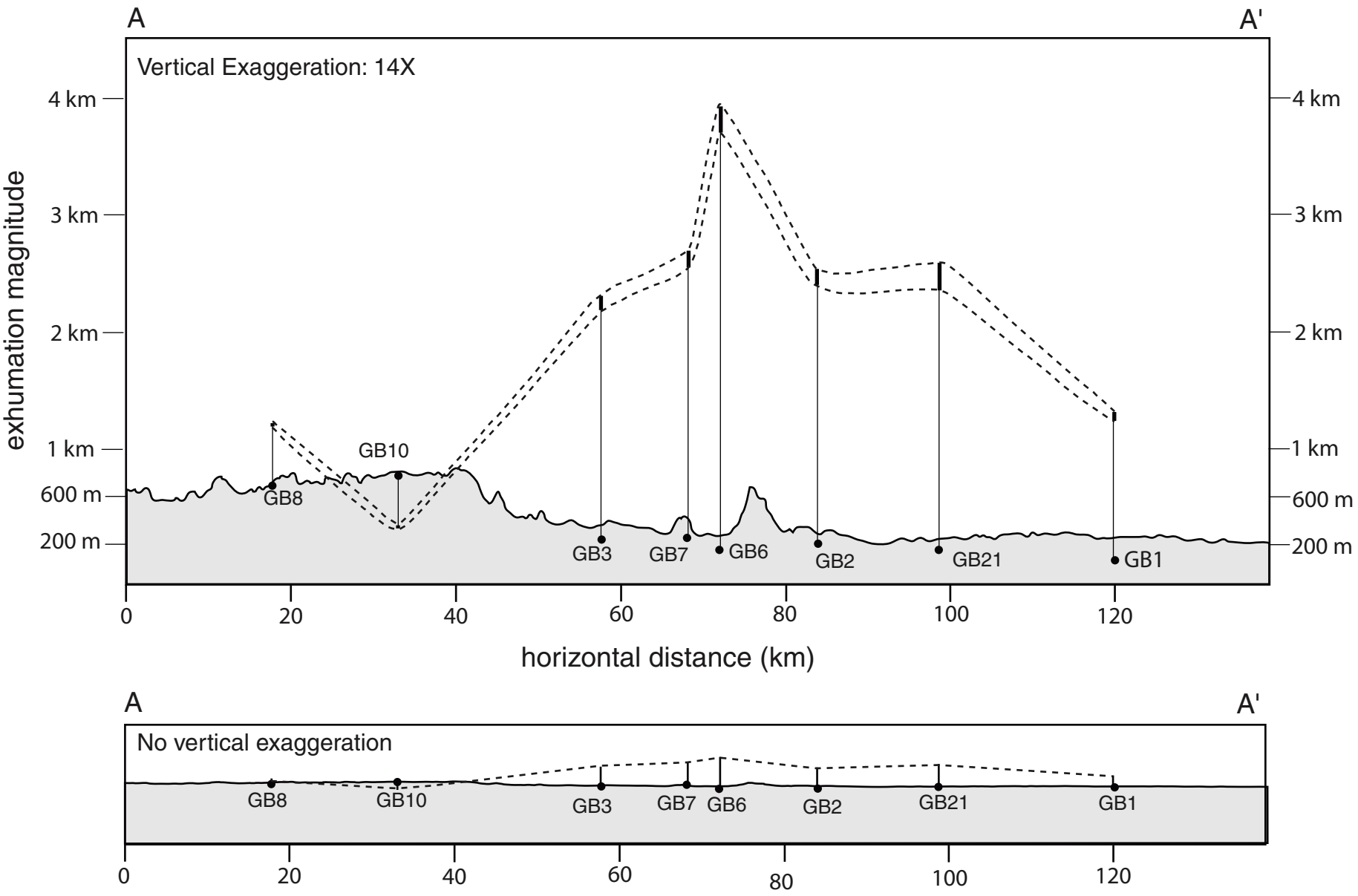
A
A'
Vertical Exaggeration: 14X
4 km
3 km
2 km
1 km
600 m
200 m
exhumation magnitude
GB8
GB10
GB3
GB7
GB6
GB2
GB21
GB1
0
20
40
60
80
100
120
horizontal distance (km)
A
A'
No vertical exaggeration
GB8
GB10
GB3
GB7
GB6
GB2
GB21
GB1
0
20
40
60
80
100
120

Table 5

Sample	Lat., min.		Long., min		elev, m	Location notes		
GB1	36	1.11	80	3.55	260	Vulcan e. quarry, south Winston-Salem, NC (311 and 52), coordinates imprecise		
GB2	36	12.951	80	25.802	246	Donnaha, NC		
GB3	36	24.467	80	33.847	268	Ararat, NC		
GB4	36	30.35	80	35.07	330	Mt. Airy, NC, North Carolina Granite Company Quarry, *coordinates imprecise		
GB6	36	43.290	79	47.192	226	near Leatherwood, VA		
GB7	36	36.686	80	2.295	281	road cut where N.Fork of Mayo River crosses Rt. 58		
GB8	36	46.006	80	43.561	750	Hillsville, VA		
GB10	36	55.092	80	10.117	792	Floyd County, near edge of Blue Ridge Escarpment; Rt. 648		
GB21	36	10.65	80	15.75	853	Vulcan North Quarry in Winston-Salem, NC		

Sample	Sample notes			Apatite notes	Volume
GB1	granite, large plag, phenocrysts, fresh			large grains, some good, clean, nice pickings	v. large
GB2	fine grained biotite gneiss, slightly weathered			big grains, some dark, a few good ones, but hard to pick	med-small
GB3	gneissic schist, fresh			long thin grains, small, little etching, good grains, easy	medium
GB4	granite, fresh			nice grains, small, zircons, lots of inclusions (SEM)	medium
GB6	amphibolite, fresh			good quality, not weathered or fractured, workable	medium
GB7	gneiss, little weathered			rounded, etched grains, few decent ones, hard to pick	v. large
GB8	biotite gneiss, fresh			weathered, crappy, fractured, hard to pick	v. large
GB10	quartz-feld gneissic metadiorite, medium sample			weathered, anhedral, rounded, crappy, difficult	medium
GB21	green gneiss, laminated, amphibolite, little weathered			perfect, great, euhedral, no inclusions, big grains	medium

Table 6

sample name	raw age (Ma)	FT	corr'd age (Ma)	est. err., Ma (2s)	mass (ng)	U ppm	Th ppm	He (ncc/mg)
Piedmont Samples								
GB1a	96.7	0.71	136	8	1.56E+04	6.7	5.2	92.6
GB1b	104	0.75	138	8	3.85E+04	10.0	9.2	154.6
GB2a	72.7	0.63	115	7	1.28E+04	5.9	0.9	53.8
GB3a	84.2	0.71	119	7	1.41E+04	27	1.2	280
GB6a	54.3	0.61	89.1	5	5.45E+03	22	62	241
GB6b	69.8	0.70	99.3	6	2.43E+04	26	70	366
GB7a	82.7	0.80	103	6	2.82E+04	4.5	15.6	82.5
GB7b	103	0.84	123	7	1.26E+05	8.5	30.7	198.5
GB21a	83.90	0.74	113	11	1.59E+07	20.7	37.0	
GB4a	169	0.60	281	17	4.28E+03	3.6	11.0	128
Upland Samples								
GB8a	136	0.83	165	10	2.87E+04	1.2	1.2	25.0
GB8b	122	0.82	149	9	7.42E+04	1.2	0.8	20.3
GB10a	129	0.66	197	13	1.54E+04	0.3	1.1	9.1

Table 7

Sample Number	Age (Ma)	Exhumation Rate (mm/yr)	Exhumation Magnitude (km)
GB1	137	0.022	3.9
GB2	115	0.026	4.6
GB3	119	0.025	4.5
GB6	94.2	0.032	5.6
GB7	113	0.026	4.7
GB21	113	0.026	4.7
Piedmont averages	**115.6**	**0.026**	**4.6**
Upland			
GB8	157	0.019	
GB10	197	0.015	
Upland Averages	**177**	**0.017**	**3.0**
thermal conditions:			
T_c = 65º C	$^{dT}/_{dZ}$ = 20º C/km	$T_{ambient}$ = 5º C	

T_c – closure temperature of apatite (U-Th)/He technique

$^{dT}/_{dZ}$ – geothermal gradient

$T_{ambient}$ – the average assumed surface temperature

Exhumation Magnitude – the amount of exhumation experienced at a particular location relative to an arbitrary isochron (e.g. 177 Ma isochron); i.e., amount of exhumation experienced over the past 177 Ma, using the exhumation rate for each sample site.

Chapter 5 –Conclusions

5.1 Elimination of Hypotheses

This study has employed three very different approaches in order to examine the origins of the Blue Ridge Escarpment. Each approach on its own has yielded valuable, if complicated, information that can be used to interpret the landscape age and the magnitude of exhumation experienced by the upland and Piedmont domains as well as the degree of migration experienced by the escarpment itself. When the results of these three approaches are combined, it is evident that three hypotheses on escarpment generation can be eliminated, while three remain viable.

The findings of topographic analysis, field studies, and thermochronometry have important implications for the erosion kinematics of the region of the escarpment. First, it is suggested by the analysis of topography that the Blue Ridge upland possesses an older landscape age than the Piedmont. Field studies in the form of meander geometry and stream sinuosity support this argument. Average (U-Th)/He ages from the upland and Piedmont appear to confirm that the upland landscape is older than its Piedmont counterpart. Second, divide migration appears to have occurred. Field evidence such as beheaded channels and cases of drainage basin capture demonstrate that the westward-draining upland is shrinking due to the more vigorous action of Atlantic-draining Piedmont streams. This is compatible with the changes seen with increasing downstream distance of basins draining the eastern side of the divide and with the increasingly subdued topography leading toward the base of the escarpment from the southeast. (U-Th)/He ages also lend support to the idea of divide migration. Ages tend to become younger as the divide is approached from the southeast, indicating that exhumation has been most energetic just to the east of the divide. Lastly, (U-Th)/He ages show that exhumation has not been equal in the upland and Piedmont domains over the past 150 Ma, demonstrating that the upland and Piedmont are not simply an offset erosional surface. In addition, the old ages (all > 89 Ma) found throughout the study region indicate that rejuvenation, if it has occurred, has not played a major role in shaping the topography of the Piedmont and upland or has not occurred for a long enough period to have an effect on these domains.

Based on these findings, three hypotheses can be eliminated outright because their predictions for landscape age, exhumation magnitude, and degree of divide migration do not match the observations. For example, escarpment formation by lithologic control (Figure 3) predicts that no divide migration should occur. In addition, this hypothesis predicts that little variation in exhumation in the Piedmont should take place and that the age of upland and Piedmont topography should not greatly differ. Localized geodynamic uplift (Figure 4) is another hypothesis that may be eliminated because it predicts no divide migration. It also requires that exhumation be greatest at the divide and decrease with distance to either side. Neither of these predictions is consistent with the observations. The last hypothesis that can be discarded is recent near-field normal faulting (Figure 6). There is no evidence of a border normal fault near the base of the escarpment that would have undergone enough offset to create the Blue Ridge Escarpment. Such a fault would create an exhumation pattern that contrasts with the observed pattern. Lastly, even the youngest (U-Th)/He ages are late-Mesozoic, precluding the likelihood a more recent, large-scale faulting event.

5.2 Viability of remaining Hypotheses

The three remaining hypotheses make predictions about landscape age, magnitude of exhumation, and degree of divide migration that match observations. Therefore, based on the available data, it is impossible to distinguish between the ideas. Increased (U-Th)/He dating, in combination with apatite fission track ages, may yield a more detailed exhumation history for the study area, thereby further narrowing the field of hypotheses.

It is possible, however, that the most likely answer is a combination of these three ideas. Two hypotheses, rift-flank uplift (Figure 7) and flexure and isostatic compensation (Figure 8), are genetic in nature. They describe the mechanism by with the escarpment was initiated and maintained. It is not difficult to envision a scenario in which an asymmetric divide is initiated by Mesozoic rift-flank uplift. This uplift causes increased erosion (base level drop via tectonic uplift) in the Appalachian Mountains. Mass removal and transportation from the Appalachian orogen causes loading at the Atlantic margin. Deposition at the margin and isostatic compensation within the mountain belt allows more uplift to occur, driving further erosion. In this way, both rift-flank uplift and

flexure are accommodated. The third hypothesis, headward migration of an asymmetric divide, is not genetic. It describes the nature of the divide and fits into the framework of the synthesized hypothesis presented above. The additional detail it provides is the presence of a belt of resistant rock west of the Blue Ridge (the Alleghany Plateau) that "holds up" the upland and prevents widespread denudation of the upland by westward-draining streams. This resistant belt is what has allowed the escarpment and divide remain steep over such a long timescale.

The last troubling detail is the presence of such sharp topography after >200 million years of erosion and relative tectonic passivity. Using the central Appalachian Mountains as a template, recent modeling has shown that post-orogenic decay may occur over a timescale of 100s of million years (Stephenson, 1983; Baldwin et al., submitted). Such a model, if applicable, could mean that the combined rift-flank uplift / flexure model is a viable explanation for the origin of the Blue Ridge Escarpment.

5.3 Future directions

The results of this study are promising but more work is required before a full story can be told. The methods used in this analysis have helped to shape the avenues to be taken in the future. I feel that any more forays into the use of topography to determine relative age relationship will be of little worth at this scale. Instead, approaches should bear down on particular components of topography to find answers for the larger questions. For example, studies on relict Piedmont terraces may prove very useful in constraining the timing of divide migration. These terrace may even contain material suitable for cosmogenic dating Another component of the landscape that may be examined is saprolite. Calculating saprolite formation rates, thicknesses, and distance from the escarpment would place yet another constraint on the timing of migration.

In addition to these field studies, more thermochronometric ages would prove useful. Better coverage for (U-Th)/He dating, especially across major structures such as the Brevard fault zone, will confirm whether or not displacement has occurred. Apatite fission track is also currently being performed on select samples in order to compliment the (U-Th)/He ages. Lastly, modeling of the still-viable hypotheses (flexure, loading,

rift-flank uplift) will help to fill the gaps remaining in the work on the development of the Blue Ridge Escarpment.

References

Ahnert, F. 1970 Functional relationships between denudation, relief, and uplift in large mid-latitude drainage basins. *American Journal of Science*, 268, 243-263.

Baldwin, J.A., Whipple, K.X., Tucker, G.E., submitted 2001, Implications of the shear-stress river incision model for the timescale of post-orogenic decay of topography, submitted to *Journal of Geophysical Research*.

Battiau-Queney, 1989, Constraints from deep crustal structure on long-term landform development of the British Isles and Eastern United States, *Geomorphology*, 2, 53-70.

Braun, J. and Sambridge, M., 1997, Modelling landscape evolution on geological time scales: A new method based on irregular spatial discretization. *Basin Research*., 9, 27-52.

Brown, R.W., Rust, D.J., Summerfield, M.A., Gleadow, A.J.W., De Wit, M.C.J., 1990. An Early Cretaceous phase of accelerated erosion on the south-western margin of Africa: Evidence from apatite fission track analysis and the offshore sedimentary record. *Nucl. Tracks Radiat. Meas*., 17, 339-350.

Blythe, A.E., Burbank, D.W., Farley, K.A., Fielding, E.J., 2000, Structural and topographic evolution of the central Transverse Ranges, California, from apatite fission-track, (U-Th)/He and digital elevation model analyses. *Basin Research*, 12, 97-114.

Burbank, D.W., Leland, J., Fielding, E., Anderson, R.S., Brozovic, N., Reid, M.R., Duncan, C., 1996, Bedrock incision, rock uplift and threshold hillslopes in the northwestern Himalayas, *Nature*, 379, 505-510.

Carlston, C.W., 1963, Drainage density and streamflow, *U.S.Geol Survey Prof. Paper*, 422-C, 1-8.

Carlston, C.W., 1965, The relation of free meander geometry to stream discharge and its geomorphic implications, *American Journal of Science*, 263, 864-885.

Chorley, R.J., 1957, Climate and morphometry, *Journal Geology*, 65, 628-638.

Costain, J. and Coruh, C., 1989, Tectonic setting of Triassic half-grabens in the Appalachians; seismic data acquisition, processing, and results. *AAPG Memoir*, 46, 155-174

Culling, W.E.H., 1960, Analytical theory of erosion. *Journal of Geology*, 68, 336-344.

Davis, W.M, 1903, The stream contest along the Blue Ridge, *Geog Soc Phila*, B, 3, 213-244.

Densmore, A.L. and Hovius, N., 2000, Topographic fingerprints of bedrock landslides. *Geology* (Boulder), 28, 371-374.

Dietrich, R.V., 1959, Geology and mineral resources of Floyd County of the Blue Ridge Upland, southwestern Virginia. *Bulletin of the Virginia Polytechnic Institute*, 12.

Dietrich, R.V., 1957, Origin of the Blue Ridge Escarpment directly southwest of Roanoke, Virginia. *Virginia Journal of Science*, 9, 233-246.

Espenshade, G.H., Rankin, D.W., Shaw, K.W., Neuman, R.B., 1975, Geologic map of the east half of the Winston-Salem Quadrangle, North Carolina-Virginia. USGS map.

Farley, K.A., Wolf, R.A., Silver, L.T., 1996, The effects of long alpha-stopping distances on (U-Th)/He ages, *Geochimica et Cosmochimica Acta*, 60, 4223-4229.

Farley, K.A., 2000, Helium diffusion from apatite; general behavior as illustrated by Durango fluorapatite, *Journal of Geophysical Research*, B, Solid Earth and Planets, 105, 2903-2914.

Farley, K.A., Rusmore, M.E., Bogue, S.W., 2001, Post-10 Ma uplift and exhumation of the northern Coast Mountains, British Columbia, *Geology*, 29, 99-102.

Friedkin, J.F., 1945, [Monograph] A laboratory study of the meandering of alluvial rivers, 60 pp.

Gardner, T.W. and Sevon, W.D., 1989, [Monograph] Appalachian geomorphology, *Geomorphology*, 2, 318 pp.

Gilbert, G.K., 1909, The convexity of hilltops. *Journal of Geology*, 17, 344-350.

Gilbert, G.K., 1914, The transportation of debris by running water. *U.S.G.S. Prof. Paper* 86, 263 pp.

Gilchrist, A.R., Kooi, H., Beaumont, C., 1994, Post-Gondwana geomrphic evolution of southwestern Africa: Implications for the controls on landscape development from observations and numerical experiments. *Journal of Geophysical Research*, 99, 12,211-12,228.

Granger, D.E. and Kirchner, J.W., 1995, Downcutting rate of the New River, Virginia, from (super 26) Al/ (super 10) Be in buried river gravels, *Eos, Transactions*, American Geophysical Union, 76, 689 pp.

Gregory, K.J. and Gardiner V., 1975, Drainage density and climate, *Zeitschrift fur Geomorphologie Neue Folge*, 19, 287-298.

Guth, P.L., 1995, Slope and aspect calculations on gridded digital elevation models: Examples from a geomorphometric toolbox for personal computers: *Zeitschrift fur Geomorphologie N.F. Supplementband* 101, 31-52.

Hack, J.T., 1957, Studies of longitudinal stream profiles in Virginia and Maryland, *USGS Professional Paper* 294-B, 97 pp.

Hack, J.T., 1973, Drainage adjustment in the Appalachians. in Morisawa, Marie, ed., *Fluvial Geomorphology*, 51-69.

Hack, J.T., 1978, [Monograph] Rock control and tectonism; their importance in shaping the Appalachian Highlands, *Open-File Report - U. S. Geological Survey, Report*: OF 78-403, 39 pp.

Hack, J.T., 1982, [Monograph] Physiographic divisions and differential uplift in the Piedmont and Blue Ridge, *U.S. Geological Survey Professional Paper*, Report: P 1265, 49 pp.

Hayes, C.W. and Campbell, M.R., 1894, Geomorphology of the southern Appalachians, *National Geographic*, 63-126.

Henika, W.S., Beard, J., Tracy, R., Wilson, J.R., 2000, Structure and tectonics field trip to the eastern Blue Ridge and western Piedmont near Martinsville, Virginia. *Virginia Minerals*, 46, 17-31.

Horton, R.E., 1945, Erosional development of streams and their drainage basins; hydrographical approach to quantitative morphology, *Geol. Soc. Amer Bull*., 56, 275-370.

House, M.A., Wernicke, B.P., Farley, K.A., 1998, Dating topography of the Sierra Nevada, California, using apatite (U-Th)/He ages, *Nature*, 396, 66-69.

Hubbard, S.S., Coruh, C., Costain, J.K., 1991, Paleozoic and Grenvillian structures in the southern Appalachians: extended interpretation of seismic reflection data. *Tectonics*, 10, 141-170

Hurtrez, J.E., Sol, C., Lucazeau, F., 1999, Effect of drainage area on hypsometry from an analysis of small-scale drainage basins in the Siwalik Hills (central Nepal)., *Earth Surface Processes and Landforms*, 24, 799-808.

Hurtrez, J.E., Lave, J., Avouac, J.P., 1999b, Investigation of the relationships between basin morphology, tectonic uplift, and denudation from the study of an active fold belt in the Siwalik Hills, central Nepal, *Journal of Geophysical Research*, 104, 12,779-12,796.

Jacobson, R.B., McGeehin, J.P., Jacobson, A.R., 1991, Geographic information system analysis of landslide locations, *Eos, Transactions,* American Geophysical Union, vol.72, 137 pp.

Johnson, D.W., 1933, Origin of the Blue Ridge Escarpment (abstract). *Geol. Soc. Am. Bull.* 44, 87.

Jones, J.G. and Veevers, J.J., 1982, A Cainozoic history of Australia's Southeast Highlands, *Journal of the Geological Society of Australia*, 29, 1-12.

King, L.C., 1953, Cannons of landscape evolution, *Geological Society of America Bulletin*, 64, 721-752.

King, L.C., 1955, Pediplanation and isostacy: an example from South Africa, *Q.J. Geol. Soc. London*, 111, 353-359.

Kirchner, J.W., 1993, Statistical inevitability of Horton's laws and the apparent randomness of stream channel networks, *Geology* (Boulder), vol.21, 591-594.

Kirkby, M.J., 1980, The stream head as a significant geomorphic threshold, in Thresholds in Geomorphology, eds: Coates, D.R. and Vitek, J.D., pp. 53-73.

Kirkby, M.J., 1987, Modelling some influences of soil erosion, landslides, and valley gradient on drainage density and hollow development, *Catena Supplement*, 10, 1-14.

Kirby, M.J., 1993, Long term interactions between networks and hillslopes, in *Channel Network Hydrology*, eds: Beven, K. and Kirkby, M.J., pp. 255-293

Kohn, B.P., Wagner, M.E., Lutz, T.M., Organist, G., Anomalous Mesozoic thermal regime, central Appalachian Piedmont; evidence from sphene and zircon fission-track dating, *Journal of Geology*, 101, 779-794.

Leopold, L.B. and Maddock, T., 1953, [Monograph] The hydraulic geometry of stream channels and physiographic implications, *U. S. Geological Survey Professional Paper*, Report: P 0252, 57 pp.

Leopold, L.B., Wolman, M.G., and Miller, J.P., 1964. Fluvial processes in geomorphology, W.H. Freeman and Company, San Francisco, 522 p.

Lippolt, H.J., Leitz, M., Wernicke, R.S., Hagedorn, B., 1994, (Uranium+thorium)/helium dating of apatite; experience with samples from different geochemical environments, *Chemical Geology*, 112, 179-191.

Lifton, N.A. and Chase, C.G., 1992, Tectonic, climatic and lithologic influences on landscape fractal dimension and hypsometry: implications for landscape evolution in the Sand Gabriel Mountains, California, *Geomorphology*, 5, 77-114.

Meigs A. and Sauber J., 2000, Southern Alaska as an example of the long-term consequences of mountain building under the influence of glaciers, *Quaternary Science Reviews*, 19, 1543-1562.

Melton, M.A., 1958, Correlation structure of morphometric properties of drainage systems and their controlling agents, *Journal of Geology*, 66, 442-460.

Mills, H.H., 1978, Downstream rounding of pebbles; a quantitative review, *Journal of Sedimentary Petrology*, 49, 295-302.

Moglen, G.E., Eltahir, E.A.B., Bras, R.L., 1998, On the sensitivity of drainage density to climate changes, *Water Resource Research*, 34, 855-862.

Mosley, M.P., 1972, An experimental study of rill erosion, M.S. Thesis, Colorado State University, Fort Collins, CO.

Oguchi, T., 1997, Drainage density and relative relief in humid steep mountains with frequent slope failure, *Earth Surface Processes and Landforms*, 22, 107-120.

Ohmori, H., 1993, Changes in the hypsometric curve through mountain building resulting from concurrent tectonics and denudation, *Geomorphology*, 8, 263-277

Ollier, C.D., 1982. The Great Escarpment of eastern Australia: tectonic and geomorphic significance. *Geol. Soc. Aust. Journal*, 39, 431-435.

Ollier, C.D., 1985, Morphotectonics of continental margins with great escarpments, Binghamton Symposia in Geomorphology: International Series, 15, 3-25

Parker, R.S., 1977, [Monograph] Experimental study of basin evolution and its hydrologic implications, 351 pp.

Paterson, W.S.B., 1981, The physics of glaciers: Pergamon Press, 380 pp.

Pavich, M.J., and Obermeier, S.F., 1985, Saprolite formation beneath Coastal Plain sediments near Washington, D.C., *Geological Society of America Bull*., 96, 886-900.

Pazzaglia, F.J. and Gardner, T.W., 1994, Late Cenozoic flexural deformation of the middle U.S. Atlantic passive margin. *Journal of Geophysical Research*, 99, 12143-12157.

Pike, R.J. and Wilson, S.E., 1971, Elevation-relief ration, hypsometric integral, and geomorphic area-altitude analysis. *Geological Society of America Bulletin*, 82, 1079-1084.

Pratt, T.L., Coruh, C., Costain, J.K., Glover, L., 1988, A geophysical study of the earth's crust in central Virginia: implications for Appalachian crustal structure. *Journal of Geophysical Research*, 93, 6649-6667.

Reed, J.C. and Bryant, B., 1964, Evidence for strike-slip faulting along the Brevard Zone in North Carolina. *Geol. Soc. America Bulletin*, 75, 1177-1195.

Reed, J.C., Bryant, B., and Myers, W.B., 1970, The Brevard zone; a reinterpretation. *Studies of Appalchian Geology: Central and Southern*, 261-269.

Reiners, P.W. and Farley, K.A., 2000, Helium diffusion and (U-Th)/He thermochronometry of titanite, *Geochimica et Cosmochimica Acta*, 63, 3845-3859.

Rinaldo, A., Dietrich, W.E., Rigon, R., Vogel, G., Rodriguez-Iturbe, I., 1995, Geomorphological signatures of varying climate, *Nature*, 374, 632-634.

Roden, M.K., 1991, Apatite fission-track thermochronology of the southern Appalachian basin: Maryland, West Virginia, and Virginia. *Journal of Geology*, 99, 41-53.

Roering, J.J., Kirchner, J.W., Sklar, L.S., Dietrich, W.E., 2001, Hillslope evolution by nonlinear creep and landsliding: An experimental study. *Geology*, 29, 143-146.

Roper, P.J. and Justus P.S., 1973, Polytectonic evolution of the Brevard Zone. *American Journal of Science*, 273-A, 105-132.

Sadler, P.M and Reeder, W.A., 1983, Upper Cenozoic, quartzite-bearing gravels of the San Bernardino Mountains, Southern California; recycling and mixing as a result of transpressional uplift, in *Tectonics and sedimentation along faults of the San Andreas system*, eds. Andersen, D.W. and Rymer, M.J., pp. 45-57.

Schumm, S.A., 1956, Evolution of drainage systems and slopes in badlands at Perth Amboy, New Jersey, *Geol. Soc. Am. Bull*., 67, 597-646.

Schumm, S.A., 1963, The disparity between present rates of denudation and orogeny, *U. S. Geological Survey Professional Paper*, Report: P 0454-H, pp.H1-H13

Schumm, S.A., Mosley, M.P., Weaver, W.E., 1987, [Monograph] Experimental fluvial geomorphology, 413 pp.

Seidl, M.A., Weissel, J.K., Pratson, L.F., 1996, The kinematics and pattern of escarpment retreat across the rifted continental margin of SE Australia. *Basin Research*, 8, 301-316.

Snyder, N.P., Whipple, K.X., Tucker, G.E., Merritts, D.J., 2000, Landscape response to tectonic forcing: Digital evlevation model analysis of stream profiles in the Mendocino triple junction region, northern California, *Geol. Soc. Amer. Bull.*, 112, 1250-1263.

Spotila, J., Farley, K.A., Seih, K., 1998, Uplift and erosion of the San Bernardino Mountains associated with transpression along the San Andreas fault, California, as constrained by radiogenic helium thermochrometry. *Tectonics*, 17, 360-378.

Spotila, J., House, M., Blythe, A., Niemi, N., Bank, G.C., in press., Controls on the erosion and geomorphic evolution of the San Bernardino and San Gabriel Mountains, southern California, *Geological Society of America Memoir*, in press.

Stephenson, R., 1983, Flexural models of continental lithosphere based on the long-term erosional decay of topography. *Geophysical Journal of the Royal Astronomical Society*, 77, 385-413.

Strahler, A.N., 1952, Hypsometric (area-altitude) analysis of erosional topography. *Bulletin of the Geological Society of America*, 63, 1117-1142.

Strahler, A.N., 1957, Qunatitative analysis of watershed geomorphology, *American Geophysical Union Trans*., 38, 913-920.

Suess, E., 1904, *The Face of the Earth*, 1, 604 pp.

Tucker, G.E. and Bras, R.L., Hillslope processes, drainage density, and landscape morphology, *Water Resources Research*, 34, 2751-2764.

Tucker, G.E., and Slingerland, R., 1994, Erosional dynamics, flexural isostasy, and long-lived escarpments; a numerical modeling study, *Journal of Geophysical Research*, B, Solid Earth and Planets, 99 12,229-12,243.

Tucker, G.E. and Slingerland, R., 1997, Drainage basin responses to climate change, *Water Resources Research*, 33, 2031-2047.

Tucker G.E. and Bras, R.L., 1998, Hillslope processes, drainage density, and landscape morphology. *Water Resources Research*, 34, 2751-2764.

van der Beek, P. and Braun, J., 1999, Controls on post-Mid-Cretaceous landscape evolution in the southeastern highlands of Australia; insights from numerical surface

process models. *Journal of Geophysical Research, B, Solid Earth and Planets*, 104, 4945-4966.

Waller, J.O., 1971, Additional evidence for Roanoke River drainage development by stream piracy of New River drainage areas, near Blacksburg, Virginia. *Abstracts with Programs - Geological Society of America*, vol.3, no.5, pp.355-356.

Warnock, A.C., Zeitler, P.K., Wolf, R.A., Bergman, S.C., 1997, An evaluation of low-temperature apatite U-Th/He thermochronometry, *Geochimica et Cosmochimica Acta*, 61, 24, 5371-5377.

Weissel, J.K. and Seidl, M.A., 1997, Influence of rock strength properties on escarpment retreat across passive continental margins. *Geology*, 25, 631-634

Weissel, J.K and Seidl, M.A., 1998, Inland propagation of erosional escarpments and river evolution across the southeast Australian passive continental margin. *Rivers Over Rock: Fluvial Processes in Bedrock Channels*, geophysical monograph 107, 189-206.

Wellman, P., 1980. On the Cenozoic uplift of the southeastern Australian highland: *Geol. Soc. Aust. Journal*, 26, 1-9.

White, W.A., 1950, Blue Ridge front; a fault scarp, *Geological Society of America Bulletin*, 61, 1309-1346.

Whittecar, G.R. and Duffy, D.F., 1992, Geomorphology and stratigraphy of late Cenozoic alluvial fans, Augusta County, Virginia. *Southeastern Friends of the Pleistocene Field Trip Guidebook*, 128 pp.

Willemin, J.H. and Knuepfer, P.L.K, 1994, Kinematics of arc-continent collision in the eastern Central Range of Taiwan inferred from geomorphic analysis. *Journal of Geophysical Research*, 99, 20267-20280.

Willgoose, G., Bras, R.L., Rodriguez-Iturbe, I., 1991, A couple channel network growth and hillslope evolution model: 1. Theory. *Water Resources Research*, 27, 1671-1684.

Willgoose, G., Bras, R.L., Rodriguez-Iturbe, I., 1991, A couple channel network growth and hillslope evolution model: 2. Nondimensionalization and applications. *Water Resources Research*, 27, 1685-1696.

Willgoose, G. and Hancock, G., 1998, Revisiting the hypsometric curve as an indicator of form and process in transport-limited catchment, *Earth Surface Processes and Landforms*, 23, 611-623.

Whipple, K.X. and Tucker, G.E., 1999, Dynamics of the stream-power river incision model; implications for height limits of mountain ranges, landscape response timescales, and research needs. *Journal of Geophysical Research, B, Solid Earth and Planets*, 104, 17661-17674

Wolf, R.A., Farley, K.A., Silver, L.T., 1996, Helium diffusion and low-temperature thermochronometry of apatite, *Geochimica et Cosmochimica Acta*, 60, 4231-4240.

Wolf, R.A., Farley, K.A., Kass, D.M., 1998, Modeling of the temperature sensitivity of the apatite (U-Th)/He thermochronometer, *Chemical Geology*, 148, 105-114.

Wright, F.J., 1927, The Blue Ridge of Southern Virginia and western North Carolina, *Bulletin of the Scientific Laboratories of Dension University*, 22, 116-132.

Wright, F.J., 1927, Gravels on the Blue Ridge, *Bulletin of the Scientific Laboratories of Dension University*, 22, 133-135.

Zeitler, P.K., Herczeg, A.L., McDougall, I., Honda, M., 1987, U-Th-He dating of apatite; a potential thermochronometer, *Geochimica et Cosmochimica Acta*, 51, 2865-2868.

VITA

Gregory C. Bank

Work Experience

Research Analyst - September 2001 to present
Advanced Resources International
1110 North Glebe Road
Suite 600
Arlington, Virginia 22201

Education

Master of Science, Geology - August 1999 to August 2001
Virginia Polytechnic Institute and State University
Blacksburg, Virginia

Bachelor of Science, Geology - September 1995 to June 1999
Washington & Lee University
Lexington, Virginia Tech

Publications

Spotila, J., House, M., Blythe, A., Niemi, N., Bank, G.C., in press., Controls on the erosion and geomorphic evolution of the San Bernardino and San Gabriel Mountains, southern California, *Geological Society of Amereica Memoir*, in press.

Bank, Gregory C., and J. Spotila, Testing Origins of a Passive-Margin Great Escarpment along the Blue Ridge of the Southern Appalachians, Using Topographic Analysis and Geochronology. *Abstracts with Programs - Geological Society of America*, 2000.

Bank, G.C., D. Harbor, and D.W. Morriss, Quaternary Erosional History of the St. Marys River, Western Virginia. *Banisteria*, no. 13, pp.161-169, 1999

Bank, Gregory C. and D. Harbor, Headward advance of the James River basin by the capture of St. Marys River from the Shenandoah River basin, Virginia. *Abstracts with Programs - Geological Society of America*, vol. 30, no. 7, pp.140, 1998

Bank, Gregory C. Quartz weathering characteristics of Maury River terraces, Rockbridge County, VA. *Virginia Journal of Science*, vol. 49, no. 2, pp.84, 1998